TOMBUSVIRIDS AVOID AND EXPLOIT A PLANT EXORIBONUCLEASE

CHAMINDA GUNAWARDENE

A DISSERTATION SUBMITTED TO THE FACULTY OF GRADUATE STUDIES IN PARTIAL FULFILLMENT OF THE REQUIREMENTS FOR THE DEGREE OF

DOCTOR OF PHILOSOPHY

GRADUATE PROGRAM IN BIOLOGY

YORK UNIVERSITY

TORONTO, ONTARIO

NOVEMBER 2021

ABSTRACT

Tombusviridae is a family of plus-strand RNA plant viruses that contain single-stranded RNA genomes with no 5' cap or 3' poly(A) tail. The 5' cap is an essential post-transcriptional modification that increases the stability of mRNA molecules, by protecting them from 5'-to-3' exoribonuclease decay. The lack of this modification in this virus family raised the question of how these viruses protect their vulnerable genomic 5' ends from nuclease attack during infections. Carnation Italian ringspot virus (CIRV) from the genus *Tombusvirus*, family *Tombusviridae*, has a plus-strand RNA genome with a structured 5' untranslated region that I hypothesized could serve as a protective substitute for the 5' cap. Results from my *in vitro* and *in vivo* studies with CIRV showed that the higher-order RNA structure at the 5' end of its genome was able to effectively prevent access of a 5'-to-3' exoribonuclease (Xrn), thereby protecting it from being degraded by Xrn during infections. In a second related study, I investigated a small viral RNA (svRNA) that accumulated in infections with another member of the family *Tombusviridae*, Tobacco necrosis virus-D (TNV-D; genus *Betanecrovirus*). In this case, I hypothesized that the svRNA represented a stable degradation product that could be functionally relevant to successful TNV-D infections. Through *in vitro* and *in vivo* analyses of TNV-D, I determined that the svRNA was indeed generated from incomplete digestion of the TNV-D genome by Xrn, and that its accumulation was beneficial in infections. Collectively, these findings extend and broaden our knowledge of the roles of novel viral RNA structures in facilitating successful viral infections by either evading (CIRV) or exploiting (TNV-D) the activity of the cellular exoribonuclease, Xrn.

ACKNOWLEDGEMENTS

First and foremost, I would like to thank my parents, Chandralal and Irshani Gunawardene, for their unwavering support during these difficult years; my academic success up to this point would not have been possible without their help and encouragement. I would also like to extend my gratitude to my brother, Praveen Gunawardene, and my sister-in-law, Vaishnavi Somasundaram, along with her family, who have provided a vital support network for me during my graduate studies.

I was lucky enough to make some good friends while in grad school, including Jennifer Im, Chun Chih Chen, and Tamari Chkuaseli, who were able to enhance my experience and make things warmer and more enjoyable for me, especially during my final years. I would also like to acknowledge some of my lab members and students, past and present, that have helped me over the years with my work, and with some of whom I've shared many enjoyable experiences and conversations: Baodong Wu, Hyukho Sheen, Slava Rubanov, Joseph Benjamen, Julia Arrigo, Laura Newburn, and many of the undergraduate students from the labs that I taught over the years.

Last but not least, I would like to thank my supervisor and mentor, Andy White, for imparting his knowledge and guiding me through this monumental achievement, along with my two supervisory committee members, Mark Bayfield and Kathi Hudak, whose insight and suggestions over the years have been integral to the development of the content of my dissertation.

TABLE OF CONTENTS

LIST OF FIGURES

LIST OF ABBREVIATIONS

3'	three prime
3'CITE	3' cap-independent translation element
5'	five prime
5'RACE	5' rapid amplification of cDNA ends
BaMV	bamboo mosaic virus
BNYVV	beet necrotic yellow vein virus
BTE	barley yellow dwarf virus-like translation element
BVDV	bovine viral diarrhea virus
CCR4	carbon catabolite repression 4
CIRV	carnation Italian ringspot virus
CLSV	cucumber leafspot virus
CP	capsid protein
CR	conserved region
C-terminus	carboxyl-terminus
DCP	decapping protein
DF	decay factors
DI RNA	defective interfering RNA
DI-7	defective interfering RNA-7

DL	downstream linker
DmXrn1	*Drosophila melanogaster* Xrn1
DNA	deoxyribonucleic acid
DRTE	distal readthrough element
DSD	downstream domain
dsRNA	double-stranded RNA
Dxo1	decapping and 5'-to-3' exoribonuclease protein 1
eIF	eukaryotic initiation factor
EM	electron microscopy
ER	endoplasmic reticulum
HCV	hepatitis C virus
His	histidine
Hsc	heat shock cognate
Hsp	heat shock protein
IFN	interferon
IRES	internal ribosome entry site
kb	kilobases
kDa	kilodalton
KOW	kyprides/ouzounis/woese
lvRNA	long viral RNA

m^7G	7-methylguanosine
Mg	magnesium
miRNA	microRNA
MP	movement protein
mRNA	messenger RNA
MVEV	Murray Valley encephalitis virus
ncRNA	noncoding RNA
NLS	Nuclear localization signal
nm	nanometer
NMD	nonsense-mediated decay
NOT	negative on TATA-less
NS5B	nonstructural protein 5B
NSD	non-stop decay
N-terminus	amino-terminus
OPMV	opium poppy mosaic virus
ORF	open reading frame
PARN	poly(A)-specific ribonuclease
PAZ	piwi/argonaute/zwille
P-bodies	processing bodies
PK	pseudoknot

PLRV	potato leafroll virus
poly(A)	polyadenylate
PPE	promoter proximal enhancer
pre-rRNA	precursor rRNA
PRTE	proximal readthrough element
PTC	premature termination codon
PTGS	post-transcriptional gene silencing
RCNMV	red clover necrotic mosaic virus
RdRp	RNA-dependent RNA polymerase
RISC	RNA-induced silencing complex
RNA	ribonucleic acid
RNAi	RNA interference
rRNA	ribosomal RNA
S1	stem-1
SCNMV	sweet clover necrotic mosaic virus
sfRNA	subgenomic flaviviral RNA
sg mRNA	subgenomic mRNA
SH3	SRC homology 3
SHAPE	selective 2' hydroxyl acylation analyzed by primer extension
siRNA	small interfering RNA

SL	stem-loop
snoRNA	small nucleolar RNA
SUP	suppressor of gene silencing protein
svRNA	small viral RNA
TBSV	tomato bushy stunt virus
TCV	turnip crinkle virus
TMV	tobacco mosaic virus
TNV-D	tobacco necrosis virus-D
tRNA	transfer RNA
Trp	tryptophan
TRV	tobacco rattle virus
TSD	t-shaped domain
TuMV	turnip mosaic virus
UL	upstream linker
UTR	untranslated region
VPg	viral protein genome-linked
VRC	viral replicase complex
xeRNA	Xrn-evading RNA
Xrn	5'-to-3' exoribonuclease
Xrn1/4	yeast/animal Xrn1 and plant Xrn4

xrRNA	exoribonuclease-resistant RNA
ZIKV	Zika virus
β	beta
γ	gamma
π	pi

CHAPTER 1:

INTRODUCTION

1.1…Eukaryotic cellular mRNA turnover

Cellular gene expression is the process by which gene products (i.e. proteins) are generated from specific instructions encoded within DNA sequences. The process occurs via two main steps: transcription and translation (Orphanides and Reinberg, 2002; Clancy and Brown, 2008). During transcription, an RNA polymerase faithfully transcribes the protein information encoded in the DNA into an RNA molecule called a messenger RNA (mRNA). The maturation process of a eukaryotic mRNA molecule requires three main modifications to be made prior to its export to the cytoplasm; these include 5'-end capping, RNA splicing, and 3'-end polyadenylation (Moore and Proudfoot, 2009). For capping, the 5' terminal nucleotide of the nascent pre-mRNA is covalently linked to a 7-methylguanosine (m^7G) cap prior to completion of transcription. RNA splicing occurs post-transcriptionally, and involves the removal of non-coding introns, leaving only the protein-coding exons in the final mRNA. This is followed by the non-templated addition of a polyadenylate [poly(A)] tail to the 3' end of the mature mRNA. Once completed, the mature mRNA is then exported to the cytoplasm, where its amino acid codons are translated sequentially by ribosomes to construct the encoded polypeptide (Cooper, 2000; Köhler and Hurt, 2007).

1.1.1. mRNA turnover

There are two main functions associated with the 5'-cap and the 3'-poly(A) tail: they serve as both recruitment signals for factors involved in protein translation, and as protective structures at the terminal ends that maintain stability of the mRNA molecule (Ramanathan et al., 2016; Nicholson and Pasquinelli, 2019). The latter purpose of these modifications relates to their ability to enhance survivability of the mRNA molecule in the cellular environment, and loss of either, usually by enzymatic removal, triggers degradation of the mRNA. The enzymes that comprise

the mRNA decay machinery have vital roles in different cellular processes, including control of gene expression, RNA quality control, and the antiviral response.

Cellular gene expression is regulated at multiple levels to fine-tune the amount of mRNA produced, based on their quantitative, spatial, or temporal requirement. One of the main ways in which a cell exerts regulatory control over mRNA expression involves the use of mRNA decay pathways (**Figure 1**). Of these, the most widely used is the deadenylation-dependent pathway (Parker and Song, 2004; Garneau et al., 2007; Schoenberg and Maquat, 2012). As the name suggests, removal of the poly(A) tail of the mature mRNA is the first step that occurs, which is carried out by a deadenylation complex, followed by 5' cap removal by a decapping complex. The resulting mRNA intermediates then serve as substrates for 5'-to-3' exoribonucleases and 3'-to-5' exoribonucleases that degrade from the 5' and 3' ends, respectively. Less often used are the deadenylation-independent and endonuclease-mediated cleavage pathways (Wilusz et al., 2001). During deadenylation-independent mRNA decay, the 5' cap is removed by the decapping complex first, which allows for immediate 5'-to-3' exoribonuclease digestion of the mRNA from the 5' end. Endonuclease-mediated cleavage of an mRNA can also occur, resulting in 5' and 3' cleaved fragments that are then degraded by 3'-to-5' and 5'-to-3' exoribonucleases, respectively; this pathway also occurs during aberrant mRNA degradation (Wilusz et al., 2001).

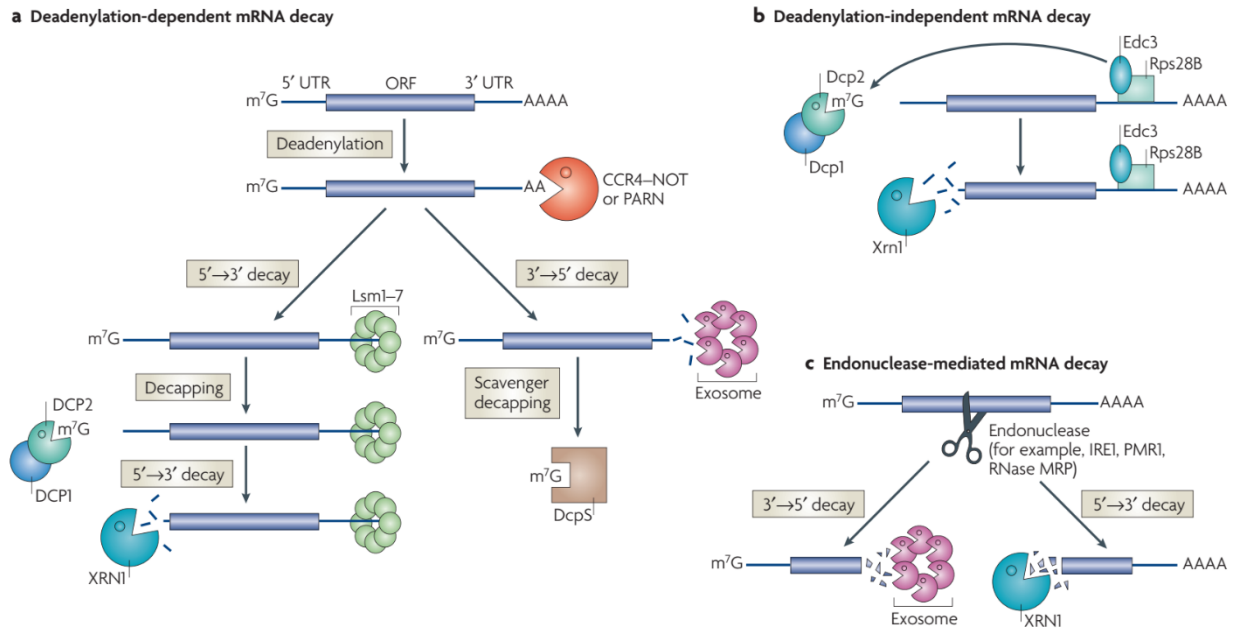

Figure 1. Cellular mRNA decay mechanisms. A) Deadenylation-dependent mRNA decay. Removal of the poly(A) tail by the deadenylation complex (CCR4-NOT or PARN) precedes exoribonuclease decay. Prior to 5'-to-3' exoribonuclease activity, the 5' cap is removed first by the decapping complex (DCP1/DCP2) followed by 5'-to-3' digestion by Xrn1. 3'-to-5' digestion from the 3' end can occur with or without 5' cap removal. **B)** Deadenylation-independent mRNA decay. Removal of the 5' cap by the decapping complex occurs independently of deadenylation, triggering 5'-to-3' degradation of the uncapped mRNA by Xrn1. **C)** Endonuclease-mediated mRNA decay. Internal endonucleolytic cleavage within the mRNA molecule results in 5' and 3' fragments, which are degraded by the exosome and Xrn1, respectively. (Adapted from Garneau et al., 2007)

mRNA surveillance factors monitor and eliminate aberrant mRNAs using endonuclease-mediated cleavage via two main mechanisms: nonsense-mediated decay (NMD), and no-go decay (Chang et al., 2007; Harigaya and Parker, 2010). The NMD pathway scans for premature termination codons (PTCs) that, if left unchecked, could result in truncated, potentially harmful proteins. NMD factors recognize PTCs and trigger endonucleolytic cleavage of the mRNA just upstream of the PTC, which activates exoribonucleases to eliminate the cleaved fragments. Similarly, during no-go decay, ribosomes that stall during translation elongation recruit endonucleases that cleave upstream of the stalled ribosome and trigger exoribonuclease decay. Both of these aberrant mRNA surveillance mechanisms trigger endonucleolytic-cleavage of the mRNA, followed by exoribonuclease decay of the resulting fragments. Non-stop decay (NSD) is another mechanism used to eliminate aberrant mRNAs, however, without the use of

endonucleolytic cleavage (Frischmeyer et al., 2002). NSD identifies mRNAs lacking a stop codon, and triggers either deadenylation followed by 3'-to-5' decay, or decapping, followed by 5'-to-3' exoribonucleolytic decay (van Hoof et al., 2002).

The host antiviral response in plants triggers a cascade of reactions, whereby foreign viral RNAs are used to generate dsRNA, which are then processed into smaller RNAs that direct endonucleolytic cleavage of the viral RNA (Muhammad et al., 2019). As with cleaved cellular mRNAs, the viral RNA fragments are then digested from their ends by exoribonucleases. Some of the most important factors that are common to all of the decay mechanisms outlined above are the exoribonucleases themselves, whose substrate-specificity include either full-length cellular mRNAs, or endonucleolytically-cleaved fragments of cellular and foreign RNAs.

1.2…Eukaryotic exoribonucleases

The term ‘exoribonuclease’ refers to a ribonuclease that hydrolyzes phosphodiester bonds between adjoining nucleotides in an RNA molecule from either its 5'- or 3'-terminus. Thus, exoribonucleases are defined in terms of the direction of their activity: 5'-to-3' exoribonucleases remove nucleotides starting at the 5' end of an RNA molecule progressing towards the 3' end, whereas 3'-to-5' exoribonucleases work in the opposite direction. As described in the previous section, exoribonucleases primarily degrade RNA substrates marked for degradation, such as cellular mRNAs and foreign RNAs. In the cell, these enzymes can be located in the nucleus, randomly dispersed in the cytosol, or contained within discrete cytoplasmic foci called processing (P) bodies (Decker and Parker, 2012). P-bodies serve as storage reservoirs and decay centers for untranslated mRNAs in the cytoplasm and contain exoribonucleases and other factors involved with mRNA decay, such as decapping and deadenylating proteins (Schoenberg and Maquat, 2012; Luo et al., 2018).

The main cytosolic 3'-to-5' exoribonuclease actually exists as a complex, referred to as the exosome (Mitchell et al., 1997). It includes a hexameric ring structure formed by six proteins, to which a trimeric 'cap' is attached, totaling nine separate proteins. This barrel-shaped, nonameric structure, however, lacks catalytic activity, which is instead provided by either by a dual 3'-to-5' exo- and endoribonuclease, Rrp44, or a 3'-to-5' exoribonuclease, Rrp6 (Kowalinski et al., 2016; Kilchert et al., 2016). The function of the exosome varies based on its location. The nuclear exosome is mainly responsible for 3' processing of nocoding RNAs such as small nucleolar RNAs (snoRNAs) and ribosomal RNAs (rRNAs), and for removal of defective precursor RNAs (Houseley et al., 2006). By contrast, the cytosolic exosome complex is primarily involved in mRNA decay and RNA silencing, and functions as the main cytosolic 3'-to-5' exoribonuclease in the cell.

5'-to-3' exoribonucleases (Xrns) can also exist in the nucleus or cytoplasm, and their functions vary based on their localization (Nagarajan et al., 2013). The two main Xrns in animals are Xrn1 and Xrn2, which localize to the cytoplasm and nucleus, respectively. Plants have no Xrn1, but instead have genes encoding Xrn2, Xrn3, and Xrn4 proteins, the first two of which are nuclear, and the latter of which is cytoplasmic (**Figure 2**) (Kastenmayer and Green, 2000). Although there is no plant ortholog for Xrn1, a cytoplasmic Xrn2 ortholog is present, which is Xrn4. The structures of Xrn1 and Xrn4 and their general functions will be discussed as the topic of the next section. One of the main functions of Xrn2 in the nucleus pertains to transcription termination via the torpedo model (West et al., 2004; Tollervey, 2004). During transcription of a nascent mRNA by RNA polymerase II, endonucleolytic cleavage is triggered following transcription of the polyadenylation signal. The 5'-liberated mRNA fragment is then polyadenylated at its free 3' end generated from the cleavage event. The 3' remaining RNA fragment still attached to the actively synthesizing polymerase, is bound by Xrn2 at its 5' end, which then degrades the remaining RNA faster than it is being synthesized by the polymerase, ultimately 'torpedoing' (i.e. knocking) the

polymerase off the DNA template (Tollervey, 2004). Xrn2 is also involved in processing of noncoding RNAs such as rRNAs, snoRNAs and tRNAs. In higher plants, an additional Xrn-family protein, Xrn3 is also present in the nucleus (Kastenmayer and Green, 2000). Xrn3 is an ortholog of Xrn2, and the two are similarly sized. Both Xrn2 and Xrn3 are endogenous suppressors of post-transcriptional gene silencing (PTGS) in plants (Gy et al., 2007). The mechanism for PTGS usually begins by the creation of dsRNA from uncapped aberrant RNA by cellular RNA-dependent RNA polymerases (RdRps). These dsRNAs are then recognized and processed by the RNA-induced silencing complex (RISC), which uses them to direct endonucleolytic cleavage of the complementary target RNA. Both of these nuclear Xrns were shown to degrade the templates for dsRNA synthesis, ultimately downregulating the PTGS system (Gy et al., 2007).

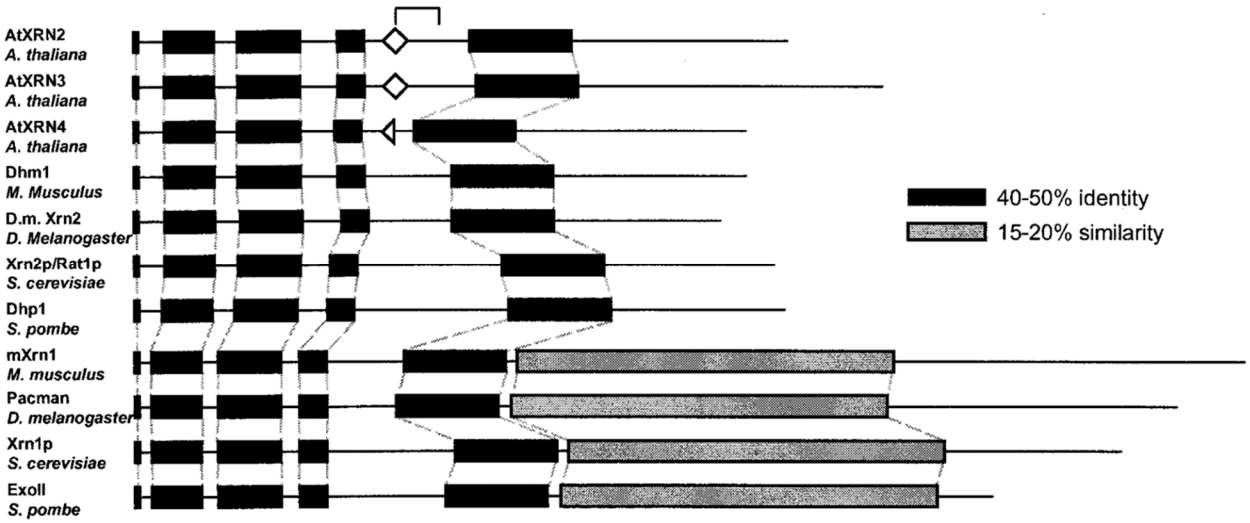

Figure 2. Protein alignment of Xrn family in higher plants, animals, and yeast. The amino acid sequence of Xrn proteins from higher plants (*A. thaliana*), animals (*M. musculus* and *D. melanogaster*) and yeast (*S. cerevisiae* and *S. pombe*) were aligned using ClustalW software by Kastenmayer and Green (2000). Horizontal black lines correspond to each full-length protein. Black bars represent regions with 40-50% sequence identity, whereas grey bars show regions with 15-20% similarity. Diamond boxes show nuclear localization signals and the half-diamond in AtXrn4 indicates a partial N-terminal NLS. (Adapted from Kastenmayer and Green, 2000). Copyright (2000) National Academy of Sciences, U.S.A.

1.3…5'-to-3' Exoribonuclease 1 (Xrn1)

5'-to-3' exoribonuclease 1 (Xrn1) is a cytoplasmic exoribonuclease that is expressed in yeast and metazoans. This ubiquitously expressed enzyme plays a major role in cellular gene expression, and was first identified, purified, and physically characterized by Audrey Stevens and colleagues beginning in the late 1970's (Stevens, 1978; Stevens, 1980; Stevens and Maupin, 1987; Stevens, 2001). In addition to its primary role in cellular mRNA turnover, Xrn1 has functions in other cellular processes related to mRNA regulation, RNA silencing, and the host antiviral response pathway (Chang et al., 2011; Jones et al., 2012). Xrn1 homologs and functional equivalents have been studied in a wide variety of model organisms ranging from animals and plants, to yeast, including detailed mutational analyses and the elucidation of crystal structures (Page et al., 1998; Xiang et al., 2009; Jinek et al., 2011; Langeberg et al., 2020). Xrn1 is mainly localized within P-bodies in the cytoplasm, where it performs the majority of its mRNA-related degradation functions. No cytoplasmic homolog for Xrn1 exists in plants, however, an ortholog of nuclear Xrn2 is present, called Xrn4 (Kastenmeyer and Green, 2000). Xrn4 has been shown to perform many of the same functions as Xrn1, and is therefore considered to be the functional equivalent of Xrn1 in plants.

1.3.1. Xrn1/4 structure and homology

The overall size of Xrn1 ranges from 1500 to 1700 amino acid residues, corresponding to a protein of approximately 175 kilodaltons in mass. Schematically, the overall structure of the enzyme resembles a bipartite, rectangular-shaped box that is divided into multiple domains, each with its own distinct function (**Figure 3**) (Chang et al., 2011; Langeberg et al., 2020). The N-terminal region is highly conserved between different species and contains the catalytic core of the enzyme, whereas the C-terminal region is more variable by comparison. This lower

conservation observed in the C-terminus reflects the different functions of Xrn1 that may be required in different species-related contexts. Indeed, truncations of the C-terminus by as many as 500 residues is well-tolerated, and the enzymes remain active *in vitro* (Page et al., 1998; Jinek et al., 2011). The nuclease domain, located at the N-terminal end, is divided into two domains called CR1 and CR2, and houses the catalytic core of the enzyme (Chang et al., 2011; Langeberg et al., 2020). In yeast, the nuclease domain is interrupted at the center, between CR1 and CR2, by an additional domain shown to interact with the 80S ribosome to degrade RNA templates on which the ribosome has stalled during translation (Tesina et al., 2019). At the C-terminal end of the nuclease domain are the PAZ and Tudor domains, which provide structural support to the catalytic motifs, and interact with the 40S ribosomal subunit in yeast. Immediately adjacent to these domains are the winged-helix and SH3-like motifs, which make contact with the tower domain in the active site and stabilize the N-terminal end, respectively (Jinek et al., 2011).

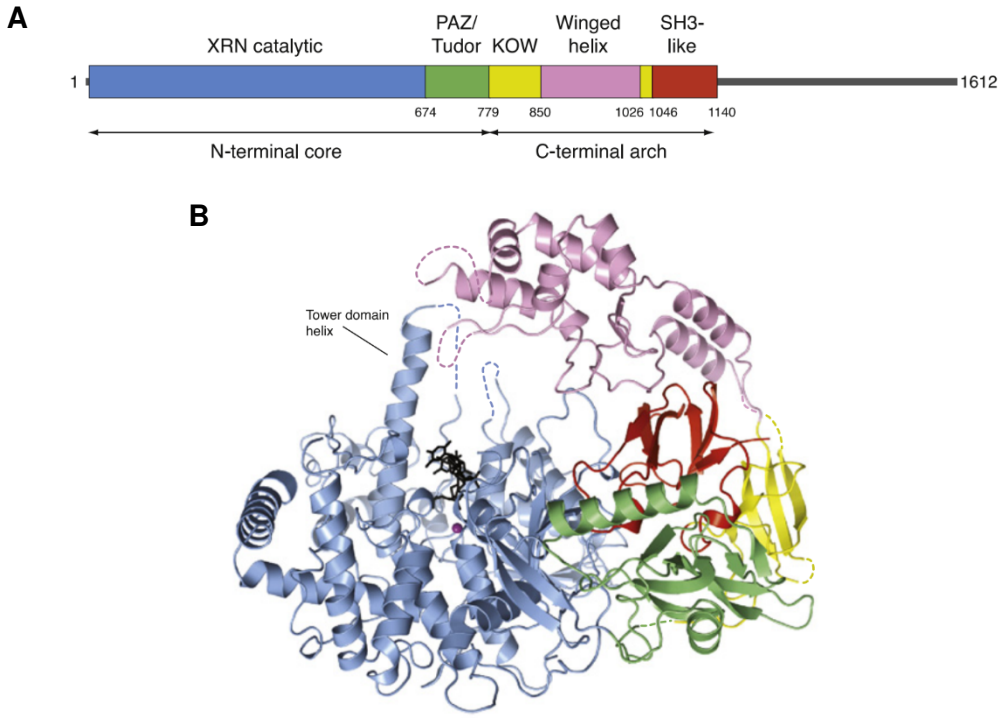

Figure 3. Structure of *D. melanogaster* Xrn1 (DmXrn1). A) Schematic representation of DmXrn1. The C-terminal region removed prior to crystallization is shown as thick grey line. The catalytic core, consisting of CR1 and CR2 domains is shown as a blue bar and the Paz/Tudor domains are shown in green. KOW, Winged Helix and SH3-like domains are shown in yellow, pink and red, respectively. **B)** Ribbon representation of a DmXrn1-substrate complex. Colour coding corresponds to the schematic diagram in panel A. A Mg^{2+} ion is represented by a purple sphere and the nucleic acid substrate is shown in black. (Adapted from Jinek et al., 2011)

The N-terminal catalytic domain of Xrn1 contains highly conserved, and some strictly conserved, residues that are involved with processive degradation of RNA substrates. The catalytic core of the enzyme is located at the base of a tower domain helix, which enables exonuclease activity exclusively (Jinek et al., 2011). Within the active site itself are a set of acidic and basic residues, which are essential for coordinating magnesium ions and water molecules, and interacting with the negatively charged 5' phosphate of the RNA substrate, respectively (Jinek et al., 2011; Langeberg et al., 2020). The basic amino acid pocket does not accommodate 5' capped and 5' triphosphorylated RNAs, allowing for only 5' monophosphorylated substrates to enter the catalytic center. The acidic residues are strictly conserved, and characteristic of Mg^{2+}-dependent nuclease enzymes (Chang et al., 2011). A π-π stacking interaction occurs between the first and third nucleotides of the substrate, capped by strictly conserved amino acid residues, His41 and Trp540 in *Drosophila melanogaster* Xrn1, at the 5' and 3' end, respectively (Jinek et al., 2011). As a result, substrate recognition by the enzyme requires three free nucleotides in the RNA for enzyme to bind, and for hydrolysis to occur. For its catalytic activity, Xrn1 uses a Brownian ratchet mechanism to direct processive degradation of the RNA substrate, via His41 and the basic pocket, which together aid in enzyme processivity, duplex unwinding, and hydrolytic directionality.

In plants, Xrn4 is the cytoplasmic ortholog of nuclear Xrn2, and thus many of the structural findings associated with Xrn2 can be extended to Xrn4 (Kastenmeyer and Green, 2000). Sequence similarity between Xrn1 and Xrn2 is relatively high around the active site, and the two share a common mechanism of action (Xiang et al., 2009; Chang et al., 2011). By contrast, the C-terminal region is much less conserved between the two, and significant portions are missing in Xrn2. Indeed, Xrn2, and its ortholog Xrn4, are much smaller than Xrn1, at approximately 950 amino acids (115 kDa). One of the main structural differences between Xrn4 and Xrn2 is that the former is missing a complete bipartite nuclear localization signal (NLS) present in the latter

(**Figure 2)** (Kastenmeyer and Green, 2000). Accordingly, the origin of Xrn4 is speculated to be due to loss of the functional NLS in Xrn2, resulting in a cytoplasmic Xrn2; the existence of a conserved N-terminal region of the NLS in Xrn4, but no C-terminus, supports this theory (Kastenmeyer and Green, 2000).

1.3.2. Xrn1/4 function

Yeast Xrn1 and plant Xrn4 (Xrn1/4) activity can only proceed on an RNA substrate bearing a monophosphate on its 5' terminal nucleotide (Stevens, 2001; Jinek et al., 2011). Therefore, mRNAs containing a 5' cap must first be decapped to generate a 5' monophosphorylated end. Uncapped viral RNAs, such as those utilized by members of the plant virus family *Tombusviridae* contain a 5' terminal triphosphate (discussed in later sections). For Xrn1/4 to engage these substrates, the γ- and β-phosphate moieties must first be removed, usually via a pyrophosphatase. In addition to their other functions, pyrophosphatases are also part of the host antiviral response, specifically responding to and removing uncapped, triphosphorylated RNA, by converting them to monophosphorylated substrates for exoribonuclease decay (Burke and Sullivan, 2017; Amador-Cañizares et al., 2018).

There is significant overlap in the molecular functions of yeast Xrn1 and plant Xrn4. Indeed, overexpression or silencing of either often produces similar molecular outcomes (Cheng et al., 2007; Jaag and Nagy, 2009). The main Xrn1 functions discovered so far involve mRNA-related activities, RNA silencing, and noncoding RNA processing. The mRNA-related activities of Xrn1 relate to its role in transcription, translation, and degradation of mRNA. The control of mRNA degradation is its main mRNA-related function. Most mRNA decay occurs via a deadenylation-dependent mechanism, whereby the poly(A) tail is first removed by the deadenylation complex, followed by removal of the 5' cap by the decapping complex (Hsu and

Stevens, 1993; Schoenberg and Maquat, 2012). The resulting mRNA molecules contain a 5' monophosphate and a partial 3' poly(A) tail, which are then degraded by Xrn1 in the 5'-to-3' direction. Deadenylation-independent mechanisms also occur, albeit less frequently.

The NMD pathway does not require deadenylation to occur, but instead requires NMD factors to scan mRNAs for PTCs, which, once found, cause endonucleolytic cleavage of the mRNA; the resulting 3' cleavage products are then degraded by Xrn1 (Gatfield and Izaurralde, 2004; Eberle et al., 2009; Nagarajan et al., 2019). Deadenylation-independent decapping of the mRNA also results in an mRNA that is an immediate substrate for Xrn1 decay (Badis et al., 2004). Degradation of mRNA can also occur co-translationally, whereby mRNAs can remain associated with translating ribosomes during deadenylation, decapping and subsequent decay by Xrn1 (Hu et al., 2009).

Similarly, during no-go decay, mRNAs containing stalled ribosomes are degraded to eliminate truncated, potentially harmful proteins from being translated, through direct physical contact between the 80S ribosome and Xrn1 (Doma and Parker, 2006; Tesina et al., 2019). Interestingly, Xrn1 was also found to function as a transcriptional activator by degrading decapped mRNAs and facilitating subsequent transport of Xrn1-complexed decay factors (DF) into the nucleus for transcription activation (Haimovich et al., 2013). These DFs, along with Xrn1, were able to bind to promoter regions in chromatinized DNA, and activate transcription of certain genes by RNA polymerase II. This model effectively links the processes of mRNA decay and transcription, placing Xrn1 in a pivotal bridging role between the two. Recently, a novel finding presented by the same researchers showed that Xrn1 activity is also able to facilitate protein translation initiation, through an interaction with the eukaryotic translation factor, eIF4G (Blasco-Moreno et al., 2019). Collectively, these unexpected findings implicate Xrn1 activity with most stages of the mRNA life cycle, including transcription, translation, and degradation. It is currently

unknown whether the translation- and transcription-related roles of Xrn1 are shared by Xrn4 in plants.

Nevertheless, a common role for both enzymes occurs during RNA silencing. The RNA silencing machinery in animals and plants is triggered by either microRNAs (miRNAs) or small interfering RNAs (siRNAs). Although their origins and biogenesis pathways differ, their mode of action is essentially the same. Following siRNA- or miRNA-directed cleavage of an mRNA substrate by the RISC complex, plant Xrn4 degrades the 3' decay intermediate of the cleaved mRNA in the 5'-to-3' direction (Souret et al., 2004; Orban and Izaurralde, 2005; Valencia-Sanchez et al., 2006). Whereas mRNA cleavage occurs often in plants, its occurrence in animals is much rarer, as small RNA-directed targeting of mRNAs usually results in reversible translation inhibition, rather than cleavage (Yekta et al., 2004; Bartel, 2009; Xu et al., 2016). Nevertheless, in the few cases in which it does occur, 5'-to-3' degradation of the 3' cleaved fragment is carried out by Xrn1.

Xrn1 is also involved with processing certain noncoding RNAs (ncRNAs). Small nucleolar RNAs (snoRNAs) are small ncRNAs in the nucleus that provide guided modification of other RNAs, such as pre-rRNAs and tRNAs (Maxwell and Fournier, 1995). Pre-rRNAs are nascent rRNA molecules that require modification in the nucleus before they can associate with ribosomes, and direct translation of proteins in the cytosol. ncRNAs such as snoRNAs and pre-rRNAs require yeast Xrn1 activity to trim their 5' ends as an essential part of their processing (Petfalski et al., 1998). It is unknown whether plant Xrn4 is required for noncoding RNA processing in plants in the same way that Xrn1 is for yeast/animals, especially because plant Xrn3 is also present in the nucleus, which may have coinciding functions in rRNA and snoRNA processing with plant Xrn2. For all three plant Xrns to have overlapping roles in certain processes would not be surprising, given that all three are related to plant Xrn2 (Kastenmayer and Green, 2000). As such, one of these roles occurs during PTGS in plants, where all three plant Xrns were shown to be endogenous suppressors of PTGS by degrading single-stranded RNA templates of

endogenous RdRps, preventing dsRNA formation and gene-specific targeting by the RISC (Gazzani et al., 2004; Gy et al., 2007).

1.4…Plus-strand RNA plant viruses

Viruses are biological entities that are often described as obligate intracellular parasites; that is, they survive by infecting a host cell and hijacking specific cellular machinery in order to replicate their genomes and make progeny viruses (Breitbart and Rohwer, 2005). Plus-strand RNA viruses are a class of virus that contain a single-stranded RNA genome that is messenger-sensed, similar to mRNA. This means that viral proteins can be translated from the viral genome directly upon entry into the cell (Ahlquist, 2006). Among the many types of plant viruses that have been identified, the majority have been found to contain plus-strand RNA genomes (Gergerich and Dolja, 2006; Hyodo and Okuno 2016). In addition, many plant diseases that affect economically important crops are caused by plus-strand RNA plant viruses. This, taken together with the fact that plant viruses serve as useful, and safer surrogates for the study of molecular virology, supports ongoing and future research involving plus-strand RNA plant viruses. One of the most extensively studied plus-strand RNA plant viruses is Tomato bushy stunt virus (TBSV), the type member of the genus *Tombusvirus* in the family *Tombusviridae*.

The typical life cycle of the plus-strand RNA plant virus, TBSV, is depicted in **Figure 4**. The TBSV life cycle begins with entry of the viral particle into the cell, which requires physical damage to breach the plant cell wall. For tombusvirus infection, this damage is mediated by a fungal vector from the genus *Olpidium* (Dias, 1970; Yamamura and Scholtof, 2005). Once inside the cell, disassembly occurs via interaction with a plant Hsp70 homolog, Hsc70, which causes conformational changes in the particle and triggers release of the plus-strand RNA genome into the cytoplasm (Alam and Rochon, 2017). The coding-sense RNA genome is then bound by host

translation factors and ribosomes that translate the viral replication proteins, including the viral RdRp (**Figure 4**). The viral replication proteins, in concert with additional host proteins, recruit the viral genome to membranous invaginations of intracellular organelles, called spherules, where the viral replicase complex (VRC) assembles and replicates viral RNA (White and Nagy, 2004; Belov and van Kuppeveld, 2012). Within the virus-induced spherule, the VRC makes multiple copies of the plus-strand RNA genome through production of a complementary minus-strand RNA intermediate. These newly synthesized viral progeny genomes are then released into the cytosol to (i) be translated by ribosomes create more replication proteins and VRCs, or (ii) be used as templates for subgenomic mRNA (sg mRNA) transcription. Viral sg mRNAs are smaller mRNAs that encode 3'-encoded viral proteins. They are generated when the RdRp stalls prematurely during synthesis of a genomic minus-strand, creating a truncated minus-strand RNA (White, 2002; Choi and White, 2002). This truncated minus-strand is then used as a template to transcribe plus-strand sg mRNAs that are 3'-coterminal with the original genome. The sg mRNAs are then released from VRCs into the cytosol where they are translated to generate additional viral proteins, such as the capsid (CP), suppressor of gene silencing (SUP), and movement (MP) proteins. The SUP protein supresses the host gene silencing response by binding and sequestering small interfering RNAs (siRNA) generated by dicer (Qiu et al., 2002; Lakatos et al., 2004). The MP protein is required for cell-to-cell movement of the viral genome to neighbouring cells through intercellular openings called plasmodesmata (Wolf et al., 1989; Desvoyes et al., 2002). Once a sufficient amount of CP protein is translated, the progeny viral genomes are packaged into infectious icosahedral particles within the cytoplasm.

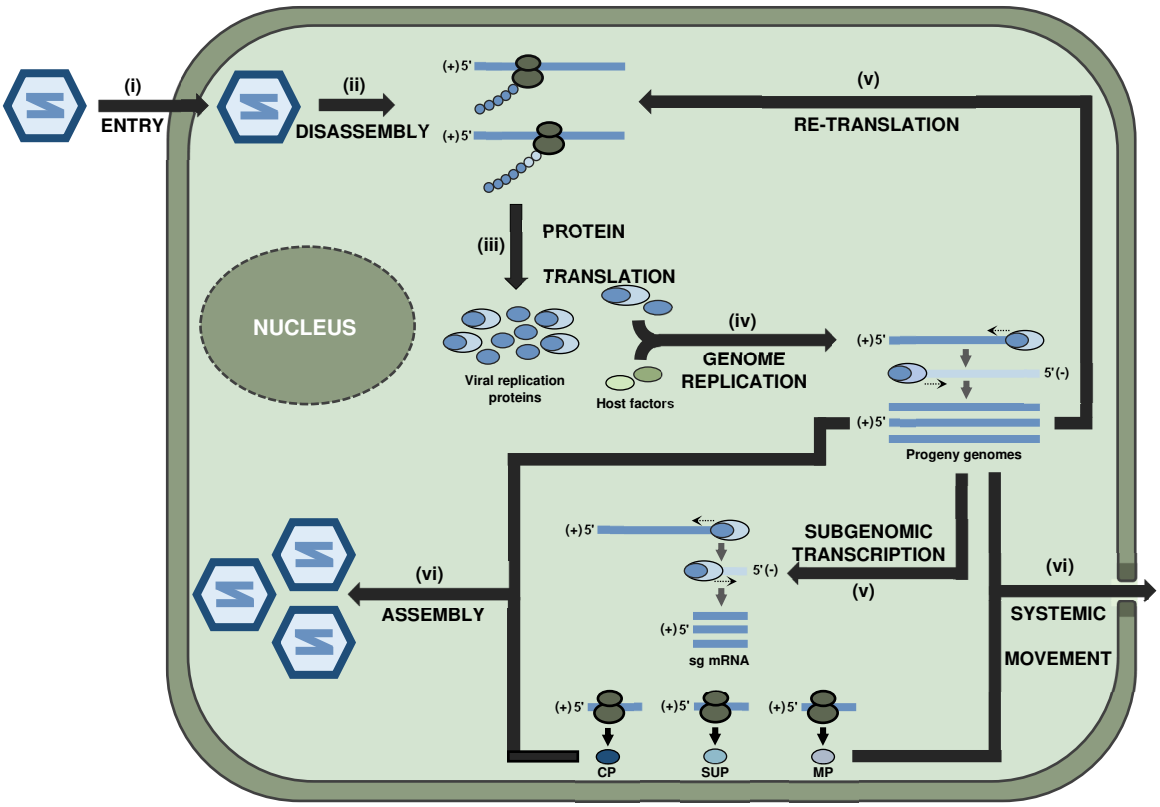

Figure 4. Plus-strand RNA plant virus (TBSV) life cycle. The TBSV lifecycle begins with entry **(i)** into the cell via a fungal vector. The virus then disassembles **(ii)** to release the plus-strand RNA genome into the cytosol, which is immediately translated by ribosomes **(iii)** to generate the viral replication proteins. The viral replication proteins, together with specific host factors, replicate the viral genome **(iv)** via a minus-strand intermediate to generate progeny genomes. Some of these progeny genomes can be re-translated **(v)** by cellular ribosomes to produce additional replication proteins. A subset of the progeny genomes are also used as templates for subgenomic mRNA transcription **(v)** to generate additional viral factors, such as coat protein (CP), gene silencing suppressor (SUP) and movement protein (MP). Once sufficient progeny viral genomes are made, some are encapsidated by CP into particles **(vi)**, while other are bound and moved through plasmodesmata to neighbouring cells by the MP **(vi)**.

1.5…Carnation Italian ringspot virus (CIRV)

Carnation Italian ringspot virus (CIRV) was first isolated from carnation plants imported to Britain from Italy and the United States (Hollings et al., 1970). It is a plus-strand RNA plant virus in the *Tombusvirus* genus of the *Tombusviridae* family. Similar to other tombusviruses, such as TBSV, it has a non-enveloped, icosahedral capsid approximately 30 nm in diameter, that is assembled with 180 identical capsid subunits arranged in T=3 symmetry. Along with TBSV, CIRV has served as an important model virus for molecular studies on tombusviruses.

1.5.1. Genome organization

The CIRV genome is made of plus-strand RNA approximately 4.8 kb in length, which lacks a 5' cap and 3' poly(A) tail (**Figure 5**). The genome is polycistronic and comprises five open reading frames (ORFs) that encode viral proteins, flanked by 5'- and 3'-untranslated regions (UTRs) at the terminal ends of the genome. The 5' proximal ORFs encode two membrane-associated replication proteins, which are translated directly from the genome immediately upon entry into the cell (White and Nagy, 2004). The three downstream auxiliary viral proteins are translated from two smaller sg mRNAs that are transcribed during infections.

1.5.2. Viral protein expression strategies

Due to the limited coding potential of a small genome, tombusviruses such as CIRV utilize unconventional protein expression strategies to translate viral proteins. These specialized strategies enable the virus to exert tight regulatory control over the quantity and timing of protein expression. The replication proteins, p36 and p95, share a common start codon, but each have their own stop codon. Expression of p95, which is the RdRp, occurs through translational

readthrough of the p36 stop codon by ribosomes, which results in a C-terminally extended p36 (Cimino et al., 2011). Translational readthrough is an inefficient process, generating twenty-fold more p36 relative to p95, which allows for optimal VRC formation during replication (Scholthof et al., 1995; Panavas et al., 2005a). In tombusviruses, subgenomic transcription occurs via a premature transcription mechanism whereby long-range RNA-RNA interactions within the genome force the RdRp to stall prematurely during synthesis of the minus-strand, creating truncated minus-strand intermediates with transcriptional promoters at their 3'-ends (White, 2002; Chkuaseli and White, 2020). The resulting minus-strands are then used to make plus-strands that are 3'-coterminal with the genome and relocate downstream genomic ORFs to the 5' end of their own message. Sg mRNA1 is used to translate the coat protein (p41) and sg mRNA2 is used to translate both movement (p22) and suppressor of gene silencing (p19) proteins (**Figure 5**). p22 and p19 are both translated from sg mRNA2, and although the start codon for p19 is located downstream of the start codon for p22 (**Figure 5**), p19 is made at higher levels (White and Nagy, 2004). This is attributed to the phenomenon of leaky scanning, whereby a weak Kozak consensus sequence for p22, along with a short 5' UTR, result in ribosomes efficiently bypassing the p22 start codon during scanning, and accessing the downstream p19 start codon instead (Scholthof et al., 1999).

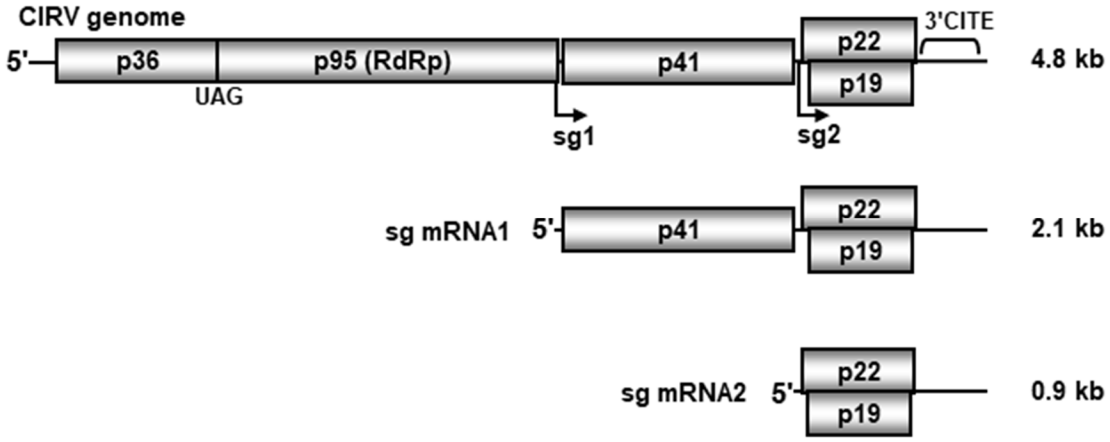

Figure 5. Schematic representation of CIRV RNAs. Viral ORFs are shown as grey boxes and the location of subgenomic promoters are delineated below the genome using black arrows. The location of the 3'CITE in the 3'UTR in shown on the genome using a bracket. Approximate RNA sizes are shown on the right, in kilobases. (Adapted from Gunawardene et al., 2021)

1.5.3. Viral protein functions

p36 is a membrane protein that is an auxiliary replication factor required during CIRV replication and subgenomic transcription. It has multiple roles including RNA template selection and recruitment to endoplasmic reticulum (ER) membranes, interacting with and recruiting multiple host factors to the sites of replication, and forming the major protein-based structural foundation of the VRC (White and Nagy, 2004; Gunawardene et al., 2017). The N-terminal end of p36 was also found to be a major determinant for organelle targeting, with its deletion resulting in VRC formation in the peroxisome instead of the ER (Burgyan et al., 1996). p95 is a C-terminal extension of p36, and contains the catalytic motifs of the RdRp (Panavas et al., 2005a). Its N-terminus corresponds to the entire p36 amino acid sequence, which allows it to interact with p36 during formation of the VRC within the membrane invaginations known as spherules. p95 is responsible for both viral processes related to RNA synthesis: genome replication and subgenomic transcription. The RdRps of tombusvirids (i.e. viruses in the family *Tombusviridae*), are highly conserved amongst members of the family, and this is a major determining factor for

inclusion into the family (Gunawardene et al., 2015). The overall structure of the tombusvirus RdRp has been compared to the poliovirus RdRp (Hansen et al., 1997; O'Reilly and Kao, 1998) and, as a supergroup II, flavivirus-like, RdRp superfamily member, was structurally modelled based on the NS5B RdRp of Hepatitis C virus (Gunawardene et al., 2017).

The coat protein, p41, is used to encapsidate the genome into an icosahedral virion of T=3 symmetry using 180 coat protein subunits per particle (White and Nagy, 2004). Studies have shown that the coat protein is not essential for local cell-to-cell spread or systemic movement of the virus through the plant, but it makes these processes more efficient (Scholtof et al., 1993; White and Nagy, 2004). p19 plays a pivotal role in suppressing the plant host's gene silencing mechanisms during viral infection. Specifically, it binds, as a homodimer, to virus-specific siRNAs that are generated during tombusvirus infection, preventing them from being loaded into the RISC (Lakatos et al., 2004). Consequently, the RISC is not able to target and cleave viral RNA, thus allowing for efficient viral genome accumulation. The p22 movement protein is essential for cell-to-cell movement of the virus within plants. It allows for viral dissemination into neighbouring cells by increasing the size exclusion limit of plasmodesmata, through which it mediates translocation of the viral genome (Desvoyes et al., 2002).

1.5.4. Viral UTRs

Similar to cellular mRNAs, the CIRV genome and associated subgenomic mRNAs both contain 5' and 3' UTRs at their termini. These nocoding sequences have been studied extensively in tombusviruses, revealing essential roles for the genomic UTRs for viral translation and replication. The fact that tombusviruses, and all members of the *Tombusviridae* family, lack a 5' cap and a 3' poly(A) tail, the question is raised as to how these and similar plus-strand RNA viruses have adapted to survive without these essential post-transcriptional modifications.

Research thus far has implicated the viral UTRs as functional substitutes for the cap and poly(A) tail during viral protein translation. It therefore stands to reason that the viral UTRs would also help to stabilize and protect the viral genomic termini from host exoribonucleases, in a similar manner to how a 5' cap and 3' poly(A) tail protects cellular mRNAs.

1.5.4.1. CIRV 5'UTR

The CIRV 5'UTR is 143 nucleotides in length and is structurally comparable to the TBSV 5'UTR, which has been studied extensively. The genomic 5'UTR is involved in two essential viral processes; namely, viral protein translation and viral genome replication (Nicholson and White, 2008; Nicholson et al., 2010; Wu et al., 2001; Ray et al., 2003, 2004). The 5'UTRs of all tombusviruses, including CIRV, are subdivided into three discrete parts: the T-shaped domain (TSD), stem-loop-5 (SL5) and the downstream domain (DSD) (**Figure 6**). (Wu et al., 2001; Ray et al., 2003, 2004). The TSD includes a three helix junction, with stem-1 (S1), containing the genomic 5' terminus, at its base. The stability of the S1 stem has been previously established as being essential for viral RNA accumulation using a subviral RNA replicon, termed a defective interfering RNA or DI RNA (Wu et al., 2001; Ray et al., 2003). The minus-strand complement of the 5' half of the TSD contains the minimal plus-strand promoter and an associated enhancer element, called the promoter proximal enhancer (PPE); the latter is essential for efficient plus-strand genome production during tombusvirus infection (Panavas et al., 2002; Panavas et al., 2003). The minus-strand complement of the 5'UTR also recruits host factors that facilitate plus-strand production (Kovalev et al., 2012). The other two stems of the TSD extending from the three-way junction are termed SL3 and SL4. It is worth noting that some tombusviruses have an additional stem region, called S2, that is absent in CIRV. For viral protein translation, tombusviruses utilize a long-range RNA-RNA interaction between the 5'UTR and a 3' cap independent translational element (3'CITE) located in the 3'UTR, to relocate 3'-CITE-bound

protein translation factors to the 5'UTR (Nicholson et al., 2010). The 5' partner sequence for this interaction lies in the loop of SL3 in the TSD. The other stem-loop, SL4, interacts with a 3'-proximal segment of the 5'UTR to form a pseudoknot, PKTD1, previously shown to be important for viral RNA synthesis (Ray et al., 2003).

Immediately 3'-adjacent to the TSD is SL5, which is a highly conserved stem-loop present in all tombusviruses that is important for viral RNA accumulation. Its location suggests that it may participate in a stacking interaction with the S1 stem of the TSD to form a quasi-continuous helix (Holbrook, 2008). The 3'-proximal DSD comprises a bulged stem-loop and a short intervening sequence of nucleotides preceding the AUG start codon, both of which are essential for viral RNA accumulation. A short 5 nt sequence that overlaps with the start codon contains the downstream partner sequence for the PKTD1 pseudoknot interaction.

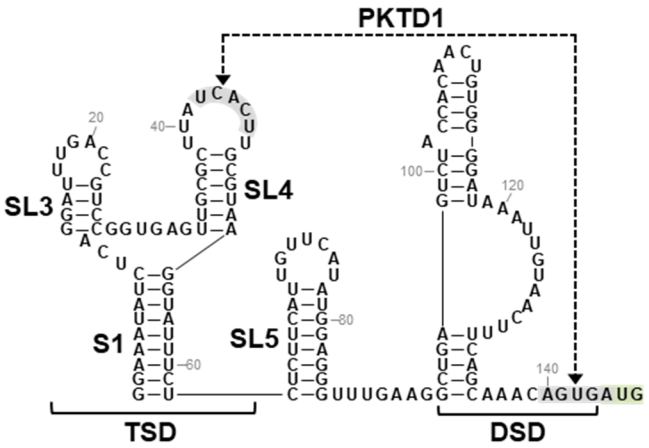

Figure 6. RNA secondary structure model of CIRV 5'UTR. The TSD and DSD are shown below using brackets. The sequences that pair to form the pseudoknot PKTD1 are highlighted in grey, and are connected with a dotted arrow. The p36 start codon, which overlaps with PKTD1, is highlighted in green. (Adapted from Gunawardene et al., 2021)

1.6…Tobacco necrosis virus-D (TNV-D)

Tobacco necrosis virus-D (TNV-D) was first isolated from tobacco seedlings displaying symptoms of necrotic lesions on the leaves (Babos and Kassanis, 1963). TNV-D is a plus-strand RNA plant virus in the genus *Betanecrovirus*, which is also in the *Tombusviridae* family. Like CIRV, it has a non-enveloped, icosahedral capsid approximately 30 nm in diameter, displaying T=3 symmetry.

1.6.1. Genome organization

The TNV-D genome is made of plus-strand RNA and is approximately 3.8 kb in length. Like all tombusvirids, the genome lacks a 5' cap and 3' poly(A) tail (**Figure 7**). The genome comprises five ORFs encoding viral proteins, flanked by 5' and 3'UTRs at the terminal ends of the genome. Similar to CIRV, the 5' proximal ORFs encode two membrane-associated replication proteins, one of which is the RdRp, which are translated directly from the genome following entry into the cell. The three downstream auxiliary viral proteins are translated from two smaller sg mRNAs that are transcribed during infections.

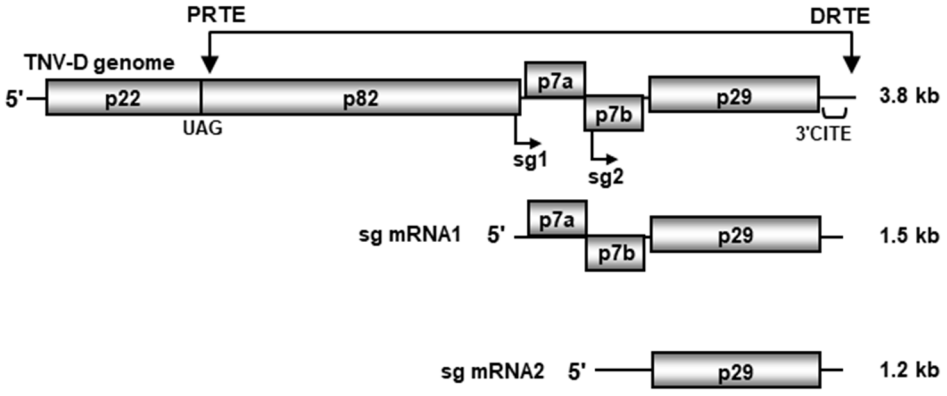

Figure 7. Schematic representation of TNV-D RNAs. Viral ORFs are shown as grey boxes and the location of subgenomic promoters are delineated below the viral genome using black arrows. The approximate location of the 3'CITE in the 3'UTR in shown on the genome using a bracket. The long-range PRTE-DRTE interaction required for genome replicaton is shown above with a double-sided arrow. Approximate RNA sizes are shown on the right, in kilobases. (Adapted from Gunawardene et al., 2019)

1.6.2. Viral protein expression strategies and functions

The viral protein expression strategies utilized by TNV-D are comparable to those used by CIRV. Although its auxiliary replication protein and RdRp, p22 and p82, respectively, are smaller than those of CIRV, they are expressed from the genome by a similar translational readthrough mechanism and perform equivalent functions during TNV-D infection (Molnár et al., 1997; Fang and Coutts, 2013). In betanecroviruses, as with tombusviruses, subgenomic transcription also occurs via the premature transcription mechanism, creating two smaller, 3' coterminal sg mRNAs for expressing the 3'-proximal proteins, p7a, p7b and p29 (**Figure 7)** (Jiwan et al., 2011). A minor difference worth noting is that, in betanecroviruses, the p29 capsid protein is also expressed from the genome, likely via the action of an internal ribosome entry site (IRES) (Chkuaseli et al., 2015). TNV-D sg mRNA1 is used to translate the movement proteins p7a and p7b, and sg mRNA2 is used to express the capsid protein, p29. p7b is translated via leaky scanning of the first encountered p7a start codon, which results in a p7a:p7b ratio of approximately 14:1. Although both proteins are required for successful cell-to-cell movement, the precise role of p7b has yet to be uncovered. p7a has been shown to interact with the viral RNA genome, which is thought to help facilitate movement of the viral RNA into adjacent cells (Offei et al., 1995). The TNV-D p29 capsid protein is required for encapsidation of the genome, and for systemic movement of the virus within infected plants (Molnár et al., 1997).

1.6.3. Viral UTRs

The TNV-D UTRs function in a similar fashion to CIRV, except that the 5'UTR of TNV-D is significantly shorter and less-structured. The 5' and 3'UTRs measure approximately 38, and 305 nucleotides in length, respectively. As with tombusviruses, the TNV-D 3'UTR has been determined to be essential for viral infection during viral protein translation and genome

replication, via the action of multiple RNA secondary and tertiary level interactions. By contrast, the roles of the 5'UTR, which, due to its small size, is only predicted to contain a short hairpin, are currently unknown.

1.6.3.1. TNV-D 3'UTR

The TNV-D 3'UTR is 305 nucleotides in length and has been extensively studied for its role in viral protein translation and genome replication (**Figure 8)** (Coutts et al., 1991). It contains several different structures and sequences that are intimately involved with the two aforementioned processes: these include SLY, SLX, the downstream linker sequence (DL), a Barley yellow dwarf virus-like translation element (BTE), the distal readthrough element (DRTE), SL2, SL1, and a replication silencer element. Interestingly, some of these elements engage in long-range RNA-RNA interactions with other regions within the TNV-D RNA to help facilitate translational readthrough or genome replication.

Mutational analysis of the two predicted hairpins, SLY and SLX, demonstrated that, of the two, SLX is particularly important for viral genome replication; although the mechanism by which it meditates this process is unknown (**Figure 8**) (Newburn et al., 2020). 3' to the SLX is an internal replication element called the DL, which forms a long-range RNA-RNA interaction with its partner sequence in the p82 coding sequence (not shown) called the upstream linker (UL). This UL-DL interaction forms the RNA-based platform on which the viral replicase complex is assembled prior to genome replication (Newburn et al., 2020). Located just downstream of the DL is the BTE, which is a type of 3'CITE (**Figure 8**) (Shen and Miller, 2004b). Its primary function is to recruit eukaryotic translation initiation factors (eIFs) to the viral 3'UTR and mediate translation of both the genome and sg mRNAs. Currently, no long-range RNA-RNA interaction between the 5' and 3'UTR has been identified in TNV-D, and therefore it is unknown how the host eIFs are relocated

to the 5' end of the genome for viral protein translation initiation (Chkuaseli et al., 2015). The overall structure of the TNV-D BTE is T-shaped, resembling a hammerhead, with two stem-loops radiating from a central point, that are connected to the rest of the 3'CITE through a long basal stem helix (Shen and Miller, 2004b). Like other BTEs, a conserved functional element within the TNV-D BTE required for eIF binding is a 17 nucleotide-long sequence overlapping SL1. This sequence has been shown to interact with the scaffolding protein, eIF4G, in the eIF4F complex, whose recruitment and activity is essential for translation initiation (Treder et al., 2008; Kraft et al., 2013).

Immediately downstream of the BTE is a bulged stem-loop RNA structure referred to as SL2, which has been shown to be involved in viral genome replication, as well as readthrough production of p82 (**Figure 8**) (Newburn and White, 2017). At the base of the 3' half of SL2 is a short pyrimidine-rich sequence called the DRTE, which participates in a long-range RNA-RNA interaction with the proximal readthrough element located at the p82 stop codon (**Figure 7**). The PRTE-DRTE interaction is required to promote translational readthrough production of p22 (Cimino et al., 2011; Newburn et al., 2014). The most 3' proximal secondary structure in the TNV-D 3'UTR is SL1, which is essential for genome replication (Shen and Miller, 2004a; Newburn and White, 2017). SL1 and the terminal four nucleotides at the 3' end of TNV-D RNA represent the genomic promoter (gPR), to which the RdRp binds in order to synthesize minus-strands. The terminal nucleotides also form a base-pairing interaction with a bulge in the 3' half of SL2, which likely protects the 3'-end of the viral genome from nuclease attack (Newburn and White, 2017). Overall, the multiple essential sequences and structures in the TNV-D 3'UTR make it a hotspot for activity related to viral RNA synthesis and viral protein translation.

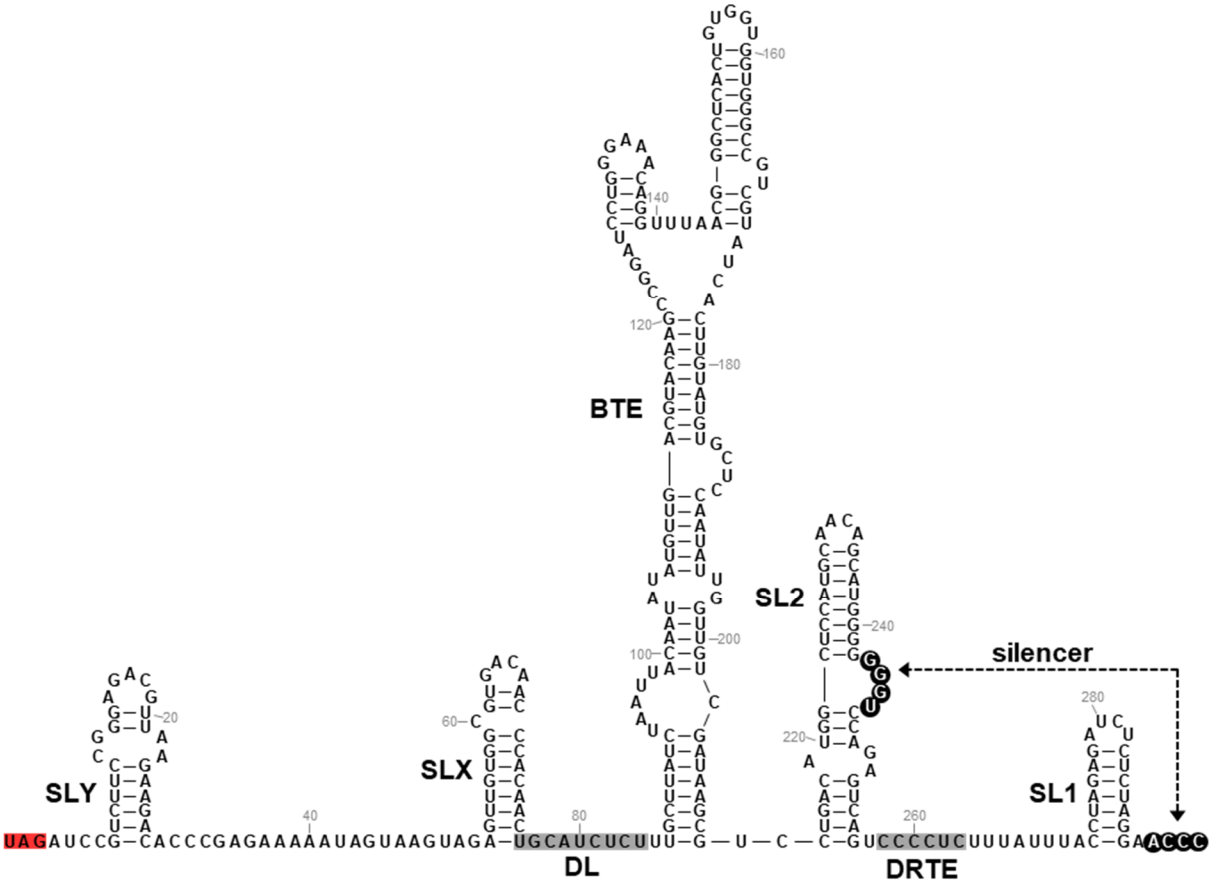

Figure 8. RNA secondary structure model of TNV-D 3'UTR. All substructures including SLY, SLX, BTE, SL2 and SL1 are labeled. The p29 stop codon is highlighted in red and the DRTE sequence is highlighted in grey. Sequences participitating in the silencer interaction are shown in black boxes with white text, and are joined by a dotted arrow.

1.7…Exoribonuclease-resistant RNAs (xrRNAs)

Over the last decade, a new field of research in RNA biology has emerged focusing on secondary and tertiary level RNA structures within viral RNAs that are able to independently resist actively digesting 5'-to-3' exoribonucleases, such as Xrns. The structural properties of these exoribonuclease-resistant RNAs (xrRNAs) have been extensively studied in members of the well-known family of arthropod-borne animal viruses, *Flaviviridae* (Kieft et al., 2015). The following section outlines the fundamental details about xrRNAs, specifically related to their structure and mechanism for blocking Xrn, and the functions of the decay intermediates they form.

1.7.1. Structure and mechanism for exoribonuclease inhibition

The primary sequence of an RNA molecule, which can be described as the phosphodiester-linked sequence of nucleosides, helps to determine the overall folding pattern of the RNA, depending on its environment. Secondary structure motifs are formed by hydrogen-bonding interactions between nearby primary sequences, and include a diverse array of structures, such as helices, terminal and internal loops, and bulges (Nowakowski and Tinoco Jr, 1997). Interactions between two or more secondary structures result in tertiary level folding, the most well-known of which is the RNA pseudoknot. Higher-order structures act to increase the thermodynamic stability of RNAs, by lowering the total free energy associated with the molecules.

1.7.1.1. Mammalian virus xrRNAs

Exoribonuclease-resistant RNAs (xrRNAs) are defined as highly structured RNA sequences that can independently block active degradation by 5'-to-3' exoribonucleases, such as Xrn (Kieft et al., 2015). The structural basis of an xrRNA involves both secondary and tertiary level interactions that cooperatively interact to form a physical barrier against actively digesting 5'-to-3' exoribonucleases. The structural properties of flavivirus xrRNAs have been studied extensively and were determined to be the structures responsible for generation of 3'UTR decay intermediates called subgenomic flaviviral RNAs (sfRNAs) (Jones et al., 2021; Vicens and Kieft, 2021). During Xrn1 digestion of the flavivirus genome, stalling of Xrn1 occurs at local, specifically-folded RNA structures in the 3'UTR, resulting in undigested, non-coding sfRNAs. The xrRNA structures of two flaviviruses, Murray Valley encephalitis virus (MVEV) and Zika virus (ZIKV), have been solved by X-ray crystallography (Chapman et al., 2014; Akiyama et al., 2016). Based on these studies, it was found that xrRNAs resist Xrn1 degradation by utilizing a local, independently-folding RNA structure-based mechanism. The xrRNA structure is highly conserved among

flaviviruses and involves an approximately 50-nucleotide long sequence forming a three-helix junction with highly conserved nucleotides near the Xrn1 stall site. A ring-like structure is formed through multiple secondary and tertiary-level interactions, which include coaxial stacking of the first two helices, and an essential pseudoknot interaction stacked on a fourth helix, which further stabilizes the fold. Together with additional interactions between the 5' leading edge of the RNA and the third helix, the 5' end is dragged through the ring-like structure (**Figure 9**). As Xrn1 approaches the stall site, a molecular 'knot' is formed around the 5' end, secured by the pseudoknot, and through specific contacts between the winged-helix domain of Xrn1 and the xrRNA, essential conformational changes required for the enzyme's processivity are prevented from occurring (Chapman et al., 2014; Akiyama et al., 2016). This effectively inhibits the enzyme's ability to unwind and degrade the xrRNA, which eventually causes the enzyme to disengage the substrate, leaving behind an undigested sfRNA.

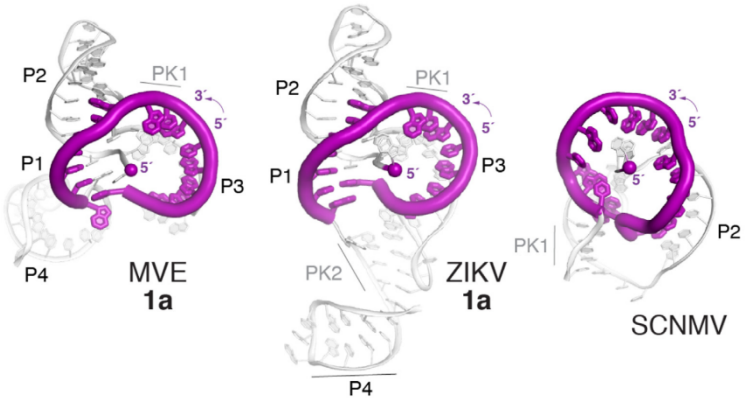

Figure 9. Ring-like RNA structures in diverse xrRNAs. 3D models of the ring-like structures formed by MVE, ZIKV and SCNMV xrRNAs are shown. The sequence comprising the ring structure is shown in magenta, and the rest of the xrRNA is shown in grey. The 5' end is shown as a magenta sphere. See text for additional details. (Adapted from Vicens and Kieft, 2021)

1.7.1.2. Plant virus xrRNAs

Research aimed at understanding the diversity of xrRNA structures has also been pursued in plant viruses, including those of the family *Tombusviridae*. Notably, the first example of an xrRNA was reported in the bi-segmented dianthovirus, Red clover necrotic mosaic virus (RCNMV) from the family *Tombusviridae* (Iwakawa et al., 2008). The study reported that during RCNMV infection, a small noncoding viral RNA, termed SR1f, was generated following incomplete digestion of the RNA1 genome by a 5'-to-3' exoribonuclease. The identity of the plant exoribonuclease responsible for generation of SR1f was not confirmed, and based on the current literature, still remains unknown. Considering its cytoplasmic localization and its functional equivalency to yeast Xrn1 (which can also generate SR1f *in vitro*), it is likely that the enzyme responsible is plant Xrn4 (Steckelberg et al., 2018a). The xrRNA structure required to stall Xrn was mapped to a ~40-nucleotide long region of the dianthovirus 3'UTR, which is significantly shorter than the ~70-nucleotide long flavivirus xrRNA. This highly conserved nuclease-resistant RNA is present in all dianthoviruses and has been solved using X-ray crystallography in Sweet clover necrotic mosaic virus (SCNMV; Steckelberg et al., 2018a). Unlike the flavivirus xrRNA, the crystal structure of the SCNMV xrRNA shows a single stem-loop comprising two stacked helices separated by an internal loop, with a single stranded region at its 3' end. Although the dianthovirus xrRNA structurally contrasts that of the flaviviruses, the underlying mechanism for exoribonuclease-blocking is the same; that is, a pseudoknot interaction formed between the terminal loop of the hairpin and the single stranded region forms a ring-link structure around the 5' end (**Figure 9**). This encircling of the 5' end occurs by co-degradational remodeling, whereby chewing of the base of the first helix by Xrn promotes formation of the pseudoknot, which is the major structure-reinforcing interaction of the xrRNA.

A crystal structure has also been solved for an xrRNA in Potato leafroll virus (PLRV), which is a polerovirus in the *Tombusviridae*-related family of plant viruses, *Luteoviridae* (Steckelberg et

al., 2020). The PLRV xrRNA has similar structural features to the dianthovirus xrRNA, with only minor differences in size, and interacting nucleotides. Despite their broader similarities, the sequences and structures that comprise the xrRNAs of dianthoviruses/poleroviruses and flaviviruses differ quite substantially from one another. For this reason, a classification system was devised to distinguish the two types of xrRNAs, where $xrRNA_D$ is used to refer to the type contained in viruses from the *Tombusviridae* and *Luteoviridae* families, and $xrRNA_F$ is used to broadly refer to those utilized by flaviviruses (Steckelberg et al., 2018b).

In Beet necrotic yellow vein virus (BNYVV), a 20-nucleotide-long sequence in the RNA3 segment of its genome, referred to as coremin, was shown to inhibit Xrn4 to produce a noncoding RNA, ncRNA3 during infection (Peltier et al., 2012; Flobinus et al., 2018; Dilweg et al., 2019). This ncRNA3 can be generated during infection, and *in vitro* using purified Xrn1. This much smaller Xrn-resistant structure, which underlies repression of Xrn4 activity by the BNYVV genome, has not been explored in detail and no atomic structural models are yet available.

1.7.1.3. Other viral xrRNAs

A different type of xrRNA was discovered in the 3'UTRs of phlebovirus and arenavirus mRNAs that stalls Xrn1. Unlike the viruses discussed thus far, the phlebo- and arenaviruses contain segmented genomes made of minus-strand RNA and their viral proteins are translated from capped plus-strand mRNAs that are transcribed during infection (Charley et al., 2018). These viral messages contain sequences in their 3'UTR that were found to stall and repress Xrn1 activity using cell-free extracts and purified recombinant Xrn1. The core region responsible for stalling Xrn1 was mapped to G-rich sequences, which are believed to form G-quadraplexes able to block Xrn1 progression. G-quadraplexes are highly stable RNA secondary structure elements that occur in regions with a high concentration of G residues (Varshney et al., 2020). Through non-

Watson Crick base pairing interactions, nearby G's interact with one another to form a tetrad, which then stack on adjacent G-tetrads to form the quadraplex. Although these unusual xrRNAs were able to independently inhibit Xrn1, the function of the resulting decay intermediates has not yet been explored.

RNA structures resembling xrRNAs have also been found within the 5'UTR of some viral genomes. In Hepatitis C virus (HCV) and Bovine viral diarrhea virus (BVDV), which are non-arthropod-borne members of the *Flaviviridae* family, it was found that structured regions in the 5'UTR of their plus-strand genomic RNA can stall actively digesting Xrn1 (Moon et al., 2015a). Stalling was attributed to multiple RNA secondary and tertiary level interactions comprising an internal ribosome entry site (IRES), located in the distal portion of the 5'UTR. A crystal structure of the HCV/BVDV resistant RNA, and the mechanistic details governing its suppression of Xrn1-mediated digestion have not yet been investigated.

1.7.1.4. Defining xrRNA activity

Yeast 20S narnavirus has a long RNA stem structure at the 5' end of its RNA genome that prevents 5'-to-3' exoribonuclease Xrn1 access to the 5' terminal nucleotides (Esteban et al., 2008). Specifically, the first four nucleotides at the 5' end of the viral genome are G residues, which base-pair with C residues in a downstream partner sequence, resulting in the 5' terminus being paired at the base of a long stem structure. Accordingly, the virus protects its 5' end by burying it within strong secondary structure, rendering it inaccessible to Xrn loading. The enzyme, being unable to load onto the RNA template, is thus unable to digest it. This contrasts with xrRNAs, which block actively digesting 5'-to-3' exoribonucleases. Unfortunately, the 5' end of the 20S narnavirus was not tested for its ability to block an actively digesting 5'-to-3' exoribonuclease

(Esteban et al., 2008). Therefore, without knowing whether it displays one of their key defining functional properties, it cannot be classified as an xrRNA.

With respect to their three-dimensional conformation, the ring-like RNA structure formed around the 5' end, stabilized by the pseudoknot, is present in all xrRNAs, and is thus a structurally defining feature (**Figure 9)** (Vicens and Kieft, 2021). Another common trait to all xrRNAs discovered so far is that they can be transposed into different sequence contexts (i.e. they are modular); this means that moving the minimal xrRNA sequence to a different RNA would result in proper folding of the xrRNA, and protection of the recipient RNA sequence downstream of the resistant structure from decay. It was also found that the xrRNA structures from both flaviviruses and dianthoviruses were able to block different types of 5'-to-3' exoribonucleases in addition to Xrn1, which include a yeast decapping and 5'-to-3' exoribonuclease protein 1 (Dxo1) and a bacterial 5'-to-3' exoribonuclease RNase J1 (MacFadden et al., 2018). This suggests that these xrRNAs utilize a general blocking mechanism that is effective against all exoribonucleases. Despite their diverse origins, the similarity of the structural features used by these different viruses for blocking Xrn, along with their transposability and common response to diverse exoribonucleases, illustrates the convergent evolution of these RNA structures, whereby different RNA sequences have independently evolved the ability to block 5'-to-3' exoribonuclease progression via a common mechanism.

1.7.2. Function of exoribonuclease-resistant RNA decay intermediates

The functional degradation intermediates generated by Xrn1 stalling at the 3'UTR of the flavivirus RNA genome are called sfRNAs. These noncoding sfRNAs are approximately 500-nucleotides in length and accumulate to high levels during flavivirus infection. Therefore, a significant amount of research has been dedicated to investigating the roles of sfRNAs during

flavivirus infection. Flaviviruses are able to infect both arthropod and vertebrate hosts, and, as a result, some of the functions attributed to sfRNAs differ between the two hosts (Slonchak and Khromykh, 2018). Two functions common to both types of hosts is the ability for sfRNAs to inhibit Xrn1 and dicer activity. sfRNAs were shown to reversibly inhibit Xrn1 *in vitro* via competitive inhibition, whereby degradation of a competitor RNA by Xrn1 was inhibited when co-treated with a full-length flavivirus 3'UTR; that is, stalling of Xrn1 at the xrRNA structure in the 3'UTR substrate led to delayed enzyme disengagement, and thus reduced engagement with the competitor RNA (Moon et al., 2012). The findings were also confirmed *in vivo*, where an increased accumulation of uncapped RNAs was observed in flavivirus-infected cells, suggesting repressed Xrn1 activity (Moon et al., 2012). By using a distinct, yet related mechanism, sfRNAs were also shown to competitively inhibit dicer activity, by binding this essential antiviral host protein and acting as a sponge, resulting in reduced levels of siRNAs derived from flavivirus RNA during infection, and disruption of the RNAi and miRNA biogenesis pathways (Moon et al., 2015b). Other effects of sfRNAs in vertebrate hosts include inhibition of the type 1 interferon (IFN) response pathway and induction of apoptosis in infected cells, which help the virus to evade the host's antiviral response and enhance viral propagation and spread to neighbouring cells, respectively. In mosquitos, sfRNAs also help flaviviruses to evade the Toll pathway, which is an antiviral response system that operates independently of RNAi. Overall, these findings demonstrate a multitude of functions for sfRNAs during flavivirus infection that are primarily centered on evading the host antiviral response, which it accomplishes via interactions with different cellular pathways.

Stalling of Xrn1 in the 5'UTR of the non-arthropod-borne members of the *Flaviviridae* family, HCV and BVDV, results in undigested near-full-length genomes containing part of the 5'UTR. The fact that they contain a fully intact IRES element, suggests that accumulation of these decay intermediates may impact viral protein translation (Moon et al., 2015a). Similar to the flavivirus sfRNAs, it was also found that the HCV and BVDV 5'UTRs were able to reversibly block

Xrn1 activity. When the HCV 5'UTR alone was added downstream of a reporter gene construct and transfected into human cells, viral infection resulted in an increase in global mRNA stability and abundance (Moon et al., 2015a), which would be expected if Xrn1 were inhibited given its pivotal role in cellular mRNA turnover. Taken together with the fact that the decay intermediates produced by Xrn1 stalling contain intact IRES structures in the undigested 5'UTR, these findings suggest that viruses like HCV and BVDV may inhibit Xrn1 activity, and consequently increase global mRNA abundance, in order to promote viral protein translation.

The degradation product SR1f, formed during infection of the plant virus RCNMV, was also determined to play a role during protein translation, mainly by inhibiting cap-independent and cap-dependent translation, suggesting a role in both viral and cellular protein translation, respectively (Iwakawa et al., 2008). Given that it contains a 3'CITE in its sequence, which is required by the virus for binding the eIF4F complex during viral cap-independent protein translation initiation, it is likely that SR1f acts as a sponge for binding and sequestering host translation factors during RCNMV infection (Miller et al., 2016).

Some decay intermediates generated by incomplete Xrn activity facilitate other aspects of the viral life cycle, beyond protein translation. For example, ncRNA3, which is produced by incomplete digestion of the BNYVV genome by Xrn4, was found to enhance long-distance systemic movement of the virus within the plant, by acting as an auxiliary viral suppressor of RNA silencing (Flobinus et al., 2016).

1.8…Plant viruses and Xrn – other examples

Although most of the research into Xrn's involvement with viral infection has focused primarily on animal viruses, there have been some studies that have also found a role for Xrn during plant virus infections. Most of these studies suggest that Xrn acts mainly as a restriction factor during infections, however, a few studies suggest that, for some plant viruses, Xrn may have a positive, or proviral role during infection. This section summarizes the current literature on the interactions between Xrn and plant viruses where, in several cases, xrRNA involvement has not been implicated.

The idea that Xrn may negatively impact survival of a single-stranded RNA virus is an intuitive notion, given that the primary substrate for Xrn is single-stranded RNA. In addition, Xrn requires a 5'-monophosphorylated terminal nucleotide for its catalytic activity, meaning that, for the cell to eliminate foreign RNAs such as viruses, those RNAs containing modified 5' ends must be unmodified first, so that exoribonucleases such as Xrn can recognize and eliminate the RNA. Potyviruses, such as Turnip mosaic virus (TuMV), are the largest genus of plant viruses, and contain plus-strand RNA genomes with a genome-linked viral protein (VPg) covalently attached to their 5' terminal nucleotide (Verma et al., 2014). The VPg protein has several functions during viral infection, including protection of the 5' end from exoribonucleases (Ullmer and Semler, 2016). Knockdown of Xrn4 in *Nicotiana benthamiana* followed by infection with TuMV resulted in an increased accumulation of viral RNAs, implicating Xrn4 as a restriction factor for these viruses (Li and Wang, 2018). Also worth noting is that the virally-encoded multifunctional proteinase, HC-Pro, was shown to bind with and inhibit Xrn4 activity during TuMV infection, suggesting that the virus has adapted to the host's antiviral response by repurposing one of its own viral proteins to suppress the activity of a major antiviral host factor (Li and Wang, 2018; Ala-Poikela et al., 2019; Ballut et al., 2005).

A restrictive role for Xrn was also observed during infection with the well-studied Tobacco mosaic virus (TMV), the first virus ever isolated. Tobamoviruses such as TMV contain a 5' methylguanosine cap structure at the 5' end of their genomes, and as a result, are also not direct substrates for Xrn during infection. Nevertheless, silencing of Xrn4 in *N. benthamiana* resulted in an increase in TMV RNA, and promoted systemic viral infection, whereas overexpression resulted in suppression of TMV viral RNA production (Peng et al., 2011; Jiang et al., 2018). Plant viruses containing genomes with unmodified 5' ends, such as tombusviruses, were also shown to be targets for Xrn4 activity in whole plant infections (Panavas et al., 2005b). Two sets of reciprocal studies analysing viral RNA accumulation in the presence or absence of Xrn4 showed that silencing Xrn4 caused an increase in tombusvirus RNA accumulation during infection, whereas overexpression of the enzyme resulted in accelerated degradation of tombusvirus RNAs (Serviene et al., 2005; Cheng et al., 2006; Cheng et al., 2007; Jaag and Nagy, 2009). Interestingly, overexpression of Xrn4 led to the accumulation of replicable 5' truncated viral RNAs lacking most of the 5'UTR that were also able to move systemically throughout the plant (Cheng et al., 2007). The replicability of these truncated RNAs is surprising considering that they lack the plus-strand initiation promoter and PPE elements, both of which are necessary for optimal tombusvirus genome replication (Panavas et al., 2002; Panavas et al., 2003).

Based on the studies described above, Xrn appears to act primarily as a restriction factor during plant virus infection, whereby it likely interacts directly with viral RNA substrates, accelerating their degradation. Despite this negative effect for Xrn on most single-stranded RNA plant viruses, there have been some roles identified for this enzyme that are proviral in nature, meaning that they enhance survivability of these types of viruses during infection. Bamboo mosaic virus (BaMV) is a potexvirus with a plus-strand RNA genome containing a 5' cap and 3' poly(A) tail. Overexpression of Xrn4 in *N. benthamiana* resulted in increased levels of BaMV accumulation, whereas silencing resulted in the opposite effect (Lee et al., 2016). Targeted

mutagenesis of the catalytic core of the enzyme implicated Xrn4 nuclease activity directly, and this proviral effect was determined not to involve Xrn4's RNAi-related function. Based on these results, along with the fact that Xrn4 was associated with a BaMV replication protein-enriched isolate, it is thought that Xrn4 may be recruited into the viral replicase complex during BaMV replication, although its exact role is still unknown (Lee et al., 2016).

Silencing of Xrn4 during Beet necrotic yellow vein virus (BNYVV) infection showed a similar result, where a decrease in viral genome replication was observed during plant infections (Flobinus et al., 2018). Benyviruses like BNYVV produce a small noncoding RNA called ncRNA3 during infection, which is required for long distance systemic movement of the virus within the plant (Flobinus et al., 2016). A 20-nucleotide-long coremin sequence in the RNA3 segment of the BNYVV genome inhibits Xrn4 to produce ncRNA3 during infection, and *in vitro,* using purified Xrn1 (Peltier et al., 2012; Flobinus et al., 2018). This coremin sequence is highly conserved in benyviruses, and sequences resembling it are also found in different plant virus families (Dilweg et al., 2019). Interestingly, Xrn4 knockdown significantly reduced viral genome accumulation, with little to no impact on ncRNA3 production, suggesting a replication-related requirement for Xrn4, similar to BaMV (Flobinus et al., 2018).

Opium poppy mosaic virus (OPMV) is a plant virus from the *Umbravirus* genus, which is a group of viruses closely related to *Tombusviridae*. OPMV infection produces two viral sg mRNAs of similar sizes, one of which is generated via an xrRNA structure (Ilyas et al., 2021). Degradation of the OPMV genome by Xrn4 is halted prematurely at an intergenic xrRNA site corresponding to a sg mRNA promoter, and the sg mRNA generated as a result encodes for a protein, called p30, that is required for efficient genome replication. Accordingly, the presence of an xrRNA site within the OPMV genome enables the virus to exploit the host antiviral Xrn4 protein to assist with the production of one of its translatable sg mRNAs. Also, the presence of the xrRNA

within an intergenic region, as opposed to the 3'UTR, suggests that these RNA species have more diverse roles during viral infection than originally thought.

Most plant viruses contain plus-strand RNA genomes, and it is therefore unsurprising that most will be susceptible to one of the main antiviral host proteins, Xrn4. It is equally predictable that viruses, in their quest to overcome the host's antiviral response, would evolve their own adaptations that seek to evade or exploit this response. Some of the examples outlined above show how a virally-encoded xrRNA structure can be used to exploit 5'-to-3' exoribonuclease activity to serve a specific viral purpose. Future research will likely uncover more xrRNA-related viral adaptations that have evolved to counteract the host antiviral response.

1.9…Purpose of research

1.9.1. Part 1

The impetus for my first project was based on previous observations made during protoplast infection of a betanecrovirus, TNV-D (family *Tombusviridae*). Infections of TNV-D resulted in the accumulation of a virally-derived small RNA species (svRNA) that was detectable during northern blotting using a 3' terminal probe (Jiwan and White, 2011). The size of the svRNA, along with the fact that it was detectable using a probe complementary to the 3' terminus of the TNV-D genome, suggested that it was derived from the 3'UTR of the viral RNA. Also, at the time, an xrRNA structure was known to exist in the 3'UTR of a *Dianthovirus* (family *Tombusviridae*), RCNMV, which led to the generation of a noncoding RNA, SR1f, that was functionally relevant (Iwakawa et al., 2008).

These two observations lead to the <u>hypothesis</u> that the TNV-D svRNA was generated via xrRNA-mediated stalling of Xrn4. Accordingly, structural and functional analyses of the TNV-D svRNA were launched.

The major goals of this project were to:

(i) Map the structure of the svRNA

(ii) Identify and characterize the RNA structural features leading to svRNA production by Xrn

(iii) Investigate the viral RNA source of the svRNA during infections

(iv) Investigate the function of the svRNA and its requirement during plant infections

This study is presented in **Chapter 2** in the form of a published research article.

1.9.2. Part 2

Plus-strand RNA plant viruses in the family *Tombusviridae* contain single-stranded RNA genomes lacking a 5' cap and 3' poly(A) tail. These two post-transcriptional modifications are essential components for enhancing the stability of mRNAs, and thus their absence in these viruses raises the question of how they are able to maintain genome integrity in a hostile cellular environment rife with exoribonucleases. Expression of the main cytosolic 5'-to-3' exoribonuclease in plants, Xrn4, has been shown to be primarily restrictive to viral infection by members of *Tombusviridae*, suggesting that some tombusvirid viral RNAs are substrates for Xrn4 activity (Serviene et al., 2005; Cheng et al., 2006; Cheng et al., 2007; Jaag and Nagy, 2009).

The absence of a 5' cap, and the presence of highly structured RNA elements in their genomic 5'UTR, led to the hypothesis that tombusviruses protect their RNA genome from Xrn4 using higher order RNA structures at the 5' end that prevent 5'-to-3' exoribonuclease access and decay. Accordingly, experiments to test this hypothesis were launched using the model tombusvirus CIRV.

The major goals of this project were to:

(i) Determine if the CIRV 5'UTR provides protection from Xrn

(ii) Identify the 5'UTR structural features that provide protection from Xrn

(iii) Ascertain if the 5'UTR is an xrRNA

(iv) Determine the importance of the 5'UTR's structural features during infections

This study is presented in **Chapter 3** in the form of a published research article.

1.10…References

Ahlquist P. 2006. Parallels among positive-strand RNA viruses, reverse-transcribing viruses and double-stranded RNA viruses. *Nat Rev Microbiol*. **4**(5):371-382.

Akiyama BM, Laurence HM, Massey AR, Costantino DA, Xie X, Yang Y, Shi PY, Nix JC, Beckham JD, Kieft JS. 2016. Zika virus produces noncoding RNAs using a multi-pseudoknot structure that confounds a cellular exonuclease. *Science*. **354**(6316):1148-1152.

Alam SB, Rochon D. 2017. Evidence that Hsc70 Is associated with cucumber necrosis virus particles and plays a role in particle disassembly. *J Virol*. **91**(2):e01555-16.

Ala-Poikela M, Rajamäki ML, Valkonen JPT. 2019. A novel interaction network used by potyviruses in virus-host interactions at the protein level. *Viruses*. **11**(12):1158.

Amador-Cañizares Y, Bernier A, Wilson JA, Sagan SM. 2018. miR-122 does not impact recognition of the HCV genome by innate sensors of RNA but rather protects the 5' end from the cellular pyrophosphatases, DOM3Z and DUSP11. *Nucleic Acids Res*. **46**(10):5139-5158.

Babos P, Kassanis B. 1963. The behaviour of some tobacco necrosis virus strains in plants. *Virology*. **20**:498-506.

Badis G, Saveanu C, Fromont-Racine M, Jacquier A. 2004. Targeted mRNA degradation by deadenylation-independent decapping. *Mol Cell*. **15**(1):5-15.

Ballut L, Drucker M, Pugnière M, Cambon F, Blanc S, Roquet F, Candresse T, Schmid HP, Nicolas P, Gall OL, et al. 2005. HcPro, a multifunctional protein encoded by a plant RNA virus, targets the 20S proteasome and affects its enzymic activities. *J Gen Virol*. **86**:2595-2603.

Bartel DP. 2009. MicroRNAs: target recognition and regulatory functions. *Cell*. **136**(2):215-233.

Belov GA, van Kuppeveld FJ. 2012. (+)RNA viruses rewire cellular pathways to build replication organelles. *Curr Opin Virol*. **2**(6):740-747.

Blasco-Moreno B, de Campos-Mata L, Böttcher R, García-Martínez J, Jungfleisch J, Nedialkova DD, Chattopadhyay S, Gas ME, Oliva B, Pérez-Ortín JE, et al. 2019. The exonuclease Xrn1 activates transcription and translation of mRNAs encoding membrane proteins. *Nat Commun*. **10**(1):1298.

Breitbart M, Rohwer F. 2005. Here a virus, there a virus, everywhere the same virus? *Trends Microbiol*. **13**(6):278-284.

Burgyan J, Rubino L, Russo M. 1996. The 5'-terminal region of a tombusvirus genome determines the origin of multivesicular bodies. *J Gen Virol*. **77**:1967-1974.

Burke JM, Sullivan CS. 2017. DUSP11 - An RNA phosphatase that regulates host and viral non-coding RNAs in mammalian cells. *RNA Biol*. **14**(11):1457-1465.

Chang JH, Xiang S, Xiang K, Manley JL, Tong L. 2011. Structural and biochemical studies of the 5'→3' exoribonuclease Xrn1. *Nat Struct Mol Biol*. **18**(3):270-276.

Chang YF, Imam JS, Wilkinson MF. 2007. The nonsense-mediated decay RNA surveillance pathway. *Annu Rev Biochem*. **76**:51-74.

Chapman EG, Costantino DA, Rabe JL, Moon SL, Wilusz J, Nix JC, Kieft JS. 2014. The structural basis of pathogenic subgenomic flavivirus RNA (sfRNA) production. *Science*. **344**(6181):307-310.

Charley PA, Wilusz CJ, Wilusz J. 2018. Identification of phlebovirus and arenavirus RNA sequences that stall and repress the exoribonuclease XRN1. *J Biol Chem*. **293**(1):285-295.

Cheng CP, Jaag HM, Jonczyk M, Serviene E, Nagy PD. 2007. Expression of the Arabidopsis Xrn4p 5'-3' exoribonuclease facilitates degradation of tombusvirus RNA and promotes rapid emergence of viral variants in plants. *Virology*. **368**(2):238-248.

Cheng CP, Serviene E, Nagy PD. 2006. Suppression of viral RNA recombination by a host exoribonuclease. *J Virol*. **80**(6):2631-2640.

Chkuaseli T, Newburn LR, Bakhshinyan D, White KA. 2015. Protein expression strategies in tobacco necrosis virus-D. *Virology*. **486**:54-62.

Chkuaseli T, White KA. 2020. Activation of viral transcription by stepwise largescale folding of an RNA virus genome. *Nucleic Acids Res*. **48**(16):9285-9300.

Choi IR, White KA. 2002. An RNA activator of subgenomic mRNA1 transcription in tomato bushy stunt virus. *J Biol Chem*. **277**(5):3760-3766.

Cimino PA, Nicholson BL, Wu B, Xu W, White KA. 2011. Multifaceted regulation of translational readthrough by RNA replication elements in a tombusvirus. *PLoS Pathog*. **7**(12):e1002423.

Clancy S, Brown W. 2008. Translation: DNA to mRNA to Protein. *Nature Education*. **1(**1):101.

Cooper GM. 2000. Translation of mRNA. In: The cell: a molecular approach. 2nd edition. Sunderland (MA): Sinauer Associates.

Coutts RH, Rigden JE, Slabas AR, Lomonossoff GP, Wise PJ. 1991. The complete nucleotide sequence of tobacco necrosis virus strain D. *J Gen Virol*. **72**:1521-1529.

Decker CJ, Parker R. 2012. P-bodies and stress granules: possible roles in the control of translation and mRNA degradation. *Cold Spring Harb Perspect Biol*. **4**(9):a012286.

Desvoyes B, Faure-Rabasse S, Chen MH, Park JW, Scholthof HB. 2002. A novel plant homeodomain protein interacts in a functionally relevant manner with a virus movement protein. *Plant Physiol*. **129**(4):1521-1532.

Dias HF. 1970. Transmission of cucumber necrosis virus by Olpidium cucurbitacearum Barr & Dias. *Virology*. **40**(4):828-839.

Dilweg IW, Gultyaev AP, Olsthoorn RC. 2019. Structural features of an Xrn1-resistant plant virus RNA. *RNA Biol*. **16**:838-845.

Doma MK, Parker R. 2006. Endonucleolytic cleavage of eukaryotic mRNAs with stalls in translation elongation. *Nature*. **440**(7083):561-564.

Eberle AB, Lykke-Andersen S, Mühlemann O, Jensen TH. 2009. SMG6 promotes endonucleolytic cleavage of nonsense mRNA in human cells. *Nat Struct Mol Biol*. **16**(1):49-55.

Esteban R, Vega L, Fujimura T. 2008. 20S RNA narnavirus defies the antiviral activity of SKI1/XRN1 in Saccharomyces cerevisiae. *J Biol Chem*. **283**(38):25812-25820.

Fang L, Coutts RH. 2013. Investigations on the tobacco necrosis virus D p60 replicase protein. *PLoS One*. **8**(11):e80912.

Flobinus A, Chevigny N, Charley PA, Seissler T, Klein E, Bleykasten-Grosshans C, Ratti C, Bouzoubaa S, Wilusz J, Gilmer D. 2018. Beet necrotic yellow vein virus noncoding RNA production depends on a 5'→3' Xrn exoribonuclease activity. *Viruses*. **10**(3):137.

Flobinus A, Hleibieh K, Klein E, Ratti C, Bouzoubaa S, Gilmer D. 2016. A viral noncoding RNA complements a weakened viral RNA silencing suppressor and promotes efficient systemic host infection. *Viruses*. **8**(10):272.

Frischmeyer PA, van Hoof A, O'Donnell K, Guerrerio AL, Parker R, Dietz HC. 2002. An mRNA surveillance mechanism that eliminates transcripts lacking termination codons. *Science*. **295**(5563):2258-2261.

Garneau NL, Wilusz J, Wilusz CJ. 2007. The highways and byways of mRNA decay. *Nat Rev Mol Cell Biol*. **8**(2):113-126.

Gatfield D, Izaurralde E. 2004. Nonsense-mediated messenger RNA decay is initiated by endonucleolytic cleavage in Drosophila. *Nature*. **429**(6991):575-578.

Gazzani S, Lawrenson T, Woodward C, Headon D, Sablowski R. 2004. A link between mRNA turnover and RNA interference in Arabidopsis. *Science*. **306**(5698):1046-1048.

Gergerich RC, Dolja VV. 2006. Introduction to plant viruses, the invisible foe. In: The plant health instructor.

Gunawardene CD, Donaldson LW, White KA. 2017. Tombusvirus polymerase: structure and function. *Virus Res*. **234**:74-86.

Gunawardene CD, Jaluba K, White KA. 2015. Conserved motifs in a tombusvirus polymerase modulate genome replication, subgenomic transcription, and amplification of defective interfering RNAs. *J Virol*. **89**(6):3236-3246.

Gy I, Gasciolli V, Lauressergues D, Morel JB, Gombert J, Proux F, Proux C, Vaucheret H, Mallory AC. 2007. Arabidopsis FIERY1, XRN2, and XRN3 are endogenous RNA silencing suppressors. *Plant Cell*. **19**(11):3451-3461.

Haimovich G, Medina DA, Causse SZ, Garber M, Millán-Zambrano G, Barkai O, Chávez S, Pérez-Ortín JE, Darzacq X, Choder M. 2013. Gene expression is circular: factors for mRNA degradation also foster mRNA synthesis. *Cell*. **153**(5):1000-1011.

Hansen JL, Long AM, Schultz SC. 1997. Structure of the RNA-dependent RNA polymerase of poliovirus. *Structure*. **5**(8):1109-1122.

Harigaya Y, Parker R. 2010. No-go decay: a quality control mechanism for RNA in translation. *Wiley Interdiscip Rev RNA*. **1**(1):132-141.

Holbrook SR. 2008. Structural principles from large RNAs. *Annu Rev Biophys*. **37**:445-464.

Hollings M, Stone OM, Bouttell GC. 1970. Carnation Italian ringspot virus. *Ann App Biol*. **65**:299-309.

Houseley J, LaCava J, Tollervey D. 2006. RNA-quality control by the exosome. *Nat Rev Mol Cell Biol*. **7**(7):529-539.

Hsu CL, Stevens A. 1993. Yeast cells lacking 5'-->3' exoribonuclease 1 contain mRNA species that are poly(A) deficient and partially lack the 5' cap structure. *Mol Cell Biol*. **13**(8):4826-4835.

Hu W, Sweet TJ, Chamnongpol S, Baker KE, Coller J. 2009. Co-translational mRNA decay in Saccharomyces cerevisiae. *Nature*. **461**(7261):225-229.

Hyodo K, Okuno T. 2016. Pathogenesis mediated by proviral host factors involved in translation and replication of plant positive-strand RNA viruses. *Curr Opin Virol*. **17**:11-18.

Ilyas M, Du Z, Simon AE. 2021. Opium poppy mosaic virus has an Xrn-resistant, translated subgenomic RNA and a BTE 3'CITE. *J Virol*. **95**:e02109-20.

Iwakawa HO, Mizumoto H, Nagano H, Imoto Y, Takigawa K, Sarawaneeyaruk S, Kaido M, Mise K, Okuno T. 2008. A viral noncoding RNA generated by cis-element-mediated protection against 5'->3' RNA decay represses both cap-independent and cap-dependent translation. *J Virol*. **82**(20):10162-10174.

Jaag HM, Nagy PD. 2009. Silencing of Nicotiana benthamiana Xrn4p exoribonuclease promotes tombusvirus RNA accumulation and recombination. *Virology*. **386**(2):344-352.

Jiang S, Jiang L, Yang J, Peng J, Lu Y, Zheng H, Lin L, Chen J, Yan F. 2018. Over-expression of Oryza sativa Xrn4 confers plant resistance to virus infection. *Gene*. **639**:44-51.

Jinek M, Coyle SM, Doudna JA. 2011. Coupled 5' nucleotide recognition and processivity in Xrn1-mediated mRNA decay. *Mol Cell*. **41**:600-608.

Jiwan SD, Wu B, White KA. 2011. Subgenomic mRNA transcription in tobacco necrosis virus. *Virology*. **418**(1):1-11.

Jones CI, Zabolotskaya MV, Newbury SF. 2012. The 5' → 3' exoribonuclease XRN1/Pacman and its functions in cellular processes and development. *Wiley Interdiscip Rev RNA*. **3**(4):455-468.

Jones RA, Steckelberg AL, Vicens Q, Szucs MJ, Akiyama BM, Kieft JS. 2021. Different tertiary interactions create the same important 3D features in a distinct flavivirus xrRNA. *RNA*. **27**(1):54-65.

Kastenmayer JP, Green PJ. 2000. Novel features of the XRN-family in Arabidopsis: evidence that AtXRN4, one of several orthologs of nuclear Xrn2p/Rat1p, functions in the cytoplasm. *Proc Natl Acad Sci U S A*. **97**(25):13985-13990.

Kieft JS, Rabe JL, Chapman EG. 2015. New hypotheses derived from the structure of a flaviviral Xrn1-resistant RNA: conservation, folding, and host adaptation. *RNA Biol*. **12**(11):1169-1177.

Kilchert C, Wittmann S, Vasiljeva L. 2016. The regulation and functions of the nuclear RNA exosome complex. *Nat Rev Mol Cell Biol*. **17**(4):227-239.

Köhler A, Hurt E. 2007. Exporting RNA from the nucleus to the cytoplasm. *Nat Rev Mol Cell Biol*. **8**(10):761-773.

Kovalev N, Pogany J, Nagy PD. 2012. A co-opted DEAD-box RNA helicase enhances tombusvirus plus-strand synthesis. *PLoS Pathog*. **8**(2):e1002537.

Kowalinski E, Kögel A, Ebert J, Reichelt P, Stegmann E, Habermann B, Conti E. 2016. Structure of a cytoplasmic 11-Subunit RNA exosome complex. *Mol Cell*. **63**(1):125-134.

Kraft JJ, Treder K, Peterson MS, Miller WA. 2013. Cation-dependent folding of 3' cap-independent translation elements facilitates interaction of a 17-nucleotide conserved sequence with eIF4G. *Nucleic Acids Res*. **41**(5):3398-3413.

Lakatos L, Szittya G, Silhavy D, Burgyán J. 2004. Molecular mechanism of RNA silencing suppression mediated by p19 protein of tombusviruses. *EMBO J*. **23**(4):876-884.

Langeberg CJ, Welch WRW, McGuire JV, Ashby A, Jackson AD, Chapman EG. 2020. Biochemical characterization of yeast Xrn1. *Biochemistry*. **59**:1493-1507.

Lee CC, Lin TL, Lin JW, Han YT, Huang YT, Hsu YH, Meng M. 2016. Promotion of bamboo mosaic virus accumulation in Nicotiana benthamiana by 5'→3' exonuclease NbXRN4. *Front Microbiol*. **6**:1508.

Li F, Wang A. 2018. RNA decay is an antiviral defense in plants that is counteracted by viral RNA silencing suppressors. *PLoS Pathog*. **14**(8):e1007228.

Luo Y, Na Z, Slavoff SA. 2018. P-bodies: composition, properties, and functions. *Biochemistry*. **57**(17):2424-2431.

MacFadden A, O'Donoghue Z, Silva PAGC, Chapman EG, Olsthoorn RC, Sterken MG, Pijlman GP, Bredenbeek PJ, Kieft JS. 2018. Mechanism and structural diversity of exoribonuclease-resistant RNA structures in flaviviral RNAs. *Nat Commun*. **9**(1):119.

Maxwell ES, Fournier MJ. 1995. The small nucleolar RNAs. *Annu Rev Biochem*. **64**:897-934.

Miller WA, Shen R, Staplin W, Kanodia P. 2016. Noncoding RNAs of plant viruses and viroids: sponges of host translation and RNA interference machinery. *Mol Plant Microbe Interact*. **29**(3):156-64.

Mitchell P, Petfalski E, Shevchenko A, Mann M, Tollervey D. 1997. The exosome: a conserved eukaryotic RNA processing complex containing multiple 3'-->5' exoribonucleases. *Cell*. **91**(4):457-466.

Molnár A, Havelda Z, Dalmay T, Szutorisz H, Burgyán J. 1997. Complete nucleotide sequence of tobacco necrosis virus strain DH and genes required for RNA replication and virus movement. *J Gen Virol*. **78**:1235-1239.

Moon SL, Anderson JR, Kumagai Y, Wilusz CJ, Akira S, Khromykh AA, Wilusz J. 2012. A noncoding RNA produced by arthropod-borne flaviviruses inhibits the cellular exoribonuclease XRN1 and alters host mRNA stability. *RNA*. **18**(11):2029-2040.

Moon SL, Blackinton JG, Anderson JR, Dozier MK, Dodd BJ, Keene JD, Wilusz CJ, Bradrick SS, Wilusz J. 2015a. XRN1 stalling in the 5' UTR of hepatitis C virus and bovine viral diarrhea virus is associated with dysregulated host mRNA stability. *PLoS Pathog*. **11**(3):e1004708.

Moon SL, Dodd BJ, Brackney DE, Wilusz CJ, Ebel GD, Wilusz J. 2015b. Flavivirus sfRNA suppresses antiviral RNA interference in cultured cells and mosquitoes and directly interacts with the RNAi machinery. *Virology*. **485**:322-329.

Moore MJ, Proudfoot NJ. 2009. Pre-mRNA processing reaches back to transcription and ahead to translation. *Cell*. **136**(4):688-700.

Muhammad T, Zhang F, Zhang Y, Liang Y. 2019. RNA interference: a natural immune system of plants to counteract biotic stressors. *Cells*. **8**(1):38.

Nagarajan VK, Jones CI, Newbury SF, Green PJ. 2013. XRN 5'→3' exoribonucleases: structure, mechanisms and functions. *Biochim Biophys Acta*. **1829**(6-7):590-603.

Nagarajan VK, Kukulich PM, von Hagel B, Green PJ. 2019. RNA degradomes reveal substrates and importance for dark and nitrogen stress responses of Arabidopsis XRN4. *Nucleic Acids Res*. **47**(17):9216-9230.

Newburn LR, Nicholson BL, Yosefi M, Cimino PA, White KA. 2014. Translational readthrough in tobacco necrosis virus-D. *Virology*. **450-451**:258-265.

Newburn LR, White KA. 2017. Atypical RNA elements modulate translational readthrough in tobacco necrosis virus D. *J Virol*. **91**(8):e02443-16.

Newburn LR, Wu B, White KA. 2020. Investigation of novel RNA elements in the 3'UTR of tobacco necrosis virus-D. *Viruses*. **12**(8):856.

Nicholson AL, Pasquinelli AE. 2019. Tales of detailed poly(A) tails. *Trends Cell Biol*. **29**(3):191-200.

Nicholson BL, White KA. 2008. Context-influenced cap-independent translation of tombusvirus mRNAs in vitro. *Virology*. **380**(2):203-212.

Nicholson BL, Wu B, Chevtchenko I, White KA. 2010. Tombusvirus recruitment of host translational machinery via the 3' UTR. *RNA*. **16**(7):1402-1419.

Nowakowski J, Tinoco Jr, I. 1997. RNA structure and stability. *Sem Virol*. **8**:153-165.

Offei SK, Coffin RS, Coutts RH. 1995. The tobacco necrosis virus p7a protein is a nucleic acid-binding protein. *J Gen Virol*. **76**:1493-1496.

Orban TI, Izaurralde E. 2005. Decay of mRNAs targeted by RISC requires XRN1, the Ski complex, and the exosome. *RNA*. **11**(4):459-469.

O'Reilly EK, Kao CC. 1998. Analysis of RNA-dependent RNA polymerase structure and function as guided by known polymerase structures and computer predictions of secondary structure. *Virology*. **252**(2):287-303.

Orphanides G, Reinberg D. 2002. A unified theory of gene expression. *Cell*. **108**(4):439-451.

Page AM, Davis K, Molineux C, Kolodner RD, Johnson AW. 1998. Mutational analysis of exoribonuclease I from Saccharomyces cerevisiae. *Nucleic Acids Res*. **26**(16):3707-3716.

Panavas T, Hawkins CM, Panaviene Z, Nagy PD. 2005a. The role of the p33:p33/p92 interaction domain in RNA replication and intracellular localization of p33 and p92 proteins of cucumber necrosis tombusvirus. *Virology*. **338**(1):81-95.

Panavas T, Panaviene Z, Pogany J, Nagy PD. 2003. Enhancement of RNA synthesis by promoter duplication in tombusviruses. *Virology*. **310**(1):118-129.

Panavas T, Pogany J, Nagy PD. 2002. Analysis of minimal promoter sequences for plus-strand synthesis by the cucumber necrosis virus RNA-dependent RNA polymerase. *Virology*. **296**(2):263-274.

Panavas T, Serviene E, Brasher J, Nagy PD. 2005b. Yeast genome-wide screen reveals dissimilar sets of host genes affecting replication of RNA viruses. *Proc Natl Acad Sci U S A*. **102**(20):7326-7331.

Parker R, Song H. 2004. The enzymes and control of eukaryotic mRNA turnover. *Nat Struct Mol Biol*. **11**(2):121-127.

Peltier C, Klein E, Hleibieh K, D'Alonzo M, Hammann P, Bouzoubaa S, Ratti C, Gilmer D. 2012. Beet necrotic yellow vein virus subgenomic RNA3 is a cleavage product leading to stable non-coding RNA required for long-distance movement. *J Gen Virol*. **93**:1093-1102.

Peng J, Yang J, Yan F, Lu Y, Jiang S, Lin L, Zheng H, Chen H, Chen J. 2011. Silencing of NbXrn4 facilitates the systemic infection of tobacco mosaic virus in Nicotiana benthamiana. *Virus Res*. **158**(1-2):268-270.

Petfalski E, Dandekar T, Henry Y, Tollervey D. 1998. Processing of the precursors to small nucleolar RNAs and rRNAs requires common components. *Mol Cell Biol*. **18**(3):1181-1189.

Qiu W, Park JW, Scholthof HB. 2002. Tombusvirus p19-mediated suppression of virus-induced gene silencing is controlled by genetic and dosage features that influence pathogenicity. *Mol Plant Microbe Interact*. **15**(3):269-280.

Ramanathan A, Robb GB, Chan SH. 2016. mRNA capping: biological functions and applications. *Nucleic Acids Res*. **44**(16):7511-7526.

Ray D, Na H, White KA. 2004. Structural properties of a multifunctional T-shaped RNA domain that mediate efficient tomato bushy stunt virus RNA replication. *J Virol*. **78**(19):10490-10500.

Ray D, Wu B, White KA. 2003. A second functional RNA domain in the 5' UTR of the tomato bushy stunt virus genome: intra- and interdomain interactions mediate viral RNA replication. *RNA*. **9**(10):1232-1245.

Schoenberg DR, Maquat LE. 2012. Regulation of cytoplasmic mRNA decay. *Nat Rev Genet*. **13**(4):246-259.

Scholthof HB, Desvoyes B, Kueckler J, Whitehead E. 1999. Biological activity of two tombusvirus proteins translated from nested genes is influenced by dosage control via context-dependent leaky scanning. *Mol Plant Microbe Interact*. **12**(8):670-679.

Scholthof HB, Morris TJ, Jackson AO. 1993. The capsid protein gene of tomato bushy stunt virus is dispensable for systemic movement and can be replaced for localized expression of foreign genes. *Mol Plant Microbe Interact*. **6**:309-322.

Scholthof KB, Scholthof HB, Jackson AO. 1995. The tomato bushy stunt virus replicase proteins are coordinately expressed and membrane associated. *Virology*. **208**(1):365-369.

Serviene E, Shapka N, Cheng CP, Panavas T, Phuangrat B, Baker J, Nagy PD. 2005. Genome-wide screen identifies host genes affecting viral RNA recombination. *Proc Natl Acad Sci U S A*. **102**(30):10545-10550.

Shen R, Miller WA. 2004a. Structures required for poly(A) tail-independent translation overlap with, but are distinct from, cap-independent translation and RNA replication signals at the 3' end of tobacco necrosis virus RNA. *Virology*. **358**(2):448-458.

Shen R, Miller WA. 2004b. The 3' untranslated region of tobacco necrosis virus RNA contains a barley yellow dwarf virus-like cap-independent translation element. *J Virol*. **78**(9):4655-4664.

Slonchak A, Khromykh AA. 2018. Subgenomic flaviviral RNAs: What do we know after the first decade of research. *Antiviral Res*. **159**:13-25.

Souret FF, Kastenmayer JP, Green PJ. 2004. AtXRN4 degrades mRNA in Arabidopsis and its substrates include selected miRNA targets. *Mol Cell*. **15**(2):173-183.

Steckelberg AL, Akiyama BM, Costantino DA, Sit TL, Nix JC, Kieft JS. 2018a. A folded viral noncoding RNA blocks host cell exoribonucleases through a conformationally dynamic RNA structure. *Proc Natl Acad Sci U S A*. **115**(25):6404-6409.

Steckelberg AL, Vicens Q, Costantino DA, Nix JC, Kieft JS. 2020. The crystal structure of a polerovirus exoribonuclease-resistant RNA shows how diverse sequences are integrated into a conserved fold. *RNA*. **26**:1767-1776.

Steckelberg AL, Vicens Q, Kieft JS. 2018b. Exoribonuclease-resistant RNAs exist within both coding and noncoding subgenomic RNAs. *mBio*. **9**(6):e02461-18.

Stevens A, Maupin MK. 1987. A 5'----3' exoribonuclease of Saccharomyces cerevisiae: size and novel substrate specificity. *Arch Biochem Biophys*. **252**(2):339-347.

Stevens A. 1978. An exoribonuclease from Saccharomyces cerevisiae: effect of modifications of 5' end groups on the hydrolysis of substrates to 5' mononucleotides. *Biochem Biophys Res Commun*. **81**(2):656-661.

Stevens A. 1980. Purification and characterization of a Saccharomyces cerevisiae exoribonuclease which yields 5'-mononucleotides by a 5' leads to 3' mode of hydrolysis. *J Biol Chem*. **255**(7):3080-3085.

Stevens A. 2001. 5'-exoribonuclease 1: Xrn1. *Methods Enzymol*. **342**:251-259.

Tesina P, Heckel E, Cheng J, Fromont-Racine M, Buschauer R, Kater L, Beatrix B, Berninghausen O, Jacquier A, Becker T, et al. 2019. Structure of the 80S ribosome-Xrn1 nuclease complex. *Nat Struct Mol Biol*. **26**(4):275-280.

Tollervey D. 2004. Molecular biology: termination by torpedo. *Nature*. **432**(7016):456-457.

Treder K, Kneller EL, Allen EM, Wang Z, Browning KS, Miller WA. 2008. The 3' cap-independent translation element of barley yellow dwarf virus binds eIF4F via the eIF4G subunit to initiate translation. *RNA*. **14**(1):134-147.

Ullmer W, Semler BL. 2016. Diverse strategies used by picornaviruses to escape host RNA decay pathways. *Viruses*. **8**(12):335.

Valencia-Sanchez MA, Liu J, Hannon GJ, Parker R. 2006. Control of translation and mRNA degradation by miRNAs and siRNAs. *Genes Dev*. **20**(5):515-524.

van Hoof A, Frischmeyer PA, Dietz HC, Parker R. 2002. Exosome-mediated recognition and degradation of mRNAs lacking a termination codon. *Science*. **295**(5563):2262-2264.

Varshney D, Spiegel J, Zyner K, Tannahill D, Balasubramanian S. 2020. The regulation and functions of DNA and RNA G-quadruplexes. *Nat Rev Mol Cell Biol*. **21**(8):459-474.

Verma RK, Mishra R, Sharma P, Choudhary DK, Gaur RK. 2014. Systemic infection of potyvirus: a compatible interaction between host and viral proteins. In: Gaur R., Sharma P. editors. *Approaches to plant stress and their management*. Springer, New Delhi.

Vicens Q, Kieft JS. 2021. Shared properties and singularities of exoribonuclease-resistant RNAs in viruses. *Comput Struct Biotechnol J*. **19**:4373-4380.

West S, Gromak N, Proudfoot NJ. 2004. Human 5' --> 3' exonuclease Xrn2 promotes transcription termination at co-transcriptional cleavage sites. *Nature*. **432**(7016):522-525.

White KA, Nagy PD. 2004. Advances in the molecular biology of tombusviruses: gene expression, genome replication, and recombination. *Prog Nucleic Acid Res Mol Biol*. **78**:187-226.

White KA. 2002. The premature termination model: a possible third mechanism for subgenomic mRNA transcription in (+)-strand RNA viruses. *Virology*. **304**(2):147-154.

Wilusz CJ, Wormington M, Peltz SW. 2001. The cap-to-tail guide to mRNA turnover. *Nat Rev Mol Cell Biol*. **2**(4):237-246.

Wolf S, Deom CM, Beachy RN, Lucas WJ. 1989. Movement protein of tobacco mosaic virus modifies plasmodesmatal size exclusion limit. *Science*. **246**(4928):377-379.

Wu B, Vanti WB, White KA. 2001. An RNA domain within the 5' untranslated region of the tomato bushy stunt virus genome modulates viral RNA replication. *J Mol Biol*. **305**(4):741-756.

Xiang S, Cooper-Morgan A, Jiao X, Kiledjian M, Manley JL, Tong L. 2009. Structure and function of the 5'-->3' exoribonuclease Rat1 and its activating partner Rai1. *Nature*. **458**(7239):784-788.

Xu K, Lin J, Zandi R, Roth JA, Ji L. 2016. MicroRNA-mediated target mRNA cleavage and 3'-uridylation in human cells. *Sci Rep*. **6**:30242.

Yamamura Y, Scholthof HB. 2005. Tomato bushy stunt virus: a resilient model system to study virus-plant interactions. *Mol Plant Pathol*. **6**(5):491-502.

Yekta S, Shih IH, Bartel DP. 2004. MicroRNA-directed cleavage of HOXB8 mRNA. *Science*. **304**(5670):594-596.

CHAPTER 2:

A 212-nt Long RNA Structure in the Tobacco Necrosis Virus-D RNA Genome is Resistant to Xrn Degradation"

Previous northern blot analyses of the betanecrovirus TNV-D (family Tombusviridae) showed that a small viral RNA (svRNA) accumulated in plant protoplast infections (Jiwan and White, 2011; doi: 10.1016/j.virol.2011.07.005). This svRNA was small, and detected using a 3'-terminal probe, which, taken together, indicated its origin from the 3'UTR of the TNV-D RNA genome. In a different tombusvirid, RCNMV, stalling of a plant 5'-to-3' exoribonuclease at an exoribonuclease-resistant RNA (xrRNA) structure in the viral RNA genome generated a 3'UTR-derived svRNA that, importantly, facilitated viral infections (Iwakawa et al., 2008; doi: 10.1128/JVI.01027-08). Based on the above observations, a study was initiated to determine the structural and functional details of the TNV-D svRNA.

This chapter is presented in the form of a peer-reviewed, published journal article. The findings of the study demonstrate that a novel xrRNA-like structure present in the 3'UTR of the TNV-D genome stalls Xrn to generate the svRNA; which has proviral functions during TNV-D infections. The article, "**A 212-nt Long RNA Structure in the Tobacco Necrosis Virus-D RNA Genome is Resistant to Xrn Degradation**" by **Chaminda D. Gunawardene, Laura R. Newburn and K. Andrew White** was published in ***Nucleic Acids Research*** on September 26, 2019 (doi: 10.1093/nar/gkz668). I conceptualized and designed the experiments for the study together with Dr. Andrew White. I performed the experiments and generated all of the data except for Figures 1C and 6, which were contributed by my co-author, Laura R. Newburn. I designed and formatted all of the figures, performed all data analyses, and wrote the first draft of the manuscript.

Published online 8 August 2019

Nucleic Acids Research, 2019, Vol. 47, No. 17 ***9329–9342***
doi: 10.1093/nar/gkz668

A 212-nt long RNA structure in the Tobacco necrosis virus-D RNA genome is resistant to Xrn degradation

Chaminda D. Gunawardene, Laura R. Newburn and K. Andrew White*

Department of Biology, York University, Toronto, Ontario, M3J 1P3, Canada

Received December 04, 2018; Revised June 26, 2019; Editorial Decision July 18, 2019; Accepted July 25, 2019

ABSTRACT

Plus-strand RNA viruses can accumulate viral RNA degradation products during infections. Some of these decay intermediates are generated by the cytosolic 5′-to-3′ exoribonuclease Xrn1 (mammals and yeast) or Xrn4 (plants) and are formed when the enzyme stalls on substrate RNAs upon encountering inhibitory RNA structures. Many Xrn-generated RNAs correspond to 3′-terminal segments within the 3′-UTR of viral genomes and perform important functions during infections. Here we have investigated a 3′-terminal small viral RNA (svRNA) generated by Xrn during infections with Tobacco necrosis virus-D (family Tombusviridae). Our results indicate that (i) unlike known stalling RNA structures that are compact and modular, the TNV-D structure encompasses the entire 212 nt of the svRNA and is not functionally transposable, (ii) at least two tertiary interactions within the RNA structure are required for effective Xrn blocking and (iii) most of the svRNA generated in infections is derived from viral polymerase-generated subgenomic mRNA1. *In vitro* and *in vivo* analyses allowed for inferences on roles for the svRNA. Our findings provide a new and distinct addition to the growing list of Xrn-resistant viral RNAs and stalling structures found associated with different plant and animal RNA viruses.

INTRODUCTION

Viruses face hostile cellular environments during infections and their genomes represent key targets for cellular nucleases. The genomes of plus-strand RNA viruses are substrates both for endo- and exoribonucleases (1), and one ribonuclease that engages viral RNAs is the cytosolic enzyme Xrn1 (2). This 5′-to-3′ exoribonuclease plays a major role in eukaryotic cellular mRNA turnover by converting messages into nucleoside monophosphates (3). Access of Xrn1 to the 5′-end of mRNAs requires prior removal of the cap structure, which creates RNAs with 5′-monophosphates, the favored substrate for Xrn1 (4). This exonuclease is highly processive, however G-rich tracts and some RNA structures can impede its progress (5).

Xrn1 is a restriction factor for some plus-strand RNA viruses (6,7), however, in some cases, its activity is beneficial to infections (8,9). An example of this latter role comes from flaviviruses where, during infections, fragments that are 3′-coterminal with their plus-strand RNA genomes, termed subgenomic flavivirus RNAs (sfRNAs), are generated by Xrn1 (10). The fragments that accumulate have well defined 5′-termini and correspond to segments of the 3′-UTRs of flavivirus RNA genomes. SfRNAs have been shown to influence symptoms and to modulate viral infections in different ways, including inhibiting host Xrn1 exoribonuclease and muting the host immune response (11). The formation of sfRNAs relies on the presence of RNA sequences which form higher-order RNA structures that cause Xrn1 to stall (12–14). Notably, the atomic structures of the stalling RNAs in two flaviviruses, Murray Valley encephalitis virus and Zika virus, have been solved (15,16). These structures revealed similar complex folds which form RNA-based braces that block Xrn1 progression. Additional analyses revealed that these structures also stall other 5′-to-3′ exonucleases, suggesting a general barrier-based mechanism for hindering nuclease movement (17). This phenomenon of Xrn1 stalling and generating distinct virally-derived 5′-ends extends beyond flaviviruses. Xrn1-resistant RNAs have also been identified in other mammalian RNA viruses such as Hepatitis C virus and Bovine viral diarrhea virus (18), as well as phleboviruses and arenaviruses (19). However, the structural nature of the RNA elements responsible for these stalling events remains undetermined.

In plants, cytosolic Xrn4 is the functional equivalent of Xrn1 (20) and can either restrict (6,21) or facilitate infections (8). Similar to flaviviruses, small virally-derived 3′-terminal fragments from different plus-strand RNA plant viruses have been reported (22) and those associated with luteoviruses are among the earliest described (23–25). The origin of these luteovirus small RNAs is currently unknown, but they may be products of Xrn4 activity during plant infections. There are, however, two plant viruses,

*To whom correspondence should be addressed. Tel: +1 416 736 5243; Fax: +1 416 736 5698; Email: kawhite@yorku.ca

Beet necrotic yellow vein virus (BNYVV; genus Benyvirus, family Benyviridae) and Red clover necrotic mosaic virus (RCNMV; genus Dianthovirus, family Tombusviridae), for which generation of Xrn-resistant RNAs have been confirmed. Non-coding RNA3 (ncRNA3), is derived from genome segment RNA3 of BNYVV and is required for long-distance movement of infections in plants (26,27). NcRNA3 production *in vitro* by recombinant Xrn1 involves a 43 nt segment that forms two hairpin structures separated by a spacer sequence (28). In RCNMV, the RNA1-derived fragment that accumulates is termed SR1f, and it facilitates plant infections, possibly by regulating viral translation, replication, or packaging (29). For RCNMV, a 43 nt long sequence is also needed for Xrn1 stalling, but its sequence is distinct from that in BNYVV (30). The crystal structure of the RCNMV stall signal inferred an RNA fold that could act as a brace against Xrn4, however, its conformation is distinct from those found in flaviviruses (30).

In addition to RCNMV, small 3′-terminal, genome-derived, RNAs have been reported for other members of the family Tombusviridae, but they have not been characterized (31–34). This group includes Tobacco necrosis virus-D in the genus Betanecrovirus, which has a ∼3.8 kb plus-strand RNA genome that is packaged into an icosahedral particle (35). The genome is neither 5′-capped nor 3′-poly(A) tailed and encodes five open reading frames (ORFs) (Figure 1A). Upon infection, the accessory replication protein (p22) and its readthrough product (p88), the RNA-dependent RNA polymerase, are translated directly from the genome (36,37). Translation is mediated by an RNA structure in the 3′-untranslated region (3′-UTR) termed the 3′ cap-independent translational enhancer (3′-CITE), which functions by binding to eukaryotic initiation factor 4G (eIF4G) (38,39). The 3′-CITE also supports translation of two subgenomic (sg) mRNAs that are transcribed during infections (32). Two small proteins that mediate virus movement within the plant, p7a and p7b, are expressed from the larger sg mRNA1, while the viral capsid protein (CP) is translated from sg mRNA2 (40) (Figure 1A).

Here, a 3′-terminal small viral RNA (svRNA) associated with TNV-D infections was investigated. The results indicate that it is generated by Xrn4 digestion and that a complex RNA structure is involved in the stalling event leading to its formation. Possible functions of this svRNA are investigated and discussed.

MATERIALS AND METHODS

TNV-D constructs

The full-length infectious TNV-D clone (GenBank D00942.1) has been reported previously (35), and all mutants were derived from this construct. The TNV-D sg mRNA1 (initiating at genome coordinate 2216) and sg mRNA2 (coordinate 2557) clones were generated as described previously (40). Standard overlapping PCR-based mutagenesis was used to introduce mutations into the genomic or subgenomic RNA clones of TNV-D. All clones were sequenced to ensure the presence of only the intended modifications.

In vitro transcription and viral RNAs

All RNA transcripts were generated by *in vitro* transcription of either SmaI-linearized clones or 3′-ends that were delineated by PCR-products, as described previously using a T7-FlashScribe transcription kit (41). Capped luciferase and wasabi mRNAs were transcribed from linearized expression vector using an AmpliCap-Max T7 Transcription Kit. Transcript integrity was verified by agarose gel electrophoresis prior to use. Transcript 50-svRNA, included the fifty contiguous viral nucleotides 5′-proximal to the primary Xrn termination site and was used for in-line probing and Xrn1 inhibition assays.

Protoplast infections and northern blot analysis

Protoplasts were isolated from 6- to 7-day-old cucumber cotyledons as described previously (42). Following isolation, 3×10^5 protoplasts were transfected with 5 μg of genomic TNV-D transcripts, mediated by PEG-$CaCl_2$. Transfected protoplasts were incubated under constant light for 22 h at 22°C. Total nucleic acids were phenol extracted and ethanol precipitated, after which one-sixth of the preparation was separated in 2% agarose gels and transferred to nylon membrane. Northern blot analysis was carried out using two internally-labeled ^{32}P-labeled DNA oligonucleotide probes that were complementary to two different regions of the 3′-UTR of TNV-D that did not overlap with regions containing nucleotide substitutions in mutants: GA CTGGGTTCCTAGAGAGATCTCTAGGTAAATAAAG AGGGGAC-3′(−), complementary to the 3′-terminal 39 nts of the viral genome (coordinates 3725–3763, underlined), and GTGATACGACGGCCCACCACCACAGT GAGCCCGTTAAACCTGTTTCCCAGGATCC-3′(−) complementary to the apical sequence of the BTE structure (coordinates 3592–3646). Both probes were used for all northern blot analyses, except for the BTE truncation mutants, where only the 3′-terminal probe was used (due to overlap between the BTE deletions and the BTE-targeted probe) (36). Probes were generated using Klenow fragment (NEB Cat# M0210L) using primer/template pairs. 3′-Terminal probe: template (+)5′-GTCCCCTCTT TATTTACCTAGAGATCTCTCTAGGAACCCAGTC and primer (−)5′-GACTGGGT. BTE-targeted probe: template: (+)5′-GGATCCTGGGAAACAGGTTTAACG GGCTCACTGTGGTGGTGGGCCGTCGTATCAC and primer (−)5′-GTGATACG). Probes were synthesized using 5 U of Klenow fragment in the presence of [α-^{32}P]-dATP and unlabeled CTP, GTP and TTP for 1 h at 25°C. Labeling reactions were stopped using 20 mM EDTA and purified via G50 sephadex columns. All protoplast infection experiments were repeated three times.

In vitro Xrn1 digestion assay

Purified Xrn1 from *Saccharomyces cerevisiae* was obtained from New England Biolabs (NEB) (Cat# M0338L). Buffer conditions for reactions were followed as described previously (14). Briefly, 2 μg of wild-type (wt) or mutant sg mRNA1 were incubated in 1× EC3 buffer (100 mM NaCl, 10 mM $MgCl_2$, 50 mM Tris, pH 7.9, 1 mM DTT) with 0.5

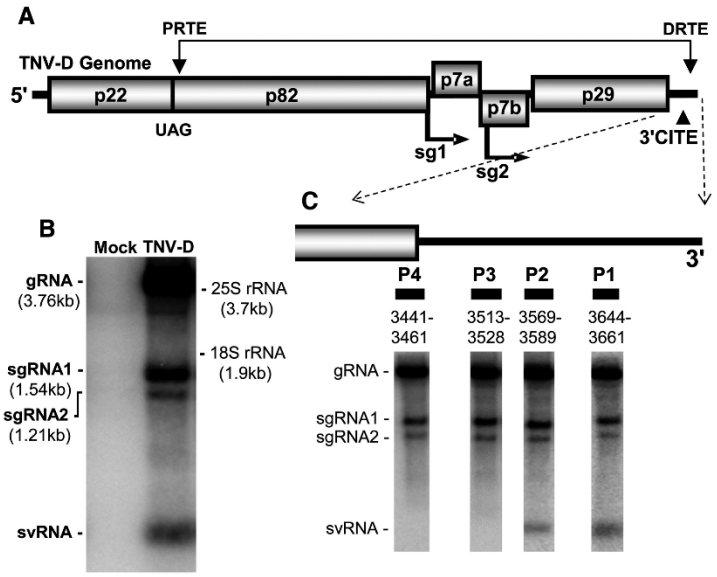

Figure 1. TNV-D genome and identification of svRNA. (**A**) Schematic representation of the TNV-D genome with encoded proteins shown as rectangles. The initiation sites of the two subgenomic (sg) mRNAs are marked below by arrows. Positions of the 3′-cap-independent translation enhancer (3′-CITE) and the complementary proximal and distal readthrough elements (PRTE and DRTE, respectively) are also shown. (**B**) Northern blot of TNV-D infection in plant protoplasts. Total RNA was separated in 2% agarose gels, transferred to nylon membrane and hybridized with ^{32}P-labelled oligonucleotides complementary to different 3′-regions of the TNV-D genome. The positions of genomic (g), subgenomic (sg) and small viral (sv) RNAs in the blots are identified to the left. The position and sizes of relevant RNAs are also shown. (**C**) Northern blot delineating the approximate 5′-end of the svRNA. The relative genomic positions of the probes (P1 to P4) are shown along with their corresponding genome coordinates.

U Xrn1 and 4 U RppH (derived from *Escherichia coli*, obtained from NEB, Cat# M0356S) in the presence of 20 U RNase inhibitor in a volume of 23 μl at 37°C for 30 min. RNA was ethanol precipitated with 20 mg glycogen and 0.2 M ammonium acetate, and dissolved in RNase-free water. Two-fifths of the RNAs recovered was separated in 2% agarose gels and transferred to nylon membrane for northern blot analysis. The signal strengths from bands were quantified using QuantityOne software. All assays were repeated three times. The level of resistant svRNA was calculated as a ratio: i.e. the level of resistant RNA divided by the level of untreated precursor, which was set as 100%. Representative northern blots used for quantification of svRNAs in Figures 3D and 4A are provided in Supplemental Material.

5′-RACE

RNAs extracted from TNV-infected protoplasts or generated by digestion with Xrn1 *in vitro* were separated in 2% agarose gels. Bands corresponding to the svRNA were excised as gel slices and the extracted RNA was ligated to an oligonucleotide adaptor sequence containing an SbfI site (bold): 5′-GATCTGCAGCTTGAG**CCTGCA GG**GTGCTGCGCAGAGTTCTACAGTCCGAC using T4 RNA ligase (NEB). RT-PCR was carried out using a reverse primer complementary to the genome 3′-terminus (underlined) and containing a SalI site (bold), 5′-GCAGCA C**GTCGAC**GGGTTCCTAGAGAGATCTCTAGG, and nested primer 5′-GCAGCTTGAGCCTGCAGGGTGC. PCR products were double-digested with SbfI and SalI and ligated into a pUC19 vector, cloned into *E. coli*, and individual clones were sequenced.

In-line probing

Wt and mutant 50-svRNAs were transcribed *in vitro*. Following 5′-end-labeling using [γ-^{32}P]-ATP, RNAs were incubated for ∼40 h at 25°C and then separated in 10% sequencing gels (43). The signal strengths from bands in each lane were quantified using QuantityOne software and plotted together.

In vitro translation competition assay

Uncapped wt TNV-D genomic (0.1 pmol), sg mRNA (0.2 pmol), capped reporter luciferase mRNA or wasabi mRNA (0.2 pmol) (Luciferase-pcDNA3, pTcI-Wasabi, obtained from Addgene) were incubated with increasing molar excesses (1:1 ratio up to 1:64) of uncapped wt svRNA or a size-matched uncapped RNA control, derived from pUC19, 5′-CUGGCGAAAGGGGGAUGUGCUGCAAGGCGA UUAAGUUGGGUAACGCCAGGGUUUUCCCAG UCACGACGUUGUAAAACGACGGCCAGUGAA UUCGAGCUCGGUACCCGGGGAUCCUCUAGA GUCGACCUGCAGGCAUGCAAGCUUGGCGUAAU CAUGGUCAUAGCUGUUUCCUGUGUGAAAUU GUUAUCCGCUCACAAUUCCACACAACAUAC, in a wheat germ extract translation system (Promega) (36). Reactions of 20 μl included 10 μl wheat germ extract and were incubated at 25°C for 2 h.

In vitro Xrn1 inhibition assay

A Xrn1-sensitive, 50 nt long, non-viral reporter RNA (Rep) 5′-GGAACAGACAGACAUACAGACGCAGA CACACACACACACACACACACACA, was used to assess the protective effect of (i) wt 50-svRNA, (ii) a mutant 50-svRNA (50-S6C) or, (iii) a size-matched, non-viral RNA sequence (NS) derived from pUC19 (i.e. the size-matched sequence provided in previous section plus the following 50 nt sequence added to its 5′-end: GAGCCGGAAGCAUAAAGUGUAAAGCCUGGG GUGCCUAAUGAGUGAGCUAA). Rep and competitor RNAs were *in vitro* transcribed with a 10-fold molar excess of GMP over GTP to generate transcripts with 5′-monophosphates, thereby obviating the need to add RppH, which could potentially be rate limiting for Xrn1 activity. Mixtures of the Rep RNA (3 ng) and each of the competitor RNAs [(i), (ii) or (iii); 1 μg each] were incubated for 1 min in the absence or presence of 1 U Xrn1 at 37°C. Upon completion of the reactions, RNA was phenol extracted, ethanol precipitated, separated in a 2% agarose gel, transferred to nylon membrane, and probed for Rep RNA.

Whole plant infections and particle isolation

Three week old *Nicotiana benthamiana* plants were rub-inoculated with transcripts of either wt or mutant genomic TNV-D RNAs as described previously (44). Plants were incubated at 23°C with a 14 h/10 h day/night cycle until developing visible symptoms (~6 days). Three plants were inoculated for each viral construct per experiment, and each experiment was repeated three times. RNA was extracted from symptomatic inoculated or upper leaves and analyzed by northern blotting. For virion preparations, plants were inoculated and incubated as described above. Virus particles were prepared from systemically-infected leaf tissue via PEG precipitation (45) and RNAs extracted from virus particles were analyzed by northern blotting as described earlier.

RESULTS

TNV-D infections contain a 3′-terminal small viral RNA

Infections of cucumber protoplasts with wt TNV-D were examined for the accumulation of viral RNAs using a probe complementary to the very 3′-terminus of the viral genome. Northern blot analysis revealed that, in addition to the expected genome and two sg mRNAs, a small viral RNA (svRNA) was detected consistently (Figure 1B). To assess how much sequence from the 3′-terminus was present in the svRNA, additional oligonucleotide probes were utilized that spanned more upstream regions of the 3′-UTR and extended into the adjacent p29 capsid-coding region. This analysis indicated that the 5′-end of the svRNA mapped between oligos-3 and -2, with the intervening sequence corresponding to genome coordinates 3528–3569 (Figure 1C). Based on these results, the size of the svRNA was estimated to be between 195 and 235 nt in length, a size consistent with its high mobility in agarose gels.

The svRNA is analogous to the products of Xrn1-digested TNV-D RNAs

The presence of Xrn1-generated 3′-terminal fragments in other plus-strand RNA virus infections prompted us to investigate the same possibility for the TNV-D svRNA. Accordingly, *in vitro* transcripts of TNV-D genomic and sg mRNAs were individually subjected to recombinant yeast Xrn1 in the presence of pyrophosphohydrolase RppH, which converts 5′-triphosphates in the transcripts to 5′-monophosphates (14). In this assay, all three viral species that were subjected to Xrn1 and RppH yielded an RNA product that comigrated to the same position as the svRNA generated in protoplast infections (Figure 2A, middle and right sections). When the 5′-termini of Xrn1-generated RNAs and *in vivo*-generated svRNA were cloned and sequenced by 5′-RACE (Figure 2B), the most frequent positions mapped to two adjacent nucleotides located just 5′-proximal to the basal stem structure of the 3′-CITE; corresponding to genomic coordinates 3552 and 3553 (Figure 2C, green asterisks). 5′-termini at these positions would yield svRNAs of lengths 211 and 212 nts, which are within with the size range estimate of 195–235 nt determined by oligonucleotide probing (Figure 1C). This equivalence in gel mobility and 5′-termini location between *in vitro*-generated small RNAs and *in vivo*-generated svRNAs is consistent with the latter being produced by plant Xrn4, the counterpart to yeast Xrn1 (28). These results also indicate that no *trans*-acting cellular or viral proteins are required for this process to occur.

svRNAs are derived primarily from sg mRNA1

In flaviviruses, which do not produce traditional protein-coding sg mRNAs, the lone source of Xrn-resistant RNAs is the viral genome. However, for TNV-D, which synthesizes two sg mRNAs during infections, either or both messages could contribute to production of svRNAs in infections. To examine this possibility, genomic mutants were assessed that were deficient in transcription of either sg mRNA1 or sg mRNA2, due to point mutations in their initiating nucleotides (Figure 2D). Inhibition of sg mRNA1 transcription resulted in a large decrease in svRNA accumulation in protoplasts, while inactivation of sg mRNA2 had nominal effects. Accordingly, most of the svRNA that accumulates during infections is derived from sg mRNA1.

Structural and functional features of the svRNA

The 3′-region of the TNV-D genome has been well characterized, both structurally and functionally. The major Xrn1-resistant fragment corresponds to a 212 nt long 3′-terminal segment that contains several functional subregions (Figure 2C). At the 5′-end is the 3′-CITE, which is composed of an extended stem structure topped by two stem-loops (SLs) (38,39,46). Just downstream from the 3′-CITE are

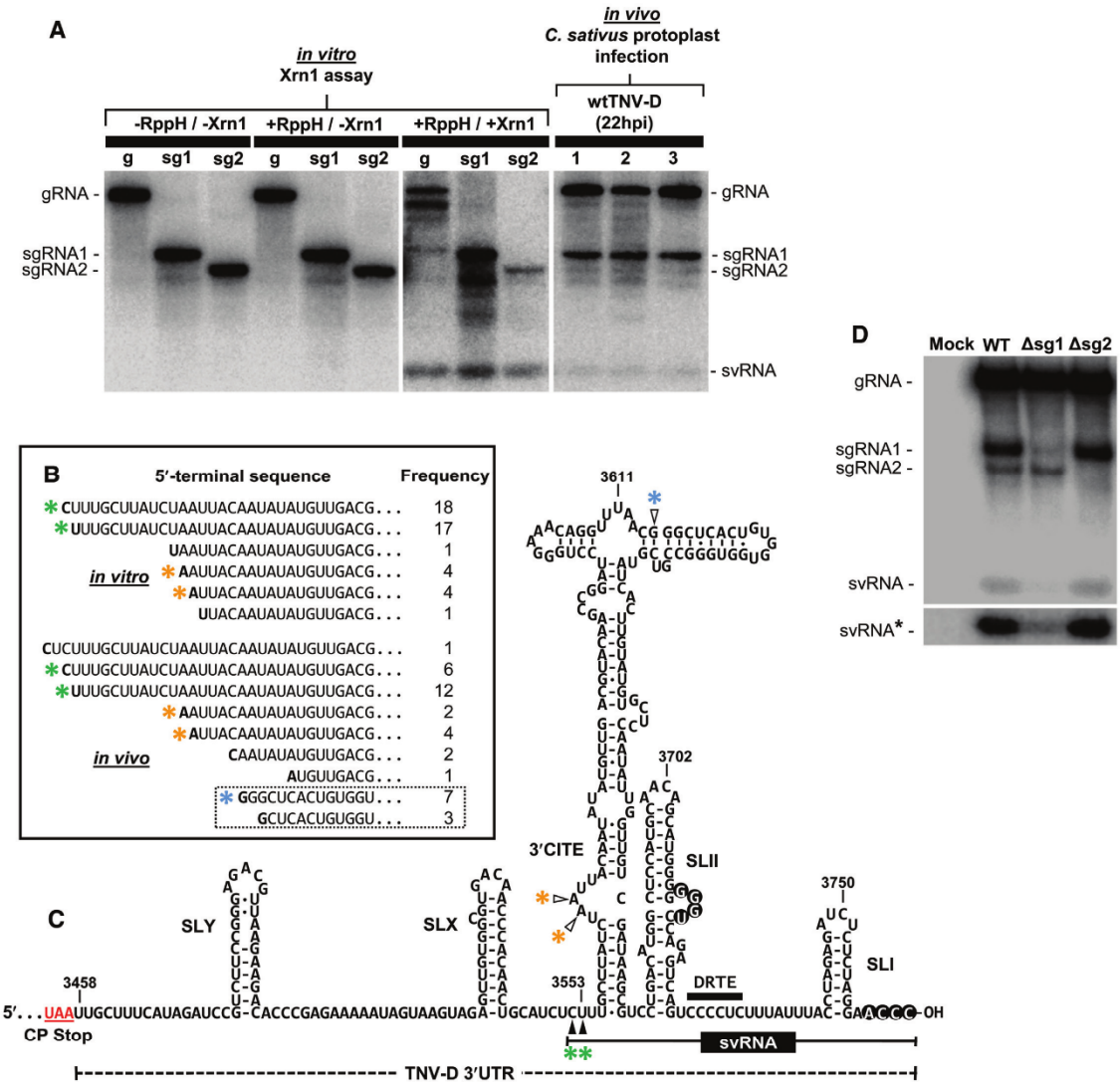

Figure 2. Comparison of *in vitro* and *in vivo*-generated svRNAs. (**A**) Northern blot comparing *in vitro*-derived svRNA produced by Xrn1 and svRNAs produced in protoplast infections. Treatment of viral RNA transcripts with (+) or without (−) RppH and Xrn1 are indicated above the lanes. All sections shown are from the same gel. (**B**) 5′-RACE analysis of svRNAs produced by Xrn1 (*in vitro*) and svRNAs produced in protoplast infections (*in vivo*). 5′-terminal sequences are shown with their corresponding frequency of occurrence. The dotted box encloses minor stall sites with 5′-ends that originate further downstream than the other sequences shown and are not aligned with those sequences above. (**C**) Secondary structure of the 3′-UTR of TNV-D. Substructures, including SLI, SLII and the 3′-CITE are indicated. Colour-coded asterisks correspond to 5′ nucleotide positions from sequence termini shown in (B). The major svRNA species (i.e. 211–212) is indicated below the structure. Complementary nucleotides in SLII and the 3′-terminus that functionally base pair are circled. (**D**) Northern blot analysis of protoplast infections of TNV-D genomes with inactivated sg mRNA1 (Δsg1) or sg mRNA2 (Δsg1) promoters. The lower panel labelled svRNA* is a longer exposure of the svRNA-containing portion of the blot above.

two hairpins, SLII and SLI. Both stem loops are critical for genome replication, as is a base pairing interaction between the 3′-terminal four nucleotides and an internal bulge in SLII (Figure 2C, circled nucleotides) (37). These two hairpins flank a 6 nt long sequence, the distal readthrough element (DRTE), which can base pair with a complementary proximal RTE (PRTE) that is present in an RNA structure 3′-adjacent to the p22 stop codon. This RNA-RNA interaction mediates translational readthrough resulting in production of p82 (Figure 1A) (36). The svRNA thus contains regulatory elements involved in translation initiation, translational readthrough, and genome replication.

Terminal regions of svRNA contain determinants of Xrn1 resistance

To examine structural features important for svRNA production we utilized transcripts of sg mRNA1 as an *in vitro* substrate for Xrn1, which, on average, generated 4.3%

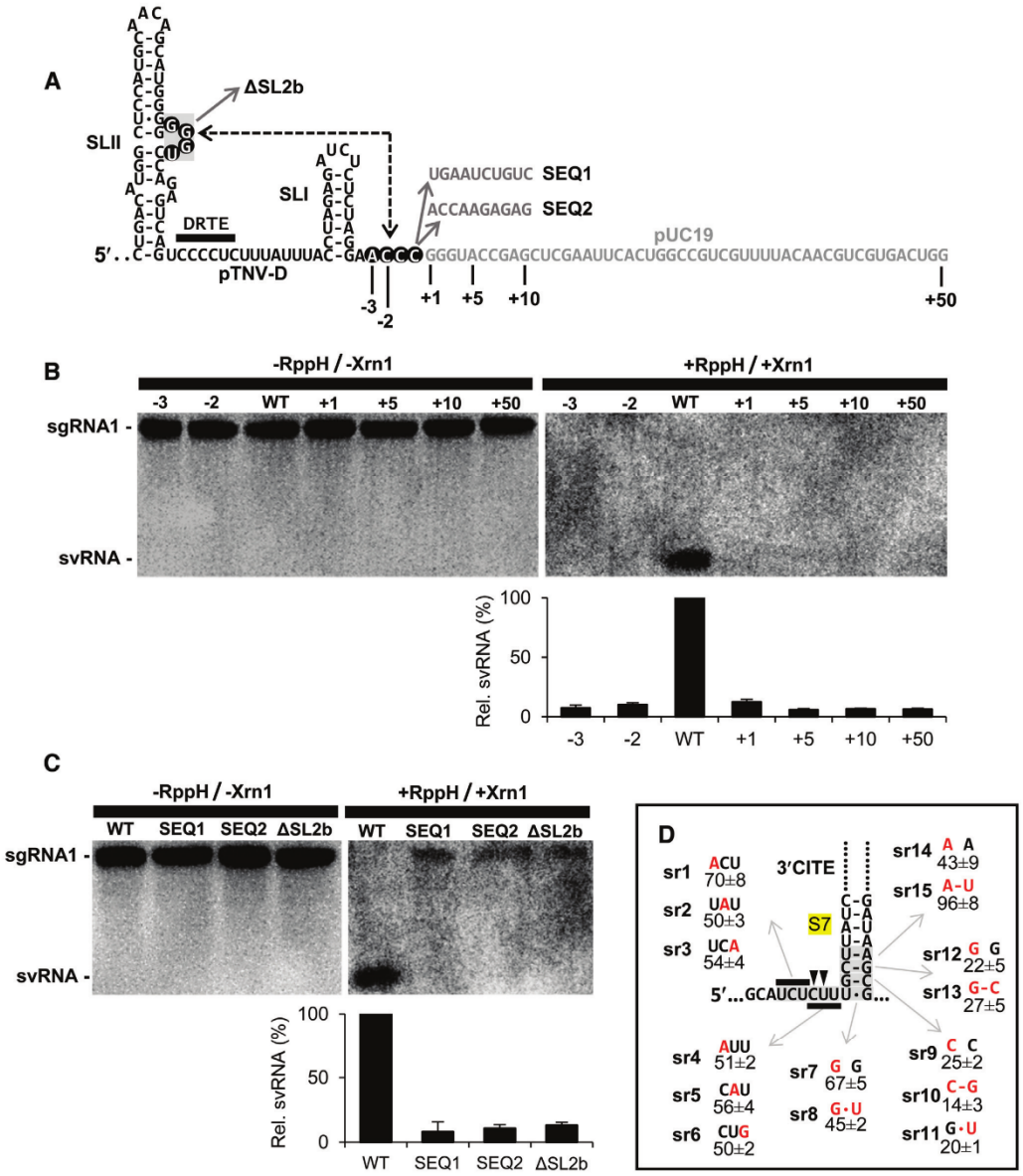

Figure 3. Mutational analysis of the 5′- and 3′-terminal regions of the svRNA in sg mRNA1. (**A**) Nucleotides were either added (from pUC19) or deleted from the 3′-end of TNV-D sg mRNA1. The SLII/3′-end interaction important for genome replication is indicated with dotted arrows. Modifications and the associated mutant names are shown. (**B** and **C**) *In vitro* Xrn1 assay of sg mRNA1 mutants depicted in (A). The substrate and product RNA species are labelled to the left, and a bar graphs below the blots quantify corresponding svRNA levels from three independent experiments, ±SE. (**D**) Mutational analysis of the 5′-terminal region of svRNA in sg mRNA1. Substitutions in each mutant are shown in red along with relative levels of accumulation of svRNAs (from three independent experiments, ±SE). Stem 7 (S7) of the 3′-CITE is highlighted in yellow. Black arrowheads indicate the primary Xrn1 stall sites.

svRNA (±0.7%, $n = 10$) from a reactant pool of sg mRNA1 set as 100%. An interesting feature of previously reported Xrn-blocking viral RNA structures is their modularity, whereby they are still functional when introduced into new sequence contexts (14,29). To assess this aspect of function, the normal 3′-terminus of sg mRNA1 was extended by one, five, ten, or fifty nucleotides of adjacent plasmid sequence (Figure 3A). Two other 10 nt 3′-terminal extensions of differing nucleotide order and composition, mutants SEQ1 and SEQ2, were also assessed, in addition to another mutant, ΔSL2b, containing a deletion of the bulge in SLII (Figure 3A). Transcripts were also produced that lacked two or three nucleotides from the 3′-end. When these viral RNAs were assayed for svRNA production *in vitro*, all modifications resulted in greatly decreased levels of svRNA (Figure 3B and C). Accordingly, small and large indels at

the 3′-terminus of the substrate RNA have major effects on its ability to stall Xrn1; as did deletion of the bulge in SLII, which is the base pairing partner sequence for the 3′-terminus (Figure 3A).

The 5′-terminus of the primary svRNA corresponds to the 5′-border of the 3′-CITE. This position would also be the location of the Xrn1 active site when the enzyme is stalled, and nearby nucleotide residues and/or RNA structures are predicted to affect this event. The substitution of single nucleotides positioned before, within, or after the major stall sites had varying effects (Figure 3D). Those changes corresponding to the region in front of (mutants sr1 to sr3) or at (sr4 and sr5) the stall sites reduced svRNA production to ∼50–70% that of wt levels, while the majority of those mapping within the closing stem of the 3′-CITE (sr7 to sr15) had more substantial negative effects (Figure 3D). For example, two of the four single substitutions in the left half of this closing stem (i.e. sr9 and sr12) caused drops in accumulation to 22% and 25% that of wt, with no or low recovery in corresponding compensatory mutations (Figure 3D). When combined with the results from analyses of the 3′-terminus, the data indicate that both ends of the svRNA contribute notably to Xrn1 stalling.

Internal regions of the svRNA confer Xrn1 resistance

The largest structural component within the svRNA is the 3′-CITE. Based on the results presented in the previous section, the closing stem of this structure, S7 (Figure 4A), is important for Xrn1 stalling. To assess the possible involvement of other parts of the 3′-CITE, truncations were designed in an sg mRNA1 substrate that progressively removed upper sections of the structure and replaced them with a terminal ultra-stable cUUCGg tetraloop (47). Deletion of upper portions in mutants ΔTop and Midi resulted in reduced levels of svRNA (∼57% and 38% of wt) (Figure 4A, green). Removal of additional structure in Mini markedly reduced svRNA accumulation (∼3% of wt), implicating the midsection of the 3′-CITE as particularly important for stalling.

Next, the structural requirements within the mid and lower regions of the 3′-CITE were investigated in more detail. Substitutions in stem 4 in mutant series S4 resulted in moderate effects that supported a role for base pairing, while those in stem 5 (series S5) had similar effects without implicating base pairing as being important (Figure 4A). Compensatory mutation sets in lower stems 6 and 7 in mutant series S6 and S7 yielded major defects in svRNA levels (i.e. down to ∼10%) and restoration of base-pairing did not recover function. Changes to the asymmetrical loop between stems 6 and 7 in series IL6, and mismatches between stems 5 and 6 in series IL5, also notably inhibited activity (∼17–23% and ∼21–57%, respectively), while perturbation of another helical interruption further up the structure in mutant ΔGCUC was well tolerated (99%) (Figure 4A). These results agree with those from internal truncations of the 3′-CITE and Figure 3C, with all findings implicating the lower region of the 3′-CITE as most important for Xrn1 stalling activity.

SLII was also investigated for possible involvement with Xrn1 stalling activities. Compensatory mutational analysis indicated that base pairing in the lower (m106, m107 and m108), middle (m135, m136 and m137), and near-upper regions (m132, m133, and m134; and m129, m130 and m131) of SLII contributed to its function, albeit to differing degrees (Figure 4A). Restoration of canonical complementarity in the base pair closing the terminal loop, did not improve svRNA production (mutants m126, m127 and m128). Also notable, was that any of eight different changes made in the terminal loop of SLII caused major decreases in svRNA production (∼14–29% of wt) (Figure 4A). Collectively, the results from examining the internal sections of the svRNA implicate SLII and the mid/lower part of the 3′-CITE as highly important elements for stalling Xrn1.

Regions within the svRNA that were required for efficient svRNA production, and which appeared to be highly dependent on sequence specificity, included the lower region of the 3′-CITE (i.e. stems 6 and 7 and their intervening internal loop) and the upper region of SLII (i.e. its terminal loop region). Accordingly, we examined the structural consequences of certain modifications in these regions by in-line probing, a solution structure analysis method that identifies flexible residues in an RNA by their propensity to undergo spontaneous cleavage (43). The viral RNAs analyzed were based on 50-svRNA, which, in addition to the svRNA sequence, contains fifty contiguous viral nucleotides 5′-proximal to the primary Xrn termination site. Like sg mRNA1, this 50-svRNA is a substrate for Xrn1, but, because its 5′-end is much closer to the stall site, analysis of reactivity in this region was more feasible. For mutant m20, which contained an AACA to GAAA substitution of the SLII terminal loop sequence and exhibited ∼29% activity, spontaneous RNA cleavage was notably increased in the region of the modified loop (Figure 4B, top trace, red asterisk) when compared to the wt control (Figure 4B, bottom trace). This suggests that these terminal loop residues are normally inflexible in the wt structure and thus may interact with other residues. Interestingly, the same loop modification also led to a small, but reproducible, increase in reactivity in the 5′-half of S6 and the adjacent asymmetrical internal loop region of the 3′-CITE (Figure 4B, top trace, green asterisk), when compared to the wt control. This result implies a structural connection between the SLII terminal loop and the lower half of the extended helix of the 3′-CITE. This notion was further supported by the analyses of mutants S6C (∼14% activity) and IL6C (∼17% activity), containing perturbations in the S6 and adjacent asymmetrical internal loop region of the 3′-CITE (Figure 4B, second and third traces, red asterisks), which induced prominent cleavages in the SLII loop region (Figure 4B, second and third traces, green asterisks). In contrast, mutant sr10 (∼14% activity) at the base of the 3′-CITE did not cause notable cleavage in the SLII loop or elsewhere. The coupled structural effects observed for mutants m20, S6C and IL6C suggest that the loop of SLII needs to interact with the lower region of the 3′-CITE to form an effective blocking structure.

Comparison of Xrn1 sensitivity *in vitro* with svRNA accumulation in virus infections

To assess how closely *in vitro* results reflected those from *in vivo* studies, several mutations that were assayed for Xrn1

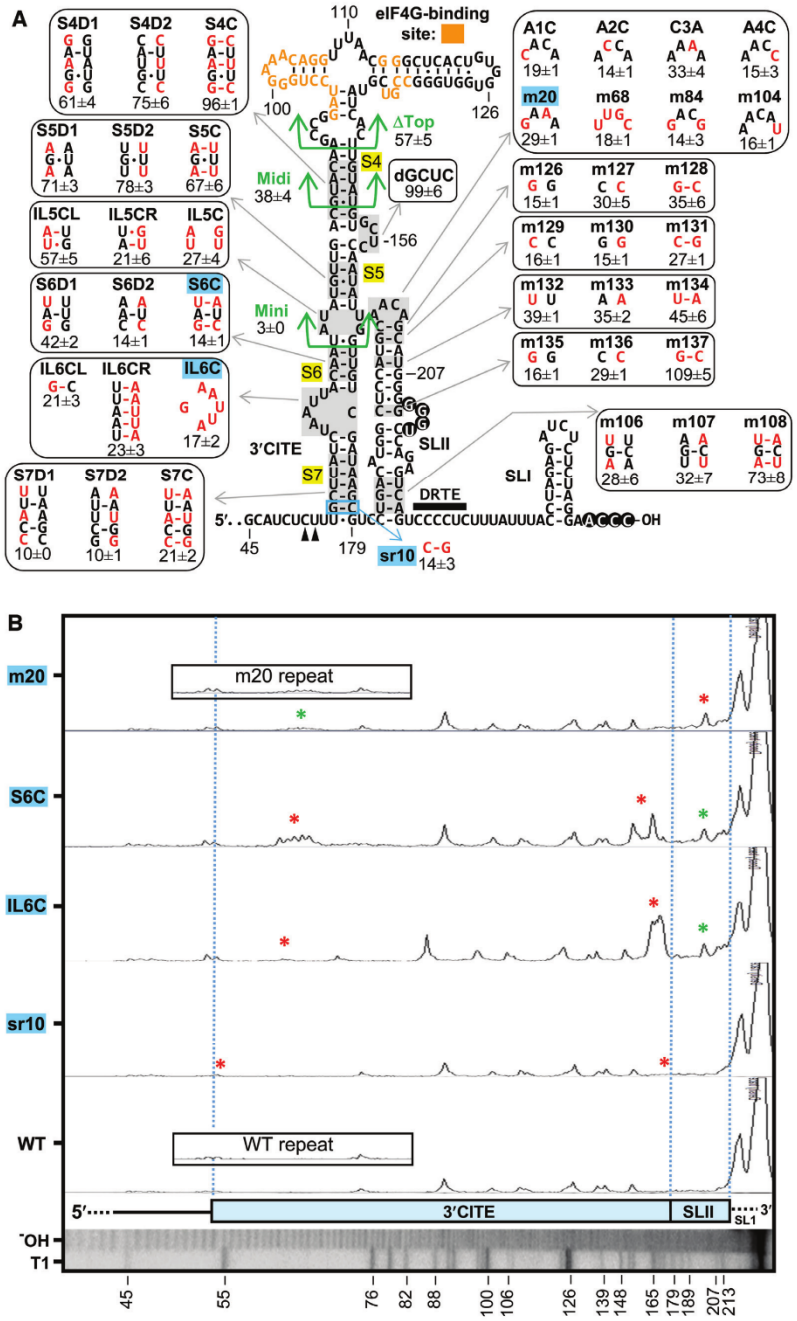

Figure 4. Mutational analysis of internal regions of the svRNA in sg mRNA1 and RNA structural analysis of selected 50-svRNA mutants defective at generating svRNAs. (**A**) Summary of *in vitro* Xrn1 assays of sg mRNA1 mutants containing substitutions or deletions in the 3′-CITE and SLII. Nucleotide substitutions in mutants are shown in red and deleted regions are outlined in green. The nucleotides in the 3′-CITE shown previously to interact with the translation factor eIF4G are shown in orange (39). Stems in the 3′-CITE are highlighted in yellow and numbered (S4 through S7). Mutants assessed by in-line probing in (B) are highlighted in blue. The primary stall sites are marked with black arrowheads below the structure. Results are from three independent experiments, ±SE. (**B**) In-line probing of svRNA-deficient mutants. The mutants assessed are shown in (A) and are highlighted in blue. *In vitro* transcripts of wt and mutant 50-svRNAs were used in the analysis and RNA reactivity for each sample was graphed. Alkaline hydrolysis (⁻OH) and T1 nuclease-treated (T1) lanes are shown along with numbering of corresponding G residues. Also shown below the profiles is a schematic depicting relevant substructures in the RNA and blue dotted lines indicate border locations of the 3′-CITE and SLII. Red asterisks indicate the positions of the modifications introduced and green asterisks indicate second-site changes in reactivity observed elsewhere in the structure. Independent repeats are shown in the insets for m20 and wt. Note that peaks in the 3′-CITE region of IL6C are shifted to the left due to the transposition of different numbers of residues in this mutant.

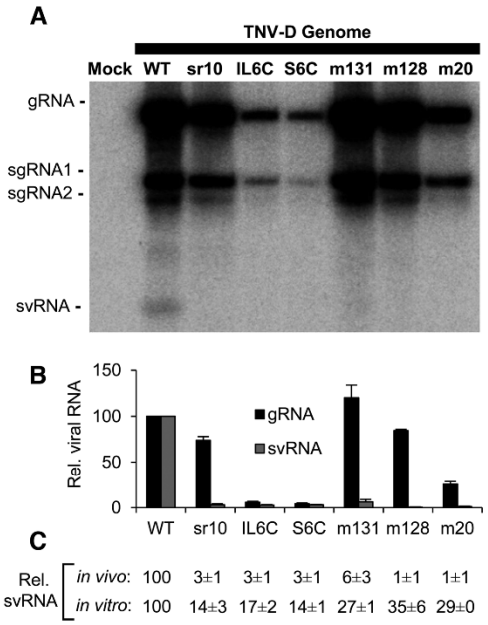

Figure 5. Replication of selected svRNA-deficient viral genomic mutants in protoplasts. (**A**) Northern blot analysis of selected mutants. Mutants are listed above the lanes and viral RNA species are labelled on the left. (**B**) Graphical representation of relative genome replication and svRNA production in (A). Black bars indicate genome replication and grey bars represent svRNA production. (**C**) Comparison of *in vivo* and *in vitro* svRNA production. *In vivo* values are derived from quantitative analysis shown in (B) and *in vitro* values were taken from Figure 4. Results are from three independent experiments, ±SE.

sensitivity (Figure 4A) were introduced into the full-length infectious clone of TNV-D and tested in protoplast infections (Figure 5A). Genome accumulation was most severely affected for IL6C, S6C and m20, containing changes to the asymmetrical internal loop, S6, or the terminal loop of SLII, respectively (Figure 5B). Thus, some changes that inhibit svRNA production *in vitro* also have major negative effects on essential viral processes. In contrast, near wt levels of genome were observed for sr10, m131 and m128 (Figure 5B). However, for these cases, the relative levels of svRNA observed *in vivo* were lower than corresponding *in vitro* levels (Figure 5C). Such differences may be a consequence of the more complex cellular environment during infections. Nonetheless, collectively, these results show that mutants exhibiting notable defects in svRNA production in *in vitro* assays also show diminished ability to generate svRNAs during infections (Figure 5C).

Functional analyses of svRNA

To gain insights into the possible function(s) of svRNA during infections, we assessed the ability of a precursor svRNA to inhibit viral RNA translation *in vitro*. We reasoned that the presence of the 3′-CITE within the svRNA could act as a sponge for eIF4F, and thus sequester this factor away from authentic viral RNAs, as was shown previously using only the TNV-D 3′-CITE as competitor (39). To test this idea, increasing amounts of svRNA or a size-matched non-specific (NS) RNA were added to *in vitro* translation reactions containing a fixed amount of either genomic or sg mRNA (Figure 6A–C). In all cases, increases in translation were observed with the NS competitor, which is likely due to it interacting non-specifically with inhibitory factors in the translation extract. For the viral RNAs, svRNA addition resulted in dose-dependent inhibition of viral RNA translation to ∼50%, at the highest level of competitor (Figure 6A–C). In contrast, similar competition assays performed with two different capped reporter mRNAs and the svRNA effectively prevented translation at the highest concentration of svRNA tested (Figure 6D and E). Thus, the svRNA can compete against both uncapped viral RNAs and capped mRNA, but is notably more effective at suppressing translation of the latter.

A second possible function of the svRNA could be to sequester Xrn1, if the enzyme stays paused at stall sites for extended periods of time. For this analysis, an Xrn1-sensitive non-viral RNA was used as a reporter (Rep). The reaction also contained either, no added RNA (M), 50-svRNA, a 50-svRNA mutant containing the S6C modification (50-S6C), or a size-matched NS RNA (Figure 7A). The Rep RNA was efficiently digested by Xrn1 in the absence of a competitor RNA. However, although all added competitor RNAs conferred a level of resistance to Xrn1, the wt viral-based 50-svRNA substrate provided the least protection when compared to the two controls. Assays were also conducted with different concentrations of Rep, competitor RNAs, and Xrn1, as well as at multiple time points, however similar results to those presented were observed in all cases (data not shown). Consequently, the findings indicate that under the conditions tested, the presence of the Xrn1 pausing sequence does not provide added protection from Xrn1 digestion to other RNAs.

A third possible function for the svRNA could be related to the assembly of viral particles. In this case, the svRNA could be included as part of the nucleic acid content of virions. To assess this possibility, we inoculated *N. benthamiana* plants with transcripts of wt TNV-D genome and isolated virus particles from infected leaves. The nucleic acid content of the isolated virus particles was subsequently assessed by northern blotting. This analysis indicated that small amounts of the two viral sg mRNAs, as well as svRNA, are packaged in TNV-D virus particles (Figure 7B).

Lastly, we wanted to determine if the absence of svRNA in whole plant infections would result in a noticeably altered phenotype. Mutant sr10 was selected for this analysis because (i) it had near wt levels of infection in protoplasts and trace levels of svRNA *in vitro* and *in vivo* (Figure 4), (ii) its modification was distal to the upper functionally-relevant region of the 3′-CITE needed for viral protein translation (38), (iii) the mutation was away from the terminal loop of SLII, which is critical for efficient translational readthrough of p82 (37) and (iv) the substitutions in it did not induce any noticeable structural changes to other regions in the svRNA (Figure 4B). *N. benthamiana* plants were rub-inoculated with transcripts of wt or sr10 mutant TNV-D genomes. At 6 days post infection, leaves inoculated with wt transcripts showed leaf curling, yellowing, and necrosis (Figure 7C).

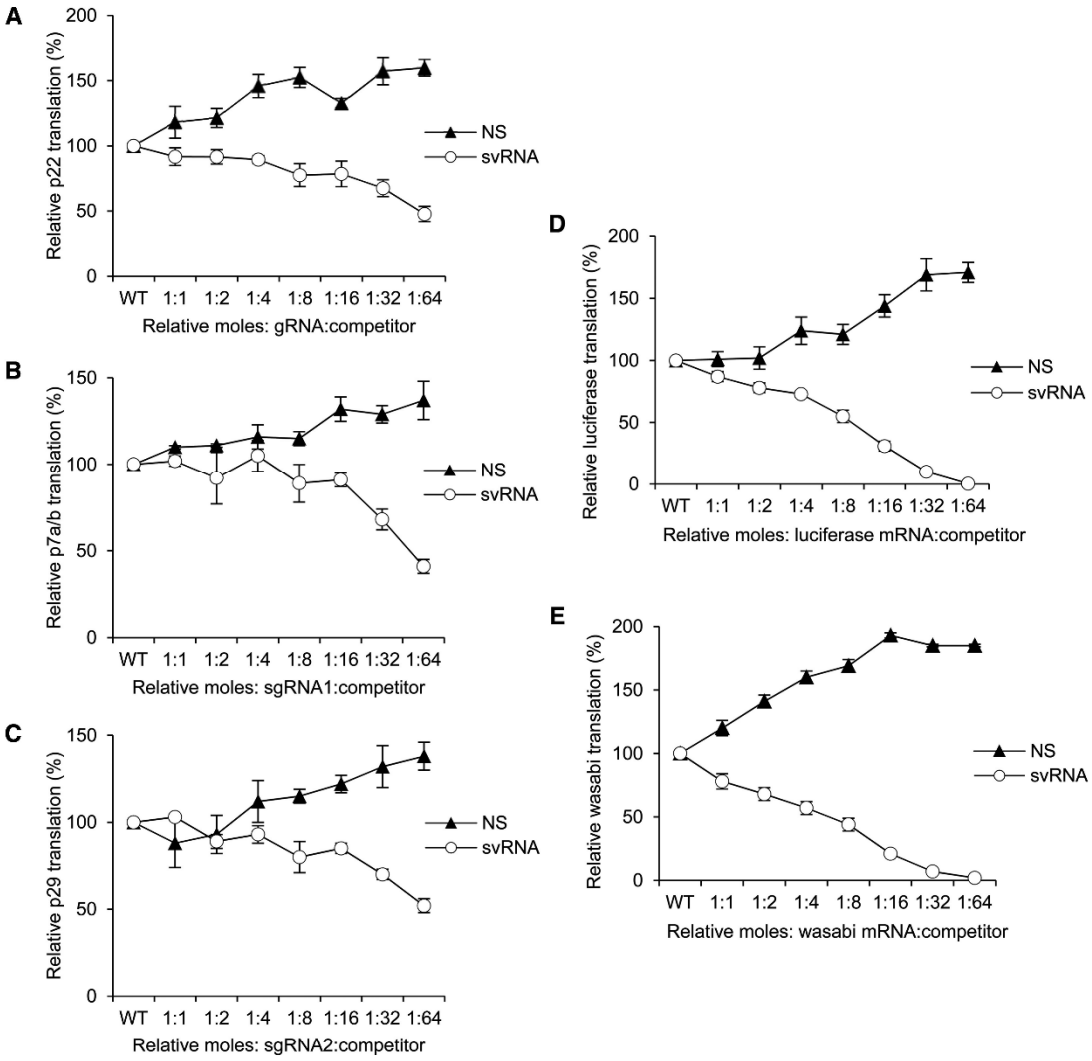

Figure 6. Translation inhibition assay using TNV-D svRNA as a competitor. (**A**) *In vitro* translation with TNV-D genomic RNA. Uncapped *in vitro* transcribed wt TNV-D genomic RNA was incubated in wheat germ extract with increasing molar amounts of 50-svRNA or a non-specific (NS) RNA in the presence of ^{35}S-labelled methionine. Levels of labeled protein were quantified and plotted for the different ratios tested. (**B**) Competition assay with sg mRNA1. (**C**) Competition assay with sg mRNA2. (**D** and **E**) Competition assay with capped luciferase and wasabi mRNAs. Results are from three independent experiments, ±SE.

In contrast, symptoms were markedly attenuated in sr10-infected leaves, which exhibited patches of small pale lesions. The yield of viral RNAs from sr10-infected plants was ∼12% that of the wt infections and, unlike for wt infections, svRNAs were not detectable and the infection did not move systemically within plants.

DISCUSSION

We have characterized an svRNA species that is generated during TNV-D infections. The svRNAs produced using recombinant Xrn1 *in vitro* were comparable in length to those generated in infected plant cells, implicating the cytosolic plant 5′-to-3′exonuclease, Xrn4, as the enzyme generating svRNAs *in vivo*. The fact that the svRNAs were generated with purified Xrn1 also indicates that other host proteins are not necessary for their production, although the possible involvement of such factors cannot be precluded. Different regions within the major svRNA species were found to be necessary for its production and distinct structural features within were determined to be essential for Xrn stalling. The implications of these and other findings are discussed.

svRNA production from a sg mRNA

Our results indicate that the majority of svRNA produced during viral infections is generated from sg mRNA1 (Figure 2D). This RNA is the more abundant of the two sg mR-

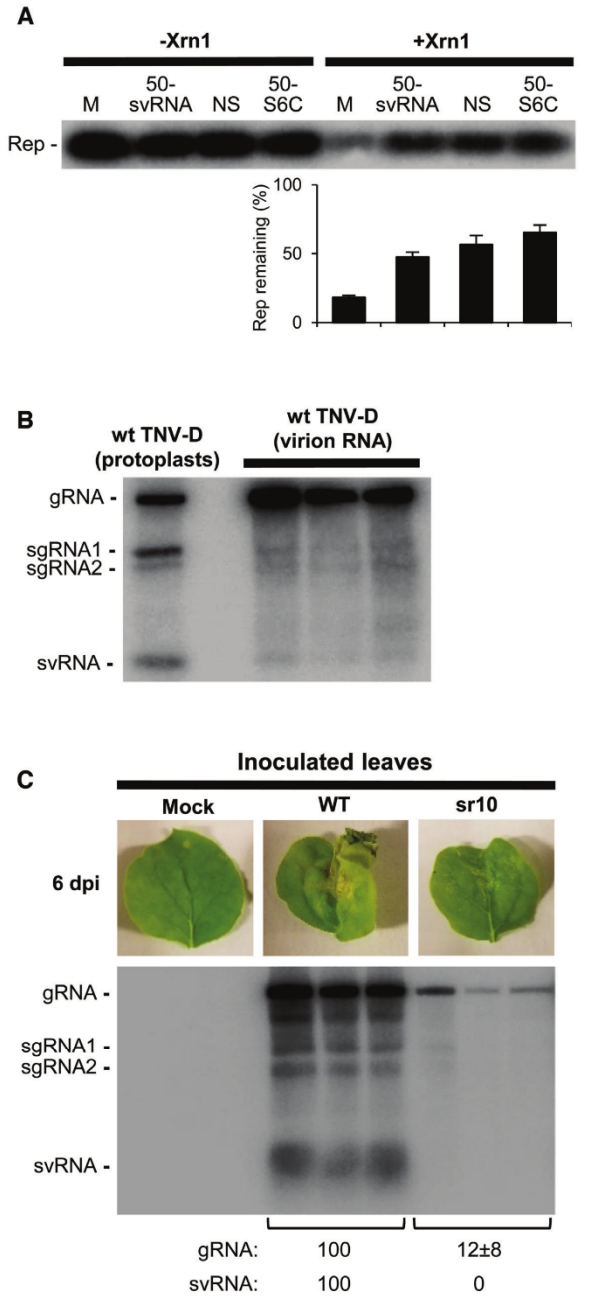

Figure 7. Functional analyses of TNV-D svRNA. (**A**) Xrn inhibition assay. A reporter RNA (Rep) was incubated with Xrn1 in the presence of competitors 50-svRNA, 50-S6C, or nonspecific RNA (NS). The amount of remaining Rep RNA was quantified by northern blotting. Results are from three independent experiments, ±SE. (**B**) Viral RNA analysis of TNV-D virions. Viral RNA was extracted from virions and analyzed by northern blotting. RNAs extracted from TNV-infected protoplasts were separated in the same gel for size comparison. Results from three independent virus isolations are shown. (**C**) Infection of *N. benthamiana* plants with svRNA-deficient mutant sr10. Total RNA was extracted from inoculated leaves of TNV-infected plants six days post infection (dpi), and analyzed by northern blotting. Representative example from three independent experiments done in triplicate.

NAs transcribed from the TNV-D genome, thus its comparatively higher level likely contributes proportionally to the production of the svRNA (Figure 1A, B). In contrast, although the viral genome accumulates to the greatest relative level in infections, it contributes minimally to svRNA production. This may be due to its efficient packaging, which could provide protection from RNases (Figure 7B). Conversely, neither sg mRNA1 nor 2 is packaged efficiently.

Both RCNMV and BNYVV produce svRNAs from genomes that also transcribe a standard sg mRNA (28,29), however the possible contribution of their sg mRNAs to the production of the svRNAs has not yet been investigated. In BYDV, inactivating sg RNA2 production in infections reduces accumulation of the svRNA, termed sgRNA3 (48), however it is not known if sgRNA3 is actually generated by Xrn (22). The possible origin of an svRNA from a transcribed viral sgRNA has been proposed for the flavivirus Japanese encephalitis virus (JEV) (49). It is well documented that many flaviviruses produce svRNAs, but these viruses do not normally transcribe sg mRNAs (11). JEV infections were shown to generate sfRNAs more efficiently in Xrn1-knockdown cells, suggesting an alternative mode for their generation. This observation, combined with *in vitro* RNA-dependent RNA polymerase promoter activity from a sequence near the stall site, prompted the notion that in JEV, sgRNA transcription mediates the production of its sfRNA (49). Further studies will be required to validate this atypical transcription-based model for svRNA production in flaviviruses.

svRNA structure

The RNA structure inhibiting Xrn exoribonucleases in TNV-D is distinct from other reported structures in terms of its (i) modularity, (ii) size, and (iii) contiguity. Other Xrn1-blocking structures have been found to be functionally modular (14,29), which contrasts our results with TNV-D, where adding sequence to the 3′-end of the structure, which alters its 3′-proximal context, abolished stalling (Figure 3). This 3′ addition would interfere with formation of the SLII/3′-terminal sequence interaction involved in genome replication. This notion is further supported by the two and three nucleotide deletions of 3′-terminal viral sequence (mutants –2 and –3) and the SLII bulge deletion (ΔSL2b) that would inhibit this interaction, and all of which yielded low levels of svRNA (Figure 3A–C). Consequently, these data implicate formation of the SLII/3′-terminal sequence interaction as an important tertiary-level stalling determinant. Residues immediately 5′-proximal to the termination site also influenced stalling function, but had more modest effects (mutants, sr1 to sr3) (Figure 3C). The substitutions in this region could potentially alter formation or stability of the downstream blocking structure. Approximately 5–6 nucleotides are predicted to reside in a protein channel leading to the active site of Xrn1 (17). In RCNMV, a sequence just downstream of the stall site is proposed to be involved in the folding of the structure mediating stalling (30). Specifically, the unwinding of a base-paired P1 stem immediately downstream of the Xrn1 stop site by Xrn1 mediates a transition of the structure from an inactive SL to an active pseudoknotted conformation; a process

termed codegradational remodelling (30). Although alternative structures are not predicted for the TNV-D region, the involvement of possible rearrangements cannot be discounted. Regardless of the mechanism of Xrn interference, the results suggest that the 5′-context of the blocking structure does influence processivity, albeit far less than the 3′-context.

The lack of modularity of the blocking RNA structure in TNV-D may in part relate to its size. Comparable functional RNA elements reported to date have been substantially smaller. For example, the linear lengths for the minimal active structures for flaviviruses, RCNMV, and BNYVV, are 72–79 nt, 43 nt and 43 nt, respectively (14,29,30). These sizes are approximately 3- to 5-fold smaller than the linear length of TNV-D sequence harbouring its stalling structure, *i.e.* 212 nt. The atomic structure of the BNYVV RNA element is yet to be explored, however those for two flaviviruses and RCNMV have been solved (15,16). Though distinct in terms of detailed conformations, all contain pseudoknots that form ring-like folds around the 5′-ends of the RNA structures. This unique type of ring structure is predicted to contact the surface of Xrn1 and act as a brace, causing it to pause. The compact nature of these RNA elements is in contrast to the region encompassing the TNV-D stall structure and may suggest that a different type of structural complexity is utilized by TNV-D to block Xrn.

Although the linear sequence involved is large, certain regions appear to be more important than others. The ability to delete the upper portion of the 3′-CITE yet maintain ∼57% activity (mutant ΔTop), rules out a critical role for this region (Figure 4A), and suggests a non-linear, or non-contiguous, arrangement of essential components. Three distinct regions were determined to be most critical; i.e. their modification led to decreases in activity to ∼10–15%. These include the lower region of the 3′-CITE (Figures 3C, 4A), SLII (Figure 3C, 4A), and the 3′-terminus (Figures 3A-C). It follows that structural coordination and/or communication between these elements is required for effective stalling. As alluded to earlier, base pairing of the SLII bulge with the 3′-terminal nucleotides is essential for TNV-D genome replication (37), and this interaction also appears to be important for formation of an effective stalling RNA structure. The requirement for specific sequence in the terminal loop of SLII and corresponding altered chemical reactivity of the lower region of the 3′-CITE upon its modification, along with reciprocal correlative evidence (Figure 4A, B), suggest an interaction between these two regions. Additionally, the hierarchical importance of sequence identity over base pairing in the lower region of the 3′-CITE (Figure 3C, and Figure 4A), suggests that non-canonical interactions and/or structural rearrangements may be involved. The detailed structural relationship between the three key structural components forming tertiary contacts, as well as the precise conformational strategy utilized to stall Xrn, remain to be elucidated.

Possible svRNA functions

Xrn-generated RNAs represent an emerging area in plant virology with a small but growing list of examples. Consequently, the functions of these RNAs in plant infections remain largely unknown (22). One exception is the svRNA of BNYVV, which has been demonstrated convincingly to be required for long-distance movement of the viral infection in plants (27,28). One can imagine a variety of possible roles for svRNAs in viral processes related to, for instance, translation, RNA replication, and/or packaging. The TNV-D svRNA inhibited translation of both viral and capped reporter mRNA *in trans* in wheat germ extract. The corresponding levels of inhibition observed in the dose-response curves for the three different viral RNA messages were similar (Figure 6A–C), suggesting that all species are supressed to comparable degrees. In contrast, the svRNA more efficiently competed against capped reporter mRNAs (Figure 6D), suggesting a possible role in preferentially downregulating cellular mRNA levels during infections. The svRNA of RCNMV was also found to inhibit translation of both viral reporter mRNAs and capped messages (29). Also, for the polymerase-generated svRNA of BYDV (24), translation of the viral genome was inhibited to a greater extent than sg mRNA1 (50). This latter observation led to the proposal that this svRNA may act as a switch to favor translation of late genes during infections. A similar regulatory role in virus translation is not predicted for TNV-D, because all viral RNAs were supressed to similar levels.

Other possible functions for the TNV-D svRNA could be to supress Xrn4 activity during infections or facilitate packaging. For TNV-D, our *in vitro* results did not support a role for its svRNA in inhibiting Xrn activity (Figure 7A), which contrasts results from other Xrn1 blocking structures in mammalian viruses (18,19,51). One could imagine that supressing Xrn4 activity during infections could be beneficial to the survival of uncapped viral RNA genomes like TNV-D. The observed lack of inhibitory activity on the enzyme could be related to the modest level of stalling (∼4.3%), which probably would not notably affect enzyme turnover. As for packaging, a small but readily detectable amount of svRNA was present in virions (Figure 7B). The svRNA of RCNMV is also packaged into virions, and could mediate assembly and/or promote particle stability (29). However, the TNV-D svRNA, and the two sg mRNAs, are not packaged efficiently. Consequently, the incorporation of these 3′-terminal sg mRNAs and svRNA in virions may be inadvertent.

Demonstrating a function for svRNA in plants has been particularly challenging. Aside from BNYVV (28,29), *in vivo* studies of viral genomes, where svRNA production has been inactivated, have resulted in only minor effects (24,29,38). Our testing of an svRNA-deficient TNV-D mutant in plants showed major differences in symptomology, viral RNA accumulation, and movement (Figure 7C). Nonetheless, it cannot be precluded that additional viral processes were affected by the modifications, even though second-site structural perturbations were not observed (Figure 4B). Indeed, the structural features that make the svRNA resistant to Xrn overlap with, or are highly integrated with, the structural elements important for a variety of viral processes. Moreover, new functions for components in this region are being discovered; *i.e.* the wt loop sequence of SLII is also required for efficient translational readthrough (37). It is thus possible that the SLII loop/lower 3′-CITE interaction needed for Xrn stalling

is also required for readthrough activity. Further detailed analyses of these overlapping features will be required to design mutants that are exclusively deficient in svRNA production.

In addition to TNV-D (Betanecrovirus) and RCNMV (Dianthovirus), at least three other genera in family Tombusviridae generate 3′-terminal svRNAs that likely originate from Xrn4 digestion. These include, tombusviruses (32), machlomoviruses (34) and carmoviruses (52). Other genera in this family may also generate svRNAs, however they may have either been overlooked or dismissed as nonrelevant degradation products (22). Recently, a bioinformatics approach was used to identify additional functional RCNMV-like stalling structures in umbraviruses (family Tombusviridae), as well as polero- and enamoviruses (family Luteoviridae) (53). Moreover, some of the svRNAs identified were predicted to encode proteins, suggesting that they could function as mRNAs for viral protein production. Their prevalence in multiple virus groups and elusive functions make Xrn-resistant RNAs intriguing subjects for further investigation.

SUPPLEMENTARY DATA

Supplementary Data are available at NAR Online.

ACKNOWLEDGEMENTS

We thank Robert Coutts for the TNV-D clone and members of our laboratory for reviewing the manuscript.

FUNDING

Natural Sciences and Engineering Research Council of Canada (NSERC); Ontario Graduate Scholarship (to C.D.G.); NSERC graduate fellowship (to L.R.N.). Funding for open access charge: York University Open Access Author Fund.
Conflict of interest statement. None declared.

REFERENCES

1. Molleston,J.M. and Cherry,S. (2017) Attacked from all Sides: RNA decay in antiviral defense. *Viruses*, **9**, E2.
2. Stevens,A. (2001) 5′-exoribonuclease 1: Xrn1. *Methods Enzymol.*, **342**, 251–259.
3. Jones,C.I., Zabolotskaya,M.V. and Newbury,S.F. (2012) The 5′ → 3′ exoribonuclease XRN1/Pacman and its functions in cellular processes and development. *Wiley Interdiscip. Rev. RNA*, **3**, 455–468.
4. Łabno,A., Tomecki,R. and Dziembowski,A. (2016) Cytoplasmic RNA decay pathways—enzymes and mechanisms. *Biochim. Biophys. Acta.*, **1863**, 3125–3147.
5. Poole,T.L. and Stevens,A. (1997) Structural modifications of RNA influence the 5′ exoribonucleolytic hydrolysis by XRN1 and HKE1 of Saccharomyces cerevisiae. *Biochem. Biophys. Res. Commun.*, **235**, 799–805.
6. Jaag,H.M. and Nagy,P.D. (2009) Silencing of Nicotiana benthamiana Xrn4p exoribonuclease promotes tombusvirus RNA accumulation and recombination. *Virology*, **386**, 344–352.
7. Li,Y., Yamane,D. and Lemon,S.M. (2015) Dissecting the roles of the 5′ exoribonucleases Xrn1 and Xrn2 in restricting hepatitis C virus replication. *J. Virol.*, **89**, 4857–4865.
8. Lee,C.C., Lin,T.L., Lin,J.W., Han,Y.T., Huang,Y.T., Hsu,Y.H. and Meng,M. (2016) Promotion of bamboo mosaic virus accumulation in Nicotiana benthamiana by 5′→3′ exonuclease NbXRN4. *Front. Microbiol.*, **6**, 1508.
9. Clarke,B.D., Roby,J.A., Slonchak,A. and Khromykh,A.A. (2015) Functional non-coding RNAs derived from the flavivirus 3′ untranslated region. *Virus Res.*, **206**, 53–61.
10. Pijlman,G.P., Funk,A., Kondratieva,N., Leung,J., Torres,S., van der Aa,L., Liu,W.J., Palmenberg,A.C., Shi,P.Y., Hall,R.A. *et al.* (2008) A highly structured, nuclease-resistant, noncoding RNA produced by flaviviruses is required for pathogenicity. *Cell Host Microbe*, **4**, 579–591.
11. Slonchak,A. and Khromykh,A.A. (2018) Subgenomic flaviviral RNAs: what do we know after the first decade of research. *Antiviral Res.*, **159**, 13–25.
12. Funk,A., Truong,K., Nagasaki,T., Torres,S., Floden,N., Balmori Melian,E., Edmonds,J., Dong,H., Shi,P.Y. and Khromykh,A.A. (2010) RNA structures required for production of subgenomic flavivirus RNA. *J. Virol.*, **84**, 11407–11417.
13 Silva,P.A., Pereira,C.F., Dalebout,T.J., Spaan,W.J. and Bredenbeek,P.J. (2010) An RNA pseudoknot is required for production of yellow fever virus subgenomic RNA by the host nuclease XRN1. *J. Virol.*, **84**, 11395–113406.
14. Chapman,E.G., Moon,S.L., Wilusz,J. and Kieft,J.S. (2014) RNA structures that resist degradation by Xrn1 produce a pathogenic Dengue virus RNA. *Elife*, **3**, e01892.
15. Chapman,E.G., Costantino,D.A., Rabe,J.L., Moon,S.L., Wilusz,J., Nix,J.C. and Kieft,J.S. (2014). The structural basis of pathogenic subgenomic flavivirus RNA (sfRNA) production. *Science*, **344**, 307–310.
16. Akiyama,B.M., Laurence,H.M., Massey,A.R., Costantino,D.A., Xie,X., Yang,Y., Shi,P.Y., Nix,J.C., Beckham,J.D. and Kieft,J.S. (2016) Zika virus produces noncoding RNAs using a multi-pseudoknot structure that confounds a cellular exonuclease. *Science*, **354**, 1148–1152.
17. MacFadden,A., O'Donoghue,Z., Silva,P.A.G.C., Chapman,E.G., Olsthoorn,R.C., Sterken,M.G., Pijlman,G.P., Bredenbeek,P.J. and Kieft,J.S. (2018) Mechanism and structural diversity of exoribonuclease-resistant RNA structures in flaviviral RNAs. *Nat. Commun.*, **9**, 119.
18. Moon,S.L., Blackinton,J.G., Anderson,J.R., Dozier,M.K., Dodd,B.J., Keene,J.D., Wilusz,C.J., Bradrick,S.S. and Wilusz,J. (2015) XRN1 stalling in the 5′ UTR of hepatitis C virus and bovine viral diarrhea virus is associated with dysregulated host mRNA stability. *PLoS Pathog.*, **11**, e1004708.
19. Charley,P.A., Wilusz,C.J. and Wilusz,J. (2018) Identification of phlebovirus and arenavirus RNA sequences that stall and repress the exoribonuclease XRN1. *J. Biol. Chem.*, **293**, 285–295.
20. Nagarajan,V.K., Jones,C.I., Newbury,S.F. and Green,P.J. (2013) XRN 5′→3′ exoribonucleases: structure, mechanisms and functions. *Biochim. Biophys. Acta.*, **1829**, 590–603.
21. Peng,J., Yang,J., Yan,F., Lu,Y., Jiang,S., Lin,L., Zheng,H., Chen,H. and Chen,J. (2011) Silencing of NbXrn4 facilitates the systemic infection of Tobacco mosaic virus in Nicotiana benthamiana. *Virus Res.*, **158**, 268–270.
22. Miller,W.A., Shen,R., Staplin,W. and Kanodia,P. (2016) Noncoding RNAs of plant viruses and viroids: sponges of host translation and rna interference machinery. *Mol. Plant Microbe Interact.*, **29**, 156–164.
23. Kelly,L., Gerlach,W.L. and Waterhouse,P.M. (1994) Characterisation of the subgenomic RNAs of an Australian isolate of barley yellow dwarf luteovirus. *Virology*, **202**, 565–573.
24. Koev,G. and Miller,W.A. (2000) A positive-strand RNA virus with three very different subgenomic RNA promoters. *J. Virol.*, **74**, 5988–5996.
25. Yamagishi,N., Terauchi,H., Kanematsu,S. and Hidaka,S. (2003) Characterization of the small subgenomic RNA of soybean dwarf virus. *Arch. Virol.*, **148**, 1827–1834.
26. Peltier,C., Klein,E., Hleibieh,K., D'Alonzo,M., Hammann,P., Bouzoubaa,S., Ratti,C. and Gilmer,D. (2012) Beet necrotic yellow vein virus subgenomic RNA3 is a cleavage product leading to stable non-coding RNA required for long-distance movement. *J. Gen. Virol.*, **93**, 1093–1102.
27. Flobinus,A., Chevigny,N., Charley,P.A., Seissler,T., Klein,E., Bleykasten-Grosshans,C., Ratti,C., Bouzoubaa,S., Wilusz,J. and Gilmer,D. (2018) Beet Necrotic yellow vein virus noncoding RNA production depends on a 5′→3′ Xrn exoribonuclease activity. *Viruses*, **10**, E137.

28. Dilweg,I.W., Gultyaev,A.P. and Olsthoorn,R.C. (2019) Structural features of an Xrn1-resistant plant virus RNA. *RNA Biol.*, **16**, 838–845.
29. Iwakawa,H.O., Mizumoto,H., Nagano,H., Imoto,Y., Takigawa,K., Sarawaneeyaruk,S., Kaido,M., Mise,K. and Okuno,T. (2008) A viral noncoding RNA generated by cis-element-mediated protection against 5′→3′ RNA decay represses both cap-independent and cap-dependent translation. *J. Virol.*, **82**, 10162–10174.
30. Steckelberg,A.L., Akiyama,B.M., Costantino,D.A., Sit,T.L., Nix,J.C. and Kieft,J.S. (2018) A folded viral noncoding RNA blocks host cell exoribonucleases through a conformationally dynamic RNA structure. *Proc. Natl. Acad. Sci. U.S.A.*, **115**, 6404–6409
31. Miller,W.A., Shen,R., Staplin,W. and Kanodia,P. (2016) Noncoding RNAs of plant viruses and viroids: sponges of host translation and RNA interference machinery. *Mol. Plant Microbe Interact.*, **29**, 156–164.
32. Jiwan,S.D., Wu,B. and White,K.A. (2011) Subgenomic mRNA transcription in Tobacco necrosis virus. *Virology*, **418**, 1–11.
32. Johnston,J.C. and Rochon,D.M. (1995) Deletion analysis of the promoter for the cucumber necrosis virus 0.9-kb subgenomic RNA. *Virology*, **214**, 100–109.
34. Scheets,K. (2000) Maize chlorotic mottle machlomovirus expresses its coat protein from a 1.47-kb subgenomic RNA and makes a 0.34-kb subgenomic RNA. *Virology*, **267**, 90–101.
35. Coutts,R.H., Rigden,J.E., Slabas,A.R., Lomonossoff,G.P. and Wise,P.J. (1991) The complete nucleotide sequence of Tobacco necrosis virus strain D. *J. Gen. Virol.*, **72**, 1521–1529.
36. Newburn,L.R., Nicholson,B.L., Yosefi,M., Cimino,P.A. and White,K.A. (2014) Translational readthrough in Tobacco necrosis virus-D. *Virology*, **450-451**, 258–265.
37. Newburn,L.R. and White,K.A. (2017) Atypical RNA elements modulate translational readthrough in Tobacco necrosis virus D. *J. Virol.*, **91**, e02443-16.
38. Shen,R. and Miller,W.A. (2004) The 3′ untranslated region of Tobacco necrosis virus RNA contains a barley yellow dwarf virus-like cap-independent translation element. *J. Virol.*, **78**, 4655–4664.
39. Kraft,J.J., Treder,K., Peterson,M.S. and Miller,W.A. (2013) Cation-dependent folding of 3′ cap-independent translation elements facilitates interaction of a 17-nucleotide conserved sequence with eIF4G. *Nucleic Acids Res.*, **41**, 3398–3413.
40. Chkuaseli,T., Newburn,L.R., Bakhshinyan,D. and White,K.A. (2015) Protein expression strategies in Tobacco necrosis virus-D. *Virology*, **486**, 54–62.
41. Gunawardene,C.D., Jaluba,K. and White,K.A. (2015) Conserved motifs in a tombusvirus polymerase modulate genome replication, subgenomic transcription, and amplification of defective interfering RNAs. *J. Virol.*, **89**, 3236–3246.
42. White,K.A. and Morris,T.J. (1994) Nonhomologous RNA recombination in tombusviruses: generation and evolution of defective interfering RNAs by stepwise deletions. *J. Virol.*, **68**, 14–24.
43. Regulski,E.E. and Breaker,R.R. (2008) In-line probing analysis of riboswitches. *Methods Mol. Biol.*, **419**, 53–67.
44. Nicholson,B.L., Zaslaver,O., Mayberry,L.K., Browning,K.S. and White,K.A. (2013) Tombusvirus Y-shaped translational enhancer forms a complex with eIF4F and can be functionally replaced by heterologous translational enhancers. *J. Virol.*, **87**, 1872–1883.
45. Hillman,B.I., Morris,T.J. and Schlegel,D.E. (1985) Effects of low molecular- weight RNA and temperature on tomato bushy stunt virus symptom expression. *Phytopathology*, **75**, 361–365.
46. Wang,Z., Kraft,J.J., Hui,A.Y. and Miller,W.A. (2010) Structural plasticity of Barley yellow dwarf virus-like cap-independent translation elements in four genera of plant viral RNAs. *Virology*, **402**, 177–186.
47. Molinaro,M. and Tinoco,I. Jr (1995) Use of ultra stable UNCG tetraloop hairpins to fold RNA structures: thermodynamic and spectroscopic applications. *Nucleic Acids Res.*, **23**, 3056–3063.
48. Shen,R., Rakotondrafara,A.M. and Miller,W.A. (2006) Trans regulation of cap-independent translation by a viral subgenomic RNA. *J. Virol.*, **80**, 10045–10054.
49. Chen,Y.S., Fan,Y.H., Tien,C.F., Yueh,A. and Chang,R.Y. (2018) The conserved stem-loop II structure at the 3′ untranslated region of Japanese encephalitis virus genome is required for the formation of subgenomic flaviviral RNA. *PLoS One*, **13**, e0201250.
50. Wang,S., Guo,L., Allen,E. and Miller,W.A. (1999) A potential mechanism for selective control of cap-independent translation by a viral RNA sequence in cis and in trans. *RNA*, **5**, 728–738.
51. Moon,S.L., Anderson,J.R., Kumagai,Y., Wilusz,C.J., Akira,S., Khromykh,A.A. and Wilusz,J. (2012) A noncoding RNA produced by arthropod-borne flaviviruses inhibits the cellular exoribonuclease XRN1 and alters host mRNA stability. *RNA*, **18**, 2029–2040.
52. Zhang,S., Sun,R., Guo,Q., Zhang,X.F. and Qu,F. (2018) Repression of turnip crinkle virus replication by its replication protein p88. *Virology*, **526**, 165–172.
53. Steckelberg,A., Vicens,Q. and Kieft,J.S. Pervasiveness of exoribonuclease-resistant RNAs in plant viruses suggests new roles for these conserved RNA structures. *mBio.*, **9**, e02461-18.

CHAPTER 3:

"RNA Structure Protects the 5'-end of an Uncapped Tombusvirus RNA Genome from Xrn Digestion"

Tombusviridae is a family of plus-strand RNA plant viruses that contain single-stranded RNA genomes lacking a 5' cap and 3' poly(A) tail. The 5' cap represents an important post-transcriptional modification that helps to enhance the stability of mRNAs by protecting them against 5'-to-3' exoribonucleases. For this reason, it was unknown how tombusvirids protect their vulnerable 5' ends from exoribonuclease attack. Previous studies had indicated that the main cytosolic 5'-to-3' exoribonuclease in plants, Xrn4, is restrictive to tombusvirus infections. Based on the susceptibility of tombusvirus infections to Xrn4 and the perceived vulnerability of their uncapped 5'-ends to this enzyme, a study was initiated to investigate how tombusviruses protect their viral genomes from Xrn4 decay.

This chapter is presented in the form of a peer-reviewed, published journal article. The findings of the study demonstrate that the genomic 5'UTR of the tombusvirus CIRV folds into a complex RNA structure that is able to evade Xrn-mediated degradation. The article, "**RNA Structure Protects the 5'-end of an Uncapped Tombusvirus RNA Genome from Xrn Digestion**" by **Chaminda D. Gunawardene, Jennifer S. H. Im and K. Andrew White** was accepted for publication in ***Journal of Virology*** on August 2021 (doi: 10.1128/JVI.01034-21). I conceptualized and designed all of the experiments for the study together with Dr. Andrew White. I performed all of the experiments except for Figure 5C and Figure 10, which were contributed by my co-author, Jennifer S.H. Im. I designed and formatted all of the figures, performed all data analyses, and wrote the first draft of the manuscript.

AMERICAN SOCIETY FOR MICROBIOLOGY | Journal of Virology®

VIRUS-CELL INTERACTIONS

RNA Structure Protects the 5′ End of an Uncapped Tombusvirus RNA Genome from Xrn Digestion

Chaminda D. Gunawardene,[a] Jennifer S. H. Im,[a] K. Andrew White[a]

[a]Department of Biology, York University, Toronto, Ontario, Canada

ABSTRACT One of the many challenges faced by RNA viruses is the maintenance of their genomes during infections of host cells. Members of the family *Tombusviridae* are plus-strand RNA viruses with unmodified triphosphorylated genomic 5′ termini. The tombusvirus *Carnation Italian ringspot virus* was used to investigate how it protects its RNA genome from attack by 5′-end-targeting degradation enzymes. *In vivo* and *in vitro* assays were employed to determine the role of genomic RNA structure in conferring protection from the 5′-to-3′ exoribonuclease Xrn. The results revealed that (i) the CIRV RNA genome is more resistant to Xrn than its sg mRNAs, (ii) the genomic 5′-untranslated region (UTR) folds into a compact RNA structure that effectively and independently prevents Xrn access, (iii) the RNA structure limiting 5′ access is formed by secondary and tertiary interactions that function cooperatively, (iv) the structure is also able to block access of RNA pyrophosphohydrolase to the genomic 5′ terminus, and (v) the RNA structure does not stall an actively digesting Xrn. Based on its proficiency at impeding Xrn 5′ access, we have termed this 5′-terminal structure an Xrn-evading RNA, or xeRNA. These and other findings demonstrate that the 5′UTR of the CIRV RNA genome folds into a complex structural conformation that helps to protect its unmodified 5′ terminus from enzymatic decay during infections.

IMPORTANCE The plus-strand RNA genomes of plant viruses in the large family *Tombusviridae* are not 5′ capped. Here, we explored how a species in the type genus *Tombusvirus* protects its genomic 5′ end from cellular nuclease attack. Our results revealed that the 5′-terminal sequence of the CIRV genome folds into a complex RNA structure that limits access of the 5′-to-3′ exoribonuclease Xrn, thereby protecting it from processive degradation. The RNA conformation also impeded access of RNA pyrophosphohydrolase, which converts 5′-triphosphorylated RNA termini into 5′-monophosphorylated forms, the preferred substrate for Xrn. This study represents the first report of a higher-order RNA structure in an RNA plant virus genome independently conferring resistance to 5′-end-attacking cellular enzymes.

KEYWORDS RNA structure, RNA folding, RNA virus, plant virus, Xrn1, Xrn4, exoribonuclease, tombusvirus, *Tombusviridae*, xrRNA, RppH

RNA viruses face the challenge of protecting their genomes from degradation during infection of host cells (1, 2). For plant RNA viruses, in addition to suppressing the host antiviral gene silencing system (3), they must also avoid canonical decay pathways designed to remove unwanted and defective cellular RNAs (4–6). Viruses with plus-strand RNA genomes are susceptible to exoribonucleases at both their 5′ and 3′ ends, and those that are uncapped and/or nonpolyadenylated are especially vulnerable. Viral genomes with unmodified 5′ ends are substrates for enzymes that digest RNA in the 5′-to-3′ direction. Xrn1 is a 5′-to-3′ exoribonuclease that functions in the cytosol of yeast and metazoans (7, 8). In plants, Xrn4 is the functional homolog of Xrn1, and both of these enzymes prefer RNA substrates with a monophosphorylated 5′-terminal nucleotide (9, 10). The termini of 5′-capped mRNAs fated for degradation become substrates for Xrn1/4 by

Citation Gunawardene CD, Im JSH, White KA. 2021. RNA structure protects the 5′ end of an uncapped tombusvirus RNA genome from Xrn digestion. J Virol 95:e01034-21. https://doi.org/10.1128/JVI.01034-21.

Editor Anne E. Simon, University of Maryland, College Park

Address correspondence to K. Andrew White, kawhite@yorku.ca.

Received 21 June 2021
Accepted 28 July 2021
Accepted manuscript posted online 4 August 2021
Published 27 September 2021

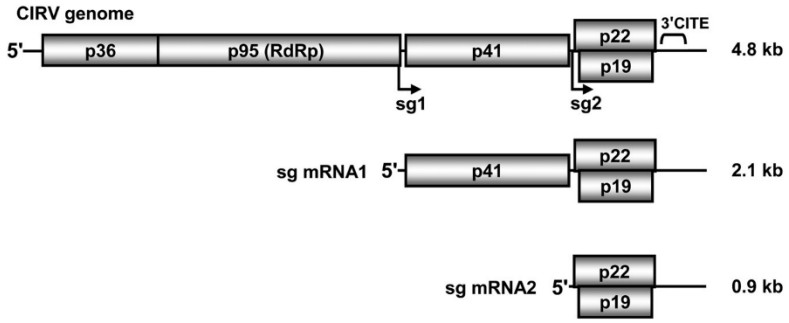

FIG 1 Schematic representation of CIRV genomic and subgenomic mRNAs. Viral ORFs are displayed as gray boxes. The location of the 3′-cap-independent translation enhancer (3′CITE) in the 3′UTR is indicated by a bracket. sg mRNA promoters are shown below the genome as black arrows. Approximate nucleotide lengths are shown, in kilobases, on the right.

decapping activities (2). For uncapped RNAs, RNA pyrophosphohydrolases (RppH) remove terminal γ- and β-phosphate groups from 5′-triphosphates, generating α-monophosphates (11). To initiate digestion of a 5′-monophosphorylated RNA substrate, Xrn1 requires two to three unpaired 5′-terminal nucleotides (12, 13). The enzyme's activity is highly processive, yielding 5′-monophosphate nucleotides; however, its progression can be impeded by certain RNA structures (14, 15).

A rapidly growing field of research has emerged that focuses on viral RNA structures that can stall actively digesting Xrn, referred to as Xrn-resistant RNAs (xrRNAs). By folding into higher-order structures in viral RNAs, xrRNAs are able to resist Xrn degradation through specific RNA-mediated contacts with the enzyme (16, 17). This inhibition can generate functional degradation intermediates, such as subgenomic flavivirus RNAs and other small virus-derived RNAs, which correspond roughly to the 3′UTRs of viral genomes or subgenomic mRNAs (18–22). Conversely, large functionally relevant xrRNAs, generated by Xrn1 termination within genomic 5′UTRs, accumulate in both hepatitis C virus and bovine viral diarrhea virus infections (23). These diverse virus-derived RNA degradation products are able to inhibit Xrn activity and/or modulate cellular processes to facilitate infections (18–23).

Carnation Italian ringspot virus (CIRV) is a plant virus in the genus *Tombusvirus* (family *Tombusviridae*). Like all tombusvirids, its plus-strand RNA genome contains no 5′-cap or 3′-poly(A) tail, making its genomic termini particularly susceptible to exoribonucleases. The polycistronic CIRV genome contains five open reading frames (ORFs) that encode an assortment of viral proteins (Fig. 1). The 5′-proximal ORFs encode two proteins that are translated directly from the genome and are essential for viral RNA synthesis: the p36 accessory replication protein and its readthrough product, p95, the RNA-dependent RNA polymerase (24). Three viral proteins are encoded further downstream that are translated from two smaller subgenomic (sg) mRNAs transcribed during infections (Fig. 1). The coat protein (p41) is translated from sg mRNA1, and the movement (p22) and suppressor of gene silencing (p19) proteins are translated from sg mRNA2. During infections, CIRV translates its proteins by utilizing long-range RNA-RNA interactions between the 5′UTRs of its three species of viral mRNAs (i.e., genome and two sg mRNAs) and a 3′-cap-independent translational enhancer (3′CITE) element located within their 3′UTRs (Fig. 1) (25).

Currently, it is not known how the 5′-triphosphorylated RNA genome and sg mRNAs of tombusviruses resist attack from plant 5′-to-3′ exoribonucleases such as plant Xrn4. Using CIRV, we have investigated the role of viral 5′-terminal RNA sequences in conferring protection from Xrn activity, focusing on the genomic 5′UTR. RNA-mediated protection of 5′-terminal triphosphates from RppH activity was also examined. Our results reveal a major role for higher-order RNA structure in the 5′UTR of the CIRV genome in blocking 5′-end access to these enzymes.

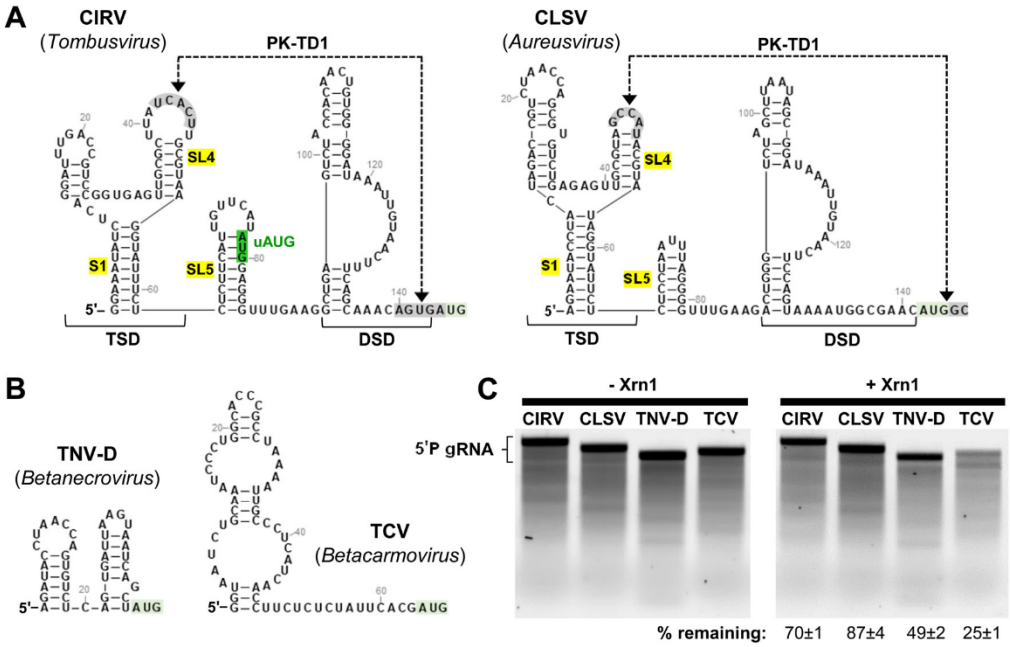

FIG 2 *In vitro* Xrn1 treatment of tombusvirid genomic RNAs. (A) RNA secondary structures of CIRV (tombusvirus) and CLSV (aureusvirus) 5′UTRs. The TSD and DSD are delineated by brackets, and the sequences involved in the PK-TD1 pseudoknot interaction are highlighted in gray. The position of the upstream AUG (uAUG) in CIRV is highlighted in green. S1, SL4, and SL5 are labeled with yellow highlighting, while the p33 and p36 start codons for CIRV and CLSV, respectively, are highlighted in light green. (B) Predicted RNA secondary structures of betanecrovirus and betacarmovirus 5′UTRs. The locations of respective p22 and p28 start codons are highlighted in light green. (C) Ethidium bromide-stained agarose gel of products from *in vitro* Xrn1 assay of tombusvirid genomes, with the percentage of input RNA remaining shown below with standard errors of the means (SEM) ($n = 3$).

RESULTS

Susceptibility of uncapped tombusvirid RNA genomes to Xrn1. Four different tombusvirid RNA genomes possessing varying degrees of higher-order RNA structure in their 5′UTRs were selected for analysis. The RNA structures in the 5′UTRs of closely related tombusviruses and aureusviruses, such as CIRV and *Cucumber leaf spot virus* (CLSV), respectively, have been characterized extensively (26–29). These 5′UTRs begin with a T-shaped domain (TSD) followed by a downstream domain (DSD), which are separated by stem-loop-5 (SL5) (Fig. 2A). Also present is a mid-range interaction involving sequences in the loop of SL4 and the DSD that forms a pseudoknot (PK-TD1). The 5′-terminal sequences of the RNA genomes in both these genera are base-paired in S1, which is positioned adjacent to SL5, providing the potential for coaxial stacking (Fig. 2A). In contrast, the 5′ ends of other tombusvirids, such as *Tobacco necrosis virus* (TNV-D, genus *Betanecrovirus*) and *Turnip crinkle virus* (TCV, genus *Betacarmovirus*), are predicted to exist in small or weak terminal hairpins, respectively (Fig. 2B). Each of these four full-length tombusvirid RNA genomes were *in vitro* transcribed under conditions that favored incorporation of a monophosphorylated 5′-terminal nucleotide, the optimal 5′-phosphorylation state for Xrn1. The viral RNAs generated were then treated with purified yeast Xrn1. Xrn1 has been utilized previously as an effective surrogate for plant Xrn4 (21). All genomes showed some susceptibility to Xrn1 degradation, with remaining full-length levels ranging from ~87% to ~25% (Fig. 2C). Notably, the degree of resistance observed correlated roughly with the predicted higher-order stability of the 5′UTRs, suggesting a role for RNA structure in protecting these uncapped genomic 5′ ends from Xrn1 activity.

Susceptibility of CIRV sg mRNAs to Xrn1. The tombusvirus CIRV was selected for further characterization, beginning with an assessment of the sensitivity of its two

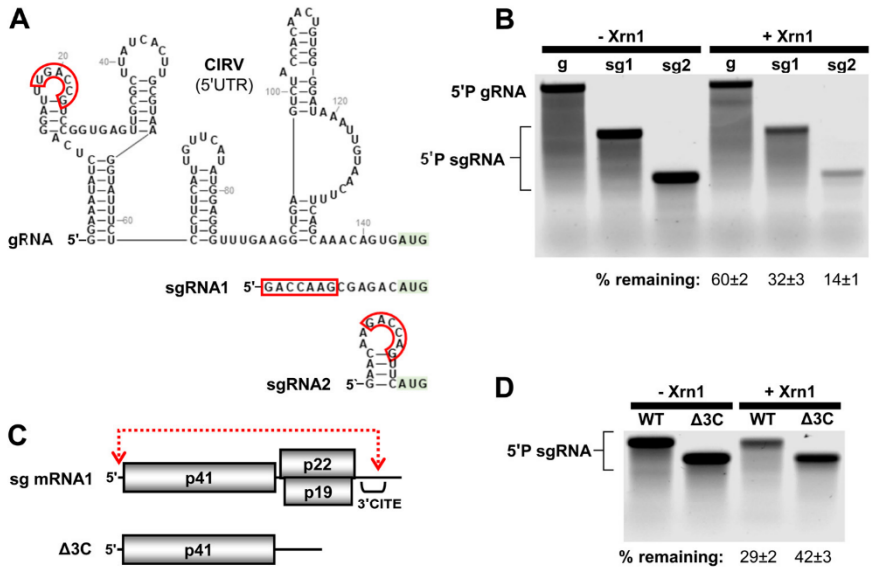

FIG 3 *In vitro* Xrn1 treatment of CIRV sg mRNAs. (A) RNA secondary structures of 5′UTRs of CIRV genome and subgenomic mRNAs. The 5′ partner sequences for the long-range RNA-RNA interaction with the 3′CITE are boxed in red. The start codon for each respective open reading frame is highlighted in light green. (B) Ethidium bromide-stained agarose gel of *in vitro* Xrn1 assay of CIRV subgenomic mRNAs. The percentage of input RNA remaining is shown below with SEM ($n = 3$). (C) Deletion of terminal region containing 3′CITE from sg mRNA1 in mutant Δ3C. The long-range RNA-RNA interaction between the 5′UTR and the 3′CITE in WT sg mRNA1 is shown as a dotted red arrow. (D) *In vitro* Xrn1 treatment of mutant Δ3C. Percentage of input RNA remaining is shown below with SEM ($n = 3$).

cognate sg mRNAs to Xrn1. The 5′ ends of both sg mRNAs are not predicted to have significant local RNA structure, although a small terminal hairpin is possible in sg mRNA2 (Fig. 3A). Treatment of transcripts of the two 5′-monophosphorylated sg mRNAs revealed that both were more sensitive to Xrn1 than their genomic counterpart (Fig. 3B). Interestingly, sg mRNA1, with the predicted linear 5′ end, was more stable than sg mRNA2. One possibility for this observation was that the 5′-terminal sequence of sg mRNA1 (Fig. 3A, red box) was paired with its partner sequence in the 3′CITE (Fig. 3A). This prospect was tested by creating a 3′-truncated sg mRNA1, Δ3C, that lacked the 3′CITE (Fig. 3C). Compared to wild-type (WT) sg mRNA1, treatment of the Δ3C RNA with Xrn1 showed moderately enhanced resistance (Fig. 3D). Thus, Xrn resistance of the 5′ end of sg mRNA1 is not dependent on an interaction with the 3′CITE.

The CIRV 5′UTR alone blocks Xrn1 access. In most tombusviruses, the 5′UTR is approximately 140 to 160 nucleotides (nt) in length and is positioned immediately upstream of the start codon for a 33-kDa accessory replication protein, p33. In the CIRV genome, in addition to an AUG at position 144 (that would produce an ~33-kDa protein), an in-frame upstream AUG (uAUG) start codon is located at genome coordinate 78 (Fig. 4A, top), positioned within the 3′ half of SL5 (Fig. 4B, left). Translation initiated at this uAUG generates an N-terminally extended accessory protein and RdRp with molecular masses of 36 kDa and 95 kDa, referred to as p36 and p95; however, the N-terminal extensions are dispensable for viral replication (30). Therefore, to match the size and structure of the CIRV 5′UTR to those of other tombusviruses and to allow for modifications of the downstream structures (i.e., SL5 and PK-TD1) without altering any underlying protein coding, the uAUG in the CIRV genome was inactivated via nucleotide substitutions. The changes made were designed to convert the uAUG to AUC while maintaining pairing in SL5 with a corresponding C-to-G nucleotide exchange in the partner strand (Fig. 4B, right). The resulting genome, termed CIRV*, contained a 143-nt-long 5′UTR, akin to those in other tombusviruses, with corresponding p33 and

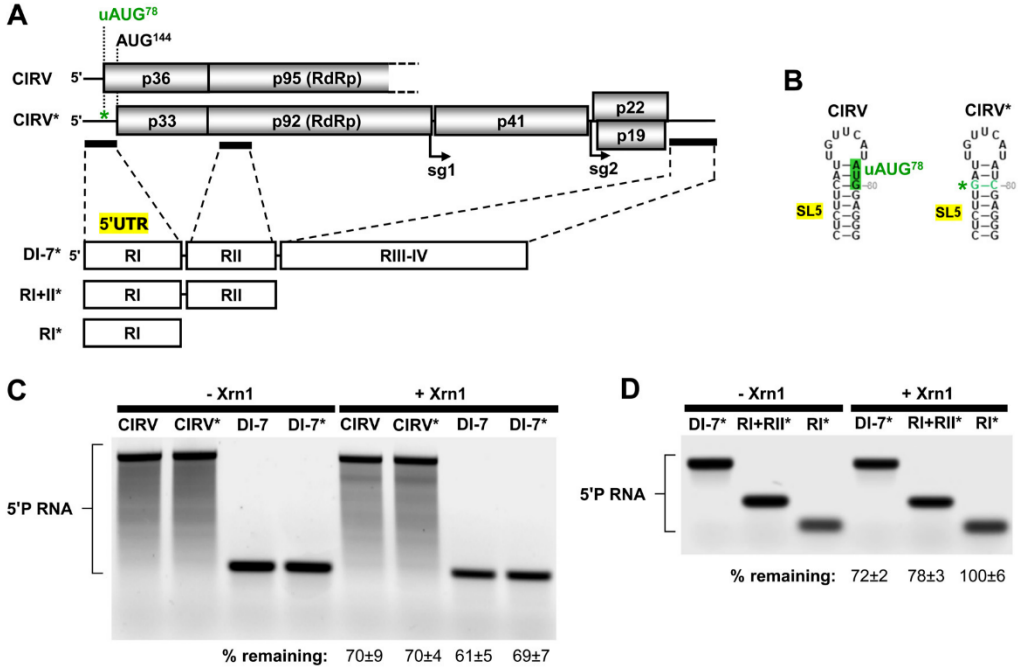

FIG 4 *In vitro* Xrn1 treatment of CIRV, CIRV*, DI-7, and DI-7*. (A) Schematic representation of CIRV, CIRV*, DI-7*, and its deletion derivatives. Open reading frames are represented by gray boxes. The relative location of the uAUG is shown at the top, along with its inactivating mutation in CIRV* and DI-7*, shown as a green asterisk. The genomic segments present in DI-7* are shown directly below the genome as thick black bars, and the corresponding regions are labeled below in white boxes. The location of the 5′UTR (i.e., RI) in DI-7* is highlighted in yellow. (B) Location of the uAUG in SL5 (green highlight) and the substitutions made (green nucleotides) to inactivate the uAUG are shown on the right in CIRV*. (C) *In vitro* Xrn1 treatment of CIRV* and DI-7* versus their WT counterparts. Percentage of input RNA remaining is shown with SEM ($n = 3$). (D) *In vitro* Xrn1 treatment of DI-7* and its truncations. Percentage of input RNA remaining is shown with SEM ($n = 3$).

p92 products translated from AUG^{144} (Fig. 4A). Importantly, the modifications made in the stem of SL5 in CIRV* had negligible impact on Xrn1 resistance compared to wild-type CIRV (Fig. 4C).

Similarly, defective interfering RNA-7 (DI-7), a viral RNA replicon composed of three discontinuous segments of the CIRV genome (Fig. 4A, lower) and its SL5-modified version, DI-7*, exhibited equivalent levels of susceptibility to Xrn1, which were also comparable to those of their full-length genome counterparts (Fig. 4C). DI-7* was constructed and tested along with CIRV* in preparation for its use as a surrogate substrate for CIRV* in later experiments assessing 5′ resistance. Because region-I (RI) of DI-7* corresponded to the 143-nt-long genomic 5′UTR and adjacent AUG^{144}, the replicon also provided a convenient way to assess whether the 5′UTR on its own was capable of blocking Xrn1 access. When viral segments downstream of RI were removed sequentially and tested, the results revealed that the 5′UTR (RI*) is highly effective at independently inhibiting Xrn1 access (Fig. 4D). Thus, the genomic 5′UTR, in the absence of other viral or cellular proteins, is an efficient blocker of Xrn entry.

The CIRV 5′UTR is not an xrRNA. The structural conformation adopted by the 5′UTR can effectively block Xrn1 from accessing 5′-terminal nucleotides (Fig. 4D). To test whether the 5′UTR is also a proficient xrRNA, that is, can efficiently stall an actively digesting Xrn1, different-sized 5′-monophosphorylated leader sequences were attached to the 5′ end of the CIRV genome to provide single-stranded access (Fig. 5A). The A-tract leader sequences appended were not predicted to interfere with 5′UTR folding based on secondary structure predictions (data not shown) (31). Compared to CIRV* (here termed WT), genomes containing a 5′ extension were considerably more

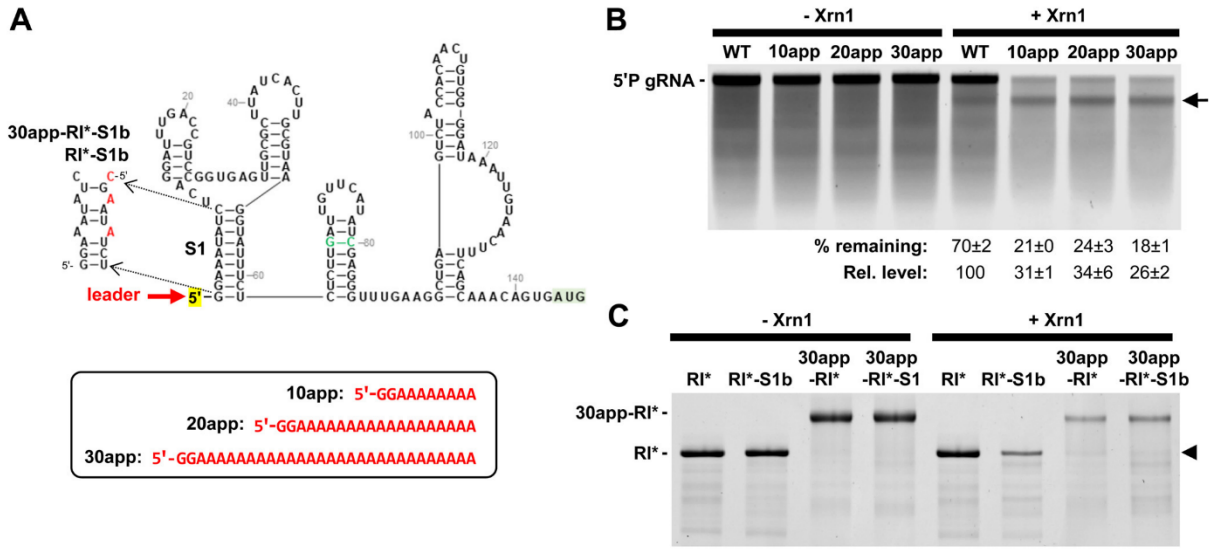

FIG 5 *In vitro* Xrn1 treatment of CIRV* genomes with and without appended poly(A) leaders. (A) RNA secondary structure diagram of the 5′UTR, with leader sequences shown below in red. (B) *In vitro* Xrn1 treatment of CIRV*-based genomes with poly(A) leader sequences. An unknown intermediate degradation product is indicated with an arrow. Percentages of input RNA remaining and relative levels of RNA remaining compared to the wild type (set at 100) are shown with SEM ($n = 3$). (C) *In vitro* Xrn1 treatment of 5′UTRs with (30app-RI*) and without (RI*) poly(A) leader sequences. Reaction products were separated in a denaturing 10% polyacrylamide gel and stained with ethidium bromide. An arrowhead on the right points to a product produced by Xrn1 stalling just upstream of the 5′UTR. A representative gel is shown ($n = 3$).

susceptible to Xrn1 digestion, indicating that the 5′UTR is not an equally effective xrRNA (Fig. 5B). Digestion of the mutants genomes did, however, lead to the accumulation of an intermediate degradation product (Fig. 5B, arrow), suggesting that there are downstream segments of the genome that possess more notable xrRNA activity.

Due to the large size of the viral genomes tested, it could not be determined if the bands corresponding to the remaining full-length genome contained or lacked the A-tracts (Fig. 5B). Accordingly, the 30-nt-long A-tract was 5′ appended to the 5′UTR only, creating 30app-RI*, which would allow for size differentiation between substrates containing the A-tract and Xrn1 products lacking it. Transcripts of RI* (WT 5′UTR) and 30app-RI* (WT 5′UTR with a 30A 5′ appendage) along with respective counterparts with a destabilized stem-1, R1*-S1b and 30app-RI*-S1b (Fig. 5A), were tested in an Xrn1 assay. As observed previously (Fig. 4D), RI* showed a high level of resistance to Xrn1, while RI*-S1b, with its destabilized S1, was notably susceptible (Fig. 5C). The addition of 30A-tracts to the WT and S1-destabilized 5′UTRs in 30app-RI* and 30app-RI*-S1b, respectively, resulted in elevated susceptibility of both to Xrn1 and the presence of a very faint band that migrated at the position of 5′UTR-only transcripts (i.e., RI* and RI*-S1b) (Fig. 5C, arrowhead). Although these minor bands likely represent very inefficient Xrn1 stalling in the A-tract just upstream of the 5′UTR structure, the generation of the band seen in 30app-RI*-S1b containing a destabilized S1, which in RI*-S1b greatly enhanced Xrn1 susceptibility, argues against the slight stalls being dependent on the previously defined higher-order RNA structure of the 5′UTR (26–28). Accordingly, these results indicate that the 5′UTR is not an xrRNA.

RNA secondary structures contribute to Xrn1 and RppH blocking activity. Having established the 5′-entry-blocking activity of the 5′UTR, the next step was to assess the contribution of the different structural components within it. Given their proximity to the 5′ end, the importance of S1 and SL5 was examined first, via compensatory mutational analysis. Destabilization of S1, which includes the 5′ terminus, markedly increased susceptibility of the 5′-monophosphorylated CIRV genome to Xrn1, while restoring base pairing resulted in a notable recovery in resistance (Fig. 6B and C). The removal of the terminal γ- and β-phosphate groups from the 5′-terminal

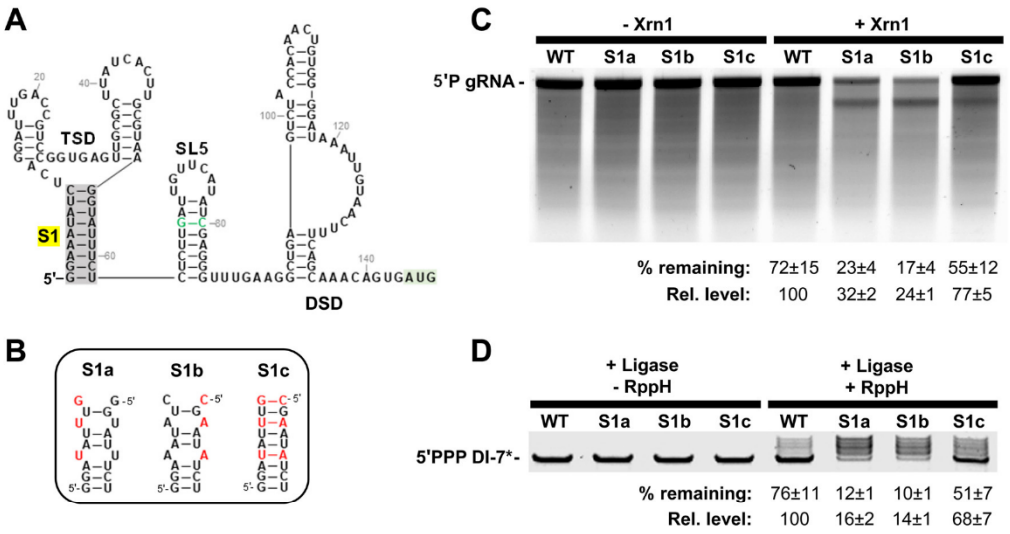

FIG 6 *In vitro* Xrn1 and RppH treatment of S1 mutants. (A) RNA secondary structure diagram of 5′UTR showing S1 stem boxed in gray. (B) S1 mutant series, with modified nucleotides shown in red. (C) *In vitro* Xrn1 treatment of CIRV*-based S1 mutants. Percentages of input RNA remaining and relative levels of RNA remaining compared to the wild type (set at 100) are shown with SEM ($n = 3$). (D) *In vitro* RppH treatment of DI-7*-based S1 mutants. Percentages of unligated RNA and relative levels of unligated RNA compared to wild type (set at 100) are shown with SEM ($n = 3$).

nucleotide triphosphate is a prerequisite for efficient Xrn1 digestion in cells. Thus, to measure accessibility of the 5′-terminal triphosphate to an RNA pyrophosphohydrolase (RppH), the same S1 modifications (Fig. 6B) were tested with *Escherichia coli* RppH in the smaller DI-7* context using a dephosphorylation assay. 5′-Triphosphorylated DI-7* and mutant transcripts treated with RppH were analyzed by PABLO (phosphorylation assay by ligation of oligonucleotides) to determine the phosphorylation state of their 5′-terminal nucleotide after RppH treatment. In this assay, only 5′-triphosphorylated DI-7* transcripts that were converted to 5′-monophosphates by RppH are ligated to a DNA oligonucleotide. This generates a larger product (or products, due to oligonucleotide concatemerization) that can be detected as covalent DI-7* RNA-DNA oligonucleotide hybrids via denaturing gel electrophoresis. Accordingly, the presence of slower-migrating bands is a positive indicator of RppH activity. DI-7* (WT), with its unmodified 5′UTR segment (i.e., RI*), provided obvious protection from RppH compared to mutants with S1 disruptions, and restoration of base pairing with transposed nucleotides notably restored resistance (Fig. 6D).

Next, the S1-adjacent SL5 was examined in a similar manner to determine its importance for 5′-end protection. Disruption of the stem of SL5 enhanced susceptibility of the genome to Xrn1, while restoration of base pairing effectively recovered resistance to wild-type levels (Fig. 7B and C). An additional SL5 mutant, S5CG, was also tested in which the two noncanonical UG base pairs in SL5 were replaced with more stable CG pairs. When challenged with Xrn1, this mutant performed marginally better than the wild type (Fig. 7C). In the RppH assay, similar results were observed for the corresponding DI-7* SL5 mutants, where predicted base pairing stability correlated with protection (Fig. 7D). Overall, these findings implicate RNA secondary structures in the viral 5′UTR, specifically S1 and SL5, as key determinants of resistance to both Xrn1 and RppH.

RNA tertiary structures contribute to Xrn1 and RppH blocking activity. A possible explanation for how SL5 limits Xrn access is that it coaxially stacks on the adjacent S1 stem, forming a tertiary interaction that would further decrease accessibility of the 5′ end (Fig. 8A). To test this idea, one or more uridylates were inserted at the junction

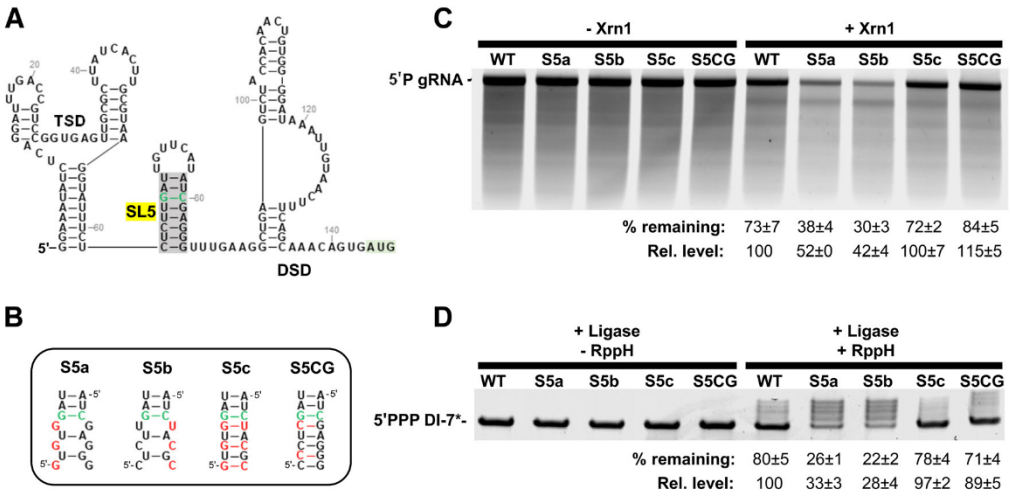

FIG 7 *In vitro* Xrn1 and RppH treatment of SL5 mutants. (A) RNA secondary structure diagram of 5′UTR showing S5 stem boxed in gray. (B) SL5 mutant series, with modified nucleotides shown in red. (C) *In vitro* Xrn1 treatment of CIRV*-based SL5 mutants. Percentages of input RNA remaining and relative levels of RNA remaining compared to wild type (set at 100) are shown with SEM ($n = 3$). (D) *In vitro* RppH treatment of DI-7*-based SL5 mutants. Percentages of unligated RNA and relative levels of unligated RNA compared to the wild type (set at 100) are shown with SEM ($n = 3$).

between the two SL structures that would impede coaxial stacking (Fig. 8A). The addition of one, two, or five residues at this position increased access of both Xrn1 and RppH (Fig. 8B and C). Curiously, mutant CS5 was less susceptible to RppH activity than either CS1 or CS2, while all three mutants were similarly susceptible to Xrn1, suggesting that RppH and Xrn1 differ somewhat in their accessibility requirements.

An additional tertiary interaction, PK-TD1, was also assessed (Fig. 9A). Destabilization of the pseudoknot interaction negatively affected the ability of the 5′UTR to block access to both Xrn1 and RppH (Fig. 9C and D). Collectively, these results are consistent with the idea that RNA tertiary interactions in the CIRV 5′UTR are important for attaining a higher-order RNA conformation that keeps 5′-proximal residues inaccessible to these two 5′-end-targeting enzymes. This notion was further supported by examining the electrophoretic mobility of 5′UTR-only fragments containing the above-described modifications in nondenaturing polyacrylamide gels. In all cases, 5′UTRs with different structurally destabilizing alterations exhibited slower migration, indicative of looser, less compact structural conformations (Fig. 10A and B).

Evidence for 5′UTR-mediated protection in a plant extract. The results presented thus far were carried out using yeast Xrn1, which is the functional homolog of the plant enzyme Xrn4. Due to its cytosolic location, Xrn4 is the most likely candidate for the 5′ targeting of cytosolic CIRV RNAs during infections (9). To gain evidence that Xrn1 was an appropriate surrogate, the effects of the 5′UTR modifications in a plant-based milieu were examined. To do so, a tobacco cell-free lysate (BYL) was employed to determine relative Xrn resistance of 5′-monophosphorylated DI-7* mutants. To confirm that the exoribonucleolytic activity observed was indeed the result of Xrn (32), the SCNMV xrRNA sequence (xrS), which forms a very efficient Xrn-stalling RNA structure (33, 34), was inserted into DI-7* (DI-7*xrS) and its mutants directly after the 5′UTR (i.e., RI*) (Fig. 11A). Stalling of Xrn4 or Xrn1 at xrS would create a readily detectable degradation product (xrS-P) and act as a positive indicator of Xrn activity (Fig. 11A). The results revealed similar trends in xrS-P accumulation from the different DI-7xrS mutants with purified Xrn1 or plant extract containing Xrn4 (Fig. 11B and C). The less intense banding patterns seen for the lysate treatments were likely due to the activity of other ribonucleases present in the plant extract. These findings suggest that the 5′UTR and its mutants respond similarly when confronted with either source of Xrn.

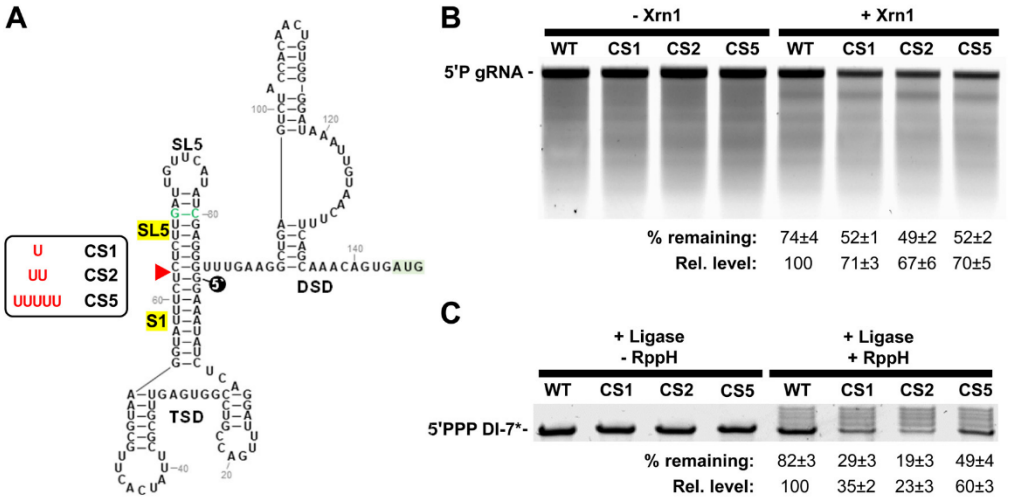

FIG 8 *In vitro* Xrn1 and RppH treatment of CS mutants impairing coaxial stacking. (A) RNA secondary structure diagram of 5′UTR depicting potential coaxial stacking between S1 and S5. The S1-S5 junction is marked by a red arrowhead, and the nucleotides inserted at this position are depicted in red. (B) *In vitro* Xrn1 treatment of CIRV*-based CS mutants. Percentages of input RNA remaining and relative levels of RNA remaining compared to the wild type (set at 100) are shown with SEM ($n = 3$). (C) *In vitro* RppH treatment of DI-7*-based CS mutants. Percentages of unligated RNA and relative levels of unligated RNA compared to the wild type (set at 100) are shown with SEM ($n = 3$).

Effects of monophosphorylation and adenylate capping on viral genome accumulation in plant cells. To test the effect of different 5′ modifications on genome accumulation during plant cell infections, CIRV genomes were transcribed *in vitro* to generate 5′ ends containing either a natural triphosphate (PPP), an adenylate-cap (A-), or a monophosphate (P) (Fig. 12A). The latter two modifications would be present in the *in vitro*-transcribed genomes used to transfect the protoplasts but would be converted to 5′-triphosphates in accumulating progeny genomes. Thus, the major effect of the alterations would occur at the beginning of the infection, immediately following

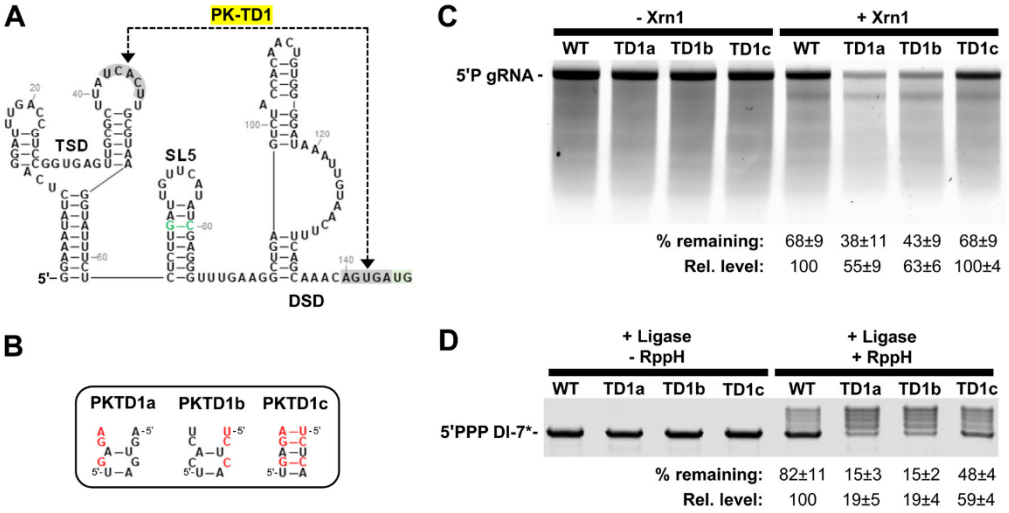

FIG 9 *In vitro* Xrn1 and RppH treatment of PK-TD1 mutants. (A) Secondary structure diagram of 5′UTR showing the PK-TD1 interaction. The location of the partner sequences involved in the pseudoknot are boxed in gray. (B) PK-TD1 mutant series, with modified nucleotides shown in red. (C) *In vitro* Xrn1 treatment of CIRV*-based PK-TD1 mutants. Percentages of input RNA remaining and relative levels of RNA remaining compared to wild type (set at 100) are shown with SEM ($n = 3$). (D) *In vitro* RppH treatment of DI-7*-based PK-TD1 mutants. Percentages of unligated RNA and relative levels of unligated RNA compared to the wild type (set at 100) are shown with SEM ($n = 3$).

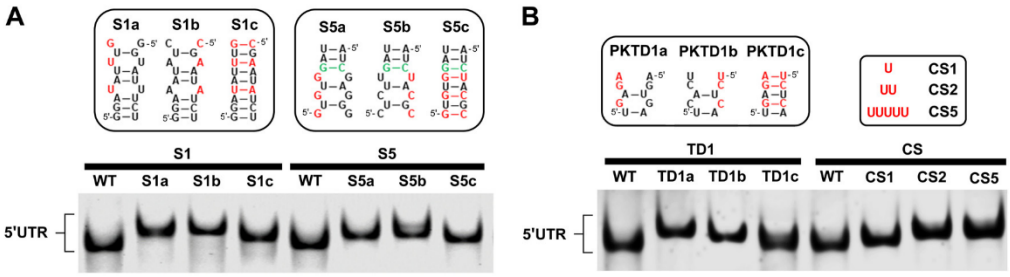

FIG 10 Gel mobility assay of 5′UTR (RI*) mutants. (A) Ethidium bromide (EtBr)-stained nondenaturing 10% polyacrylamide gel of S1 and SL5 series mutants. (B) EtBr-stained polyacrylamide gel of PK-TD1 and CS series mutants. A representative gel is shown ($n = 2$).

transfection. It was anticipated that the A-cap would increase stability of input viral genomes by providing protection against RppH and Xrn4 activity, whereas a monophosphate would decrease stability by making input genomes immediate substrates for Xrn4. Comparing progeny accumulation for input genomes with wild-type 5′UTRs (WT) and triphosphate ends (PPP, set as 100%), corresponding progeny levels for A-capped genomes were lower (A-, 82%), and notably more so for those that were monophosphorylated (P, 9%) (Fig. 12C, far left). The latter result is consistent with input genomes being immediate substrates for Xrn4. The unanticipated lower level of accumulation of progeny genomes in A-cap-modified transfections was most likely due to a defect in replication caused by the added A-cap, because such 5′ modifications are known to negatively impact replication of normally uncapped viral genomes (35). Interestingly, corresponding transfections carried out with mutant sets containing

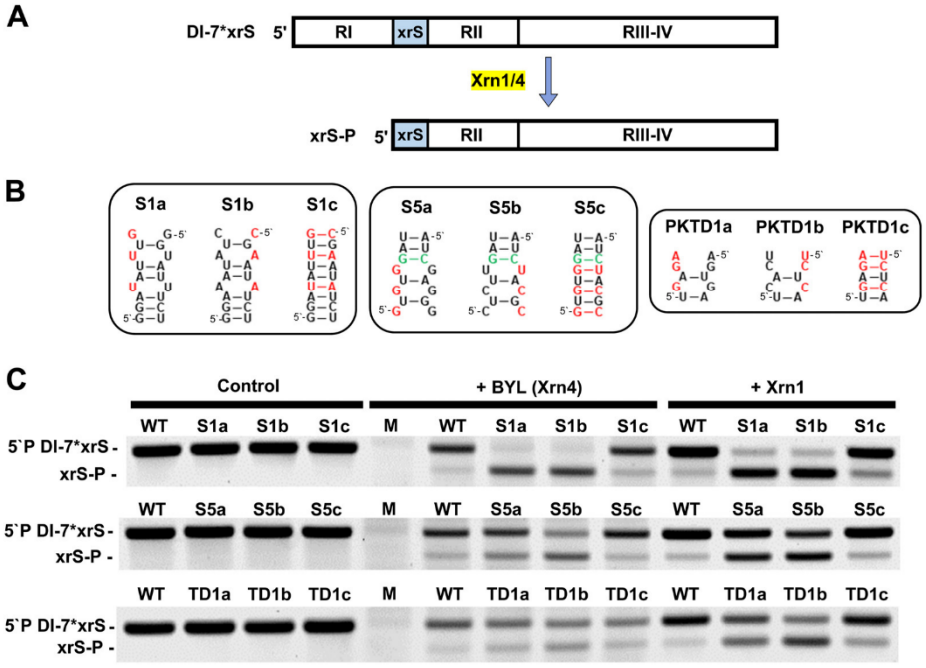

FIG 11 DI-7*xrS 5′UTR mutants treated with BYL extract. (A) Schematic representation of DI-7*xrS construct and xrS-P product formation following Xrn treatment. The blue box indicates the location of the SCNMV xrRNA sequence that stalls Xrn progression. (B) 5′UTR mutations introduced into DI-7*xrS. Nucleotide substitutions are indicated in red. (C) Control untreated DI-7*xrS and mutants (left), BYL extract-treated DI-7*xrS and mutants (middle), and *in vitro* Xrn1-treated DI-7*xrS and mutants (right). The positions of DI-7*xrS and xrS-P are indicated on the left. Representative gels are shown ($n = 2$).

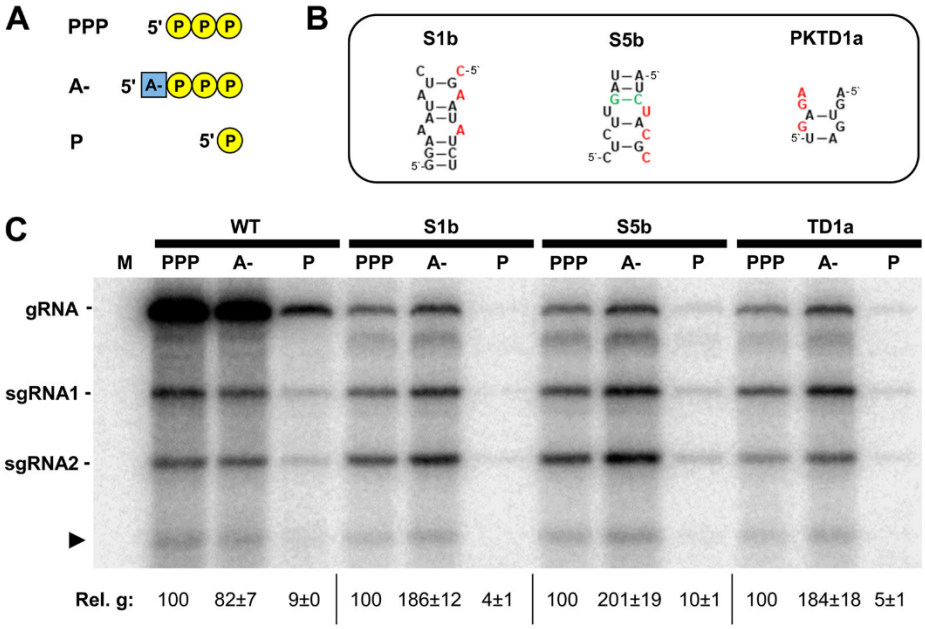

FIG 12 Protoplast infections with 5′-modified CIRV* genomes. (A) 5′ modifications introduced into CIRV*. Phosphate groups are shown as yellow circles, and the 5′-linked adenylate is represented by a blue square. PPP, triphosphate; A-, adenylate cap; P, monophosphate. (B) CIRV* 5′UTR mutants selected for 5′ modification. (C) Northern blot analysis of protoplast infection, with corresponding 5′-modified CIRV* genomes indicated above the lanes. Relative levels of genome accumulation compared to PPP (set at 100) are shown with SEM ($n = 3$).

5′UTRs with destabilized S1, SL5, or PK-TD1 showed increased levels of progeny genome production in A-cap-modified transfections compared to those with triphosphates (~2-fold relative increase) (Fig. 12C). These reciprocal effects, compared to those for WT transfections, suggest that the initial protective effect of the A-cap on input genomes was more beneficial to mutant 5′UTRs, which are more vulnerable to Xrn4. That is, for 5′UTR mutants, the negative effect of the A-cap on RNA replication was offset by its positive effect on RNA stability. Overall, these findings suggest that the low genome accumulation levels observed in mutants with destabilized 5′UTRs can be partially rescued by a protective 5′-modification (i.e., A-capping).

Finally, to examine the effects of different 5′UTR mutations during CIRV infections, protoplasts were transfected with 5′-triphosphorylated WT and variant genomes. Those with destabilized 5′UTRs accumulated much less efficiently than the wild type or genomes with restored structures (Fig. 13C). Notably, additional large virus-derived RNAs were observed in mutant infections with destabilized 5′UTRs that amassed at levels similar to or higher than those of their cognate genomes (Fig. 13C, arrow). These *in vivo*-generated truncated genomes, as well as those observed during *in vitro* Xrn1 treatment of CIRV genomes (Fig. 5C, arrow), will be investigated in detail in future studies. Nevertheless, their detection is consistent with increased 5′-end access of Xrn and implies the presence of stall sites (i.e., xrRNA structures) within the CIRV genome.

DISCUSSION

We have investigated the role of the 5′UTR of the tombusvirus CIRV in protecting its plus-strand RNA genome from 5′-terminal attack by 5′-targeting cellular enzymes. Although this genome is not 5′ capped or protein linked, its 5′UTR can fold into a structural conformation that confers resistance to terminal access by both Xrn and RppH. Here, we describe the unique features of this antidecay defense mechanism and compare and contrast the strategy with those from related studies.

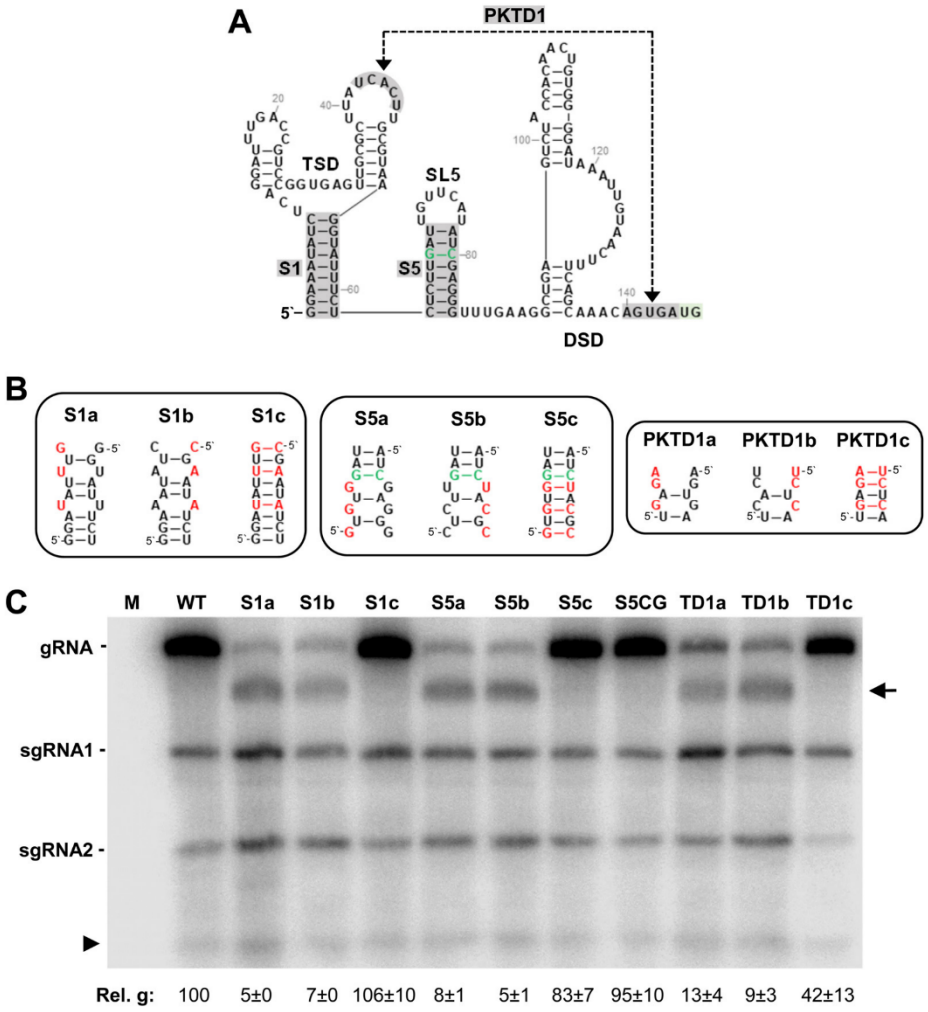

FIG 13 Protoplast infections of CIRV* 5′UTR mutants. (A) RNA secondary structure diagram of 5′UTR showing S1, SL5, and PK-TD1. The p33 start codon is boxed in light green. (B) 5′UTR mutants transfected into protoplasts. Nucleotide substitutions are indicated in red, and the uAUG inactivating mutation is shown in green. (C) Northern blot analysis of protoplast infection of CIRV 5′UTR mutants. An arrow on the right indicates 5′-truncated genomes, and the arrowhead on the left denotes a 3′-derived viral fragment. Relative levels of genome accumulation compared to the wild type (set at 100) are shown with SEM ($n = 3$).

Xrn and tombusvirids. The plus-strand RNA genomes of tombusvirids have a 5′-triphosphorylated nucleotide at their 5′ terminus, which makes them susceptible to 5′-to-3′ exoribonuclease attack. In this regard, Xrn4 has been shown to be a host restriction factor for tombusviruses and is likely also restrictive to other tombusvirids (36). Our results from assessing members of two other genera in the family *Tombusviridae*, TNV-D (genus *Betanecrovirus*) and TCV (genus *Betacarmovirus*), are consistent with the latter notion, as both genomes were more sensitive to Xrn1 attack than CIRV's genome (Fig. 2). The low level of predicted structure in the 5′UTR of the TCV genome and its high sensitivity to Xrn1 digestion suggests that it, and other viruses with less structured 5′ termini, employ alternate means of end protection during infections (e.g., protein binding). In contrast to TCV, the genome of CLSV (genus *Aureusvirus*), which contains a 5′UTR structurally comparable to that in CIRV (29), was highly resistant. This underscores the effectiveness of this shared RNA conformation and helps to explain, at least in part, why similarly folded 5′-terminal RNA structures are also present in satellite RNAs associated with viruses in these genera (37, 38).

CIRV's sg mRNAs were more susceptible to Xrn1 than the genome (Fig. 3). For sg mRNA1, the possibility of stabilization via the 5′ terminus interacting with the 3′CITE was considered but discounted (Fig. 3D). Nonetheless, it remains possible that RNA-mediated stabilization of viral RNAs occurs through long-range RNA-RNA interactions with their 5′UTRs (39). Since sg mRNAs are produced transiently during infections and are not packaged, their resistance to Xrn4 may be less crucial than it is for the genome. However, it is worth noting that susceptibility is not always detrimental, as exemplified by the unique Xrn4/sg mRNA relationship that exists in the genus *Umbravirus* (family *Tombusviridae*), where functionally relevant coding sg mRNAs are generated via Xrn4-mediated digestion (19, 20).

Noncoding xrRNAs corresponding roughly to the viral genomic 3′UTR have been identified in certain tombusvirid infections; these include the dianthovirus red clover necrotic mosaic virus (33) and the betanecrovirus TNV-D (21). Similar 3′UTR-derived genomic fragments have also been observed in some tombusvirus infections (40), including this study (Fig. 12C and 13C, arrowhead). These 3′-terminal fragments have been implicated in modulating viral processes related to translation, genome replication, and/or packaging (41). In tombusvirus infections of plants where Xrn4 was overexpressed, viral genome levels were greatly reduced (42). In some cases, 5′-truncated genomes were generated and, astonishingly, one mutant with a 138-nt-long 5′ deletion was found to be capable of limited independent replication and movement in host plants. Precisely how this viral genome, missing nearly all of its 151-nt-long 5′UTR, was able to survive, albeit minimally, is unclear. Regardless, its extremely limited levels of accumulation and spread underscore the negative impact of Xrn4 overexpression and the importance of maintaining a complete 5′UTR for maximal fitness. The structure and properties of the 5′-truncated genomes that accumulated in our protoplast infections (Fig. 13C, arrow) and *in vitro* assays (Fig. 5B, arrow) remain to be investigated. However, based on their relative sizes, ~3.3 kb, they would lack approximately 1.5 kb of 5′-proximal genomic sequence, including a significant amount of coding sequence, which would render them incapable of self-replication.

Structural features conferring Xrn blocking activity. CIRV's 5′UTR plays important roles in both genome replication and translation of 5′-proximally encoded viral proteins. Different sequence motifs and structures in the plus-strand of the 5′UTR and linear sequences in its complementary minus strand are involved in genome replication (26–28, 43–46), while efficient initiation of translation involves the 5′UTR base pairing with the 3′CITE (47). Accordingly, multiple functional elements involved in different viral processes are integrated within the complex higher-order RNA structure that confers resistance to Xrn decay.

Xrn enzymes require a single-stranded, monophosphorylated 5′-terminal sequence to initiate digestion of an RNA substrate. *In vitro* studies with Xrn1 have shown that as little as a 2-nt single-stranded 5′ extension can permit engagement by Xrn1 (13). One way for an RNA to achieve protection is to incorporate its 5′-terminal nucleotides within an SL structure, preferably one with significant overall stability and optimal base pairing strength at the bottom of the stem. The yeast 20S RNA narnavirus is an uncapped positive-strand RNA virus that protects its 5′ end from Xrn1 digestion by incorporating it in a large and stable SL structure (48). Notably, the 5′-terminal sequence of the 20S RNA genome is 5′-GGGG, which allows for tight binding with its partner sequence, CCCC, at the base of the stem and effective blocking of Xrn1 access.

In contrast, in CIRV and all tombusviruses and aureusviruses, the genomic 5′-terminal nucleotides are A/U rich due to promoter requirements, and this results in less-than-optimal stability of S1 (Fig. 6A). However, S1 stability would be bolstered if it were to coaxially stack on the adjacent helix of SL5 (Fig. 8A), and this tertiary interaction is supported by the observation that maximal Xrn-blocking activity requires both a stable SL5 (Fig. 7) and its directly adjacent placement with S1 (Fig. 8). Xrn access was also inhibited by formation of a second tertiary interaction, PK-TD1 (Fig. 9), which promoted formation of a more compact global 5′UTR structure (Fig. 10). Notably,

modification of any one of the mutationally targeted structural features in the 5′UTR resulted in a more extended structural conformation (Fig. 10). This indicates that a highly cooperative mode of RNA folding is involved in achieving the higher-order structure that effectively blocks Xrn access. Since comparable results were obtained for bacterial RppH access (Fig. 6 to 9), the same RNA structure also may confer CIRV genome protection from plant RppH enzymes. During infections, RppH activity precedes Xrn4 activity in the degradation pathway. The 10-fold higher sensitivity to decay of transfected monophosphorylated CIRV genomes over triphosphorylated counterparts indicates that, *in vivo*, RppH activities are rate limiting (Fig. 12). Furthermore, because RppHs are gatekeepers for Xrn activity, they are also predicted to be restriction factors for CIRV, as has been demonstrated for hepatitis C virus (11, 49).

Defining the anti-Xrn activity of the 5′UTR. For CIRV, the 5′UTR on its own was most resistant to Xrn1 (Fig. 4D), suggesting that sequences downstream from it interfere with proper folding of the inhibitory structure. Notably, although this RNA conformation was able to effectively prevent access of Xrn1, it was not able to stall an actively digesting Xrn1 (Fig. 5). The latter deficiency is not surprising, because as long as 5′-end generation in genome replication is reasonably accurate, there would be no selection pressure to adopt xrRNA properties. Thus, the primary activity and corresponding viral function of the 5′UTR structure is to limit access of Xrn to the viral genome and protect it from 5′-to-3′ exoribonuclease attack, respectively. Consequently, to distinguish the central nuclease-inhibiting property of this RNA structure from that of xrRNAs, we propose the term Xrn-evading RNA, or xeRNA.

Intramolecular or *cis*-xeRNA structures, as in 20S RNA narnavirus and tombusviruses, represent secondary and tertiary structural approaches, respectively, to protect vulnerable 5′-triphosphorylated plus-strand RNA genomes. A different but related tactic, the binding of miRNA-122 to its 5′UTR, is used by hepatitis C virus to guard against attack from both pyrophosphatases and Xrn1 (49–52). *In vitro* assays showed that miRNA binding alone confers genome protection from Xrn1, categorizing the bimolecular interaction as a *trans*-xeRNA structure (51). However, *in vivo*, association of the bound miRNAs with Ago likely further augments shielding of the genomic 5′ terminus, suggesting a multilayered approach to the enzyme blocking strategy (52).

Conclusions. This study has revealed an important role for the 5′UTR of the CIRV genome in conferring protection from 5′-end-targeting enzymes, such as Xrn and RppH. The RNA sequence involved is composed of secondary and tertiary structural components that fold cooperatively into a compact higher-order RNA conformation that efficiently blocks enzyme access. The structure is also highly integrated with RNA elements involved in genome replication and translation initiation, and equivalent counterparts are present in aureusviruses and subviral satellite RNA replicons. As other tombusvirids face similar challenges in their coexistence with these 5′-end-targeting enzymes, it will be interesting to explore the strategies they use to protect their vulnerable genomes and sg mRNAs.

MATERIALS AND METHODS

Viral constructs. The full-length cDNA clones used in this study have been reported previously for CIRV (53), cucumber leaf spot virus (CLSV) (54), tobacco necrosis virus-D (TNV-D) (55), turnip crinkle virus (TCV) (56), and DI-7 (24). CIRV subgenomic clones and transcripts were generated as described previously (57). Mutants were derived from CIRV* and DI-7* cDNA constructs, which lacked the upstream AUG (see Results). DI-7*xrS was generated by inserting the SCNMV xrRNA sequence downstream of the 5′UTR in DI-7* (19). Standard overlapping PCR-based mutagenesis was used to introduce mutations into the cDNA clones, which were then sequenced to ensure that only the intended modifications were incorporated.

***In vitro* transcription and viral RNAs.** All RNAs were *in vitro* transcribed from either SmaI-linearized clones or PCR-generated templates using a T7-FlashScribe transcription kit as described previously (21). Monophosphorylated RNAs were generated as described previously (21), and RNAs containing a 5′ApppG cap were transcribed using a 10-fold molar excess of cap analog over GTP. Transcript integrity was verified by agarose gel electrophoresis. All RNA structures were generated using UNAfold structure prediction software and arranged with RNA2Drawer (31, 58).

Protoplast infections and Northern blot analyses. Cucumber protoplasts were isolated from 6-day-old cotyledon leaves as described previously (40). Following isolation, approximately 3×10^5 protoplasts were transfected with 1 μg of genomic CIRV transcripts using polyethylene glycol (PEG)-$CaCl_2$. Transfected

protoplasts were incubated at 22°C for 22 h. Total nucleic acid content was extracted using phenol-chloroform-isoamyl alcohol (PCI) and then ethanol precipitated, after which one-sixth of the total volume was separated in 1.4% agarose gels. Following transfer to nylon, Northern blot analysis was performed using a previously described ^{32}P-labeled DNA oligonucleotide probe, P9, which is complementary to the 3′ terminus of the CIRV genome (59). All protoplast infections were repeated at least three times.

***In vitro* Xrn1 digestion assay.** Viral RNAs were transcribed in the presence of excess monophosphorylated-GTP, resulting in its preferential incorporation as the 5′-proximal nucleotide during *in vitro* transcription with T7 polymerase (21). The Xrn1 assay conditions used yielded ~70% remaining product for WT CIRV, which allowed for facile detection of increased (or decreased) digestion of different CIRV 5′UTR mutants as well as different viral genomes (e.g., CLSV, TNV-D, and TCV). *In vitro* Xrn1 degradation assays were performed as described previously using 2 μg of 5′-monophosphorylated *in vitro*-transcribed RNA and 0.06 U recombinant yeast Xrn1 (New England Biolabs [NEB]) (21). Xrn1 reaction mixtures were incubated at 37°C for 2 h. Following PCI extraction, samples were ethanol precipitated in the presence of glycogen. One-quarter of the recovered RNAs were separated in either 1.4% or 2% agarose gels for nondenaturing conditions or urea-polyacrylamide gels (8 M urea, 10% polyacrylamide) for denaturing conditions, followed by staining with ethidium bromide. Each experiment was repeated three times.

***In vitro* RppH treatment and PABLO analysis.** Dephosphorylation assays were performed in a manner similar to that of Xrn1 digestion assays, except that purified recombinant RppH from *E. coli* (NEB) was used. Two micrograms of *in vitro*-transcribed DI-7* RNA was treated with 5 U of RppH for 2 h at 37°C. Following PCI purification and ethanol precipitation, one-quarter of the isolated RNA was subjected to a modified PABLO (phosphorylation assay by ligation of oligonucleotides), which was described previously (60). Briefly, isolated RNAs were heat denatured at 95°C for 5 min with 20 pmol oligonucleotide X (CCCCCCCCCCCCCCCCCCCCCCCCCCCCCCCCCCCCCCCCCCCCCCCCCCCCCCCCCCCCCCCCCCCCCCCCCGAACAATATGAATGATAACTTG) and 4 pmol of oligonucleotide Y1 (TCAAATCCTGAGATATTTCCCAAGTTATCATTCATATTGTTC) or Y2 (for mutants S1a and S1c only; TCAAATCCTGACAAATATCCCAAGTTATCATTCATATTGTTC) and then cooled gradually to 30°C for 30 min. Ligation mixtures (1 μl T4 DNA ligase [NEB], 0.5 μl RNase inhibitor [40 U/μl], 2 μl 10× T4 DNA ligase buffer [NEB], 1 μl 20 mM ATP, 4.5 μl H_2O-diethyl pyrocarbonate [DEPC]) were then added to the reaction mixtures on ice, which were then incubated at 37°C for 2 h. Reactions were quenched with 10 μl of 10 mM EDTA, PCI extracted, and ethanol precipitated in the presence of glycogen. Washed pellets were then dissolved in 5 μl of H_2O-DEPC and combined with 15 μl of RNA loading buffer, after which one-quarter of the sample was separated in a 5% denaturing urea-polyacrylamide gel. All reactions were repeated three times.

RNA EMSA. RNAs subjected to electrophoretic mobility shift assays (EMSAs) were *in vitro* transcribed from PCR templates as described above. A modified version of a previously described EMSA protocol (61) was used in the present study. Briefly, 10 pmol RNA was heated at 94°C for 2 min, followed by snap cooling on ice. Reactions were then combined with 1× RNA binding buffer (5 mM HEPES, 6 mM $MgCl_2$, 100 mM KCl, 3.8% glycerol) and incubated at 37°C for 30 min. The RNAs were then placed on ice, combined with 20% glycerol (10% glycerol final), and separated in a 10% nondenaturing polyacrylamide gel in the presence of 1 mM $MgCl_2$, followed by staining with ethidium bromide.

Xrn digestion using BYL cell extract. Ten micrograms of ALiCE cell extract (Sigma) was incubated with 1 μg of DI-7*xrS RNA for 20 min at 25°C. RNAs were then PCI extracted and ethanol precipitated in the presence of glycogen. Once dissolved in DEPC-treated water, one-quarter of the reaction was separated in 2% agarose gels and stained with ethidium bromide. Each experiment was repeated twice, with similar results.

ACKNOWLEDGMENTS

We thank members of our lab for reviewing the manuscript.

This work was supported by the Natural Sciences and Engineering Research Council of Canada (NSERC). C.D.G. and J.S.H.I. were both supported by Ontario Graduate Scholarships.

REFERENCES

1. Molleston JM, Cherry S. 2017. Attacked from all sides: RNA decay in antiviral defense. Viruses 9:2. https://doi.org/10.3390/v9010002.
2. Gaglia MM, Glaunsinger BA. 2010. Viruses and the cellular RNA decay machinery. Wiley Interdiscip Rev RNA 1:47–59. https://doi.org/10.1002/wrna.3.
3. Li F, Wang A. 2019. RNA-targeted antiviral immunity: more than just RNA silencing. Trends Microbiol 27:792–805. https://doi.org/10.1016/j.tim.2019.05.007.
4. May JP, Yuan X, Sawicki E, Simon AE. 2018. RNA virus evasion of nonsense-mediated decay. PLoS Pathog 14:e1007459. https://doi.org/10.1371/journal.ppat.1007459.
5. May JP, Simon AE. 2021. Targeting of viral RNAs by Upf1-mediated RNA decay pathways. Curr Opin Virol 47:1–8. https://doi.org/10.1016/j.coviro.2020.11.002.
6. May JP, Johnson PZ, Ilyas M, Gao F, Simon AE. 2020. The multifunctional long-distance movement protein of pea enation mosaic virus 2 protects viral and host transcripts from nonsense-mediated decay. mBio 11:e00204-20. https://doi.org/10.1128/mBio.00204-20.
7. Stevens A. 2001. 5`-Exoribonuclease 1: Xrn1. Methods Enzymol 342:251–259. https://doi.org/10.1016/s0076-6879(01)42549-3.
8. Łabno A, Tomecki R, Dziembowski A. 2016. Cytoplasmic RNA decay pathways–enzymes and mechanisms. Biochim Biophys Acta 1863:3125–3147. https://doi.org/10.1016/j.bbamcr.2016.09.023.
9. Kastenmayer JP, Green PJ. 2000. Novel features of the XRN-family in Arabidopsis: evidence that AtXrn4, one of several orthologs of nuclear Xrn2p/Rat1p, functions in the cytoplasm. Proc Natl Acad Sci U S A 97:13985–13990. https://doi.org/10.1073/pnas.97.25.13985.
10. Nagarajan VK, Jones CI, Newbury SF, Green PJ. 2013. XRN 5′->3′ exoribonucleases: structure, mechanisms and functions. Biochim Biophys Acta 1829:590–603. https://doi.org/10.1016/j.bbagrm.2013.03.005.

11. Kincaid RP, Lam VL, Chirayil RP, Randall G, Sullivan CS. 2018. RNA triphosphatase DUSP11 enables exonuclease XRN-mediated restriction of hepatitis C virus. Proc Natl Acad Sci U S A 115:8197–8202. https://doi.org/10.1073/pnas.1802326115.
12. Jinek M, Coyle SM, Doudna JA. 2011. Coupled 5′ nucleotide recognition and processivity in Xrn1-mediated mRNA decay. Mol Cell 41:600–608. https://doi.org/10.1016/j.molcel.2011.02.004.
13. Langeberg CJ, Welch WRW, McGuire JV, Ashby A, Jackson AD, Chapman EG. 2020. Biochemical characterization of yeast Xrn1. Biochemistry 59:1493–1507. https://doi.org/10.1021/acs.biochem.9b01035.
14. Decker CJ, Parker R. 1993. A turnover pathway for both stable and unstable mRNAs in yeast: evidence for a requirement for deadenylation. Genes Dev 7:1632–1643. https://doi.org/10.1101/gad.7.8.1632.
15. Poole TL, Stevens A. 1997. Structural modifications of RNA influence the 5' exoribonucleolytic hydrolysis by XRN1 and HKE1 of Saccharomyces cerevisiae. Biochem Biophys Res Commun 235:799–805. https://doi.org/10.1006/bbrc.1997.6877.
16. Kieft JS, Rabe JL, Chapman EG. 2015. New hypotheses derived from the structure of a flaviviral Xrn1-resistant RNA: conservation, folding, and host adaptation. RNA Biol 12:1169–1177. https://doi.org/10.1080/15476286.2015.1094599.
17. Chapman EG, Costantino DA, Rabe JL, Moon SL, Wilusz J, Nix JC, Kieft JS. 2014. The structural basis of pathogenic subgenomic flavivirus RNA (sfRNA) production. Science 344:307–310. https://doi.org/10.1126/science.1250897.
18. Slonchak A, Khromykh AA. 2018. Subgenomic flaviviral RNAs: what do we know after the first decade of research. Antiviral Res 159:13–25. https://doi.org/10.1016/j.antiviral.2018.09.006.
19. Steckelberg AL, Vicens Q, Kieft JS. 2018. Exoribonuclease-resistant RNAs exist within both coding and noncoding subgenomic RNAs. mBio 9:e02461-18. https://doi.org/10.1128/mBio.02461-18.
20. Ilyas M, Du Z, Simon AE. 2021. Opium poppy mosaic virus has an Xrn-resistant, translated subgenomic RNA and a BTE 3' CITE. J Virol 95:e02109-20. https://doi.org/10.1128/JVI.02109-20.
21. Gunawardene CD, Newburn LR, White KA. 2019. A 212-nt long RNA structure in the tobacco necrosis virus-D RNA genome is resistant to Xrn degradation. Nucleic Acids Res 47:9329–9342. https://doi.org/10.1093/nar/gkz668.
22. Charley PA, Wilusz CJ, Wilusz J. 2018. Identification of phlebovirus and arenavirus RNA sequences that stall and repress the exoribonuclease XRN1. J Biol Chem 293:285–295. https://doi.org/10.1074/jbc.M117.805796.
23. Moon SL, Blackinton JG, Anderson JR, Dozier MK, Dodd BJ, Keene JD, Wilusz CJ, Bradrick SS, Wilusz J. 2015. XRN1 stalling in the 5' UTR of hepatitis C virus and bovine viral diarrhea virus is associated with dysregulated host mRNA stability. PLoS Pathog 11:e1004708. https://doi.org/10.1371/journal.ppat.1004708.
24. Cimino PA, Nicholson BL, Wu B, Xu W, White KA. 2011. Multifaceted regulation of translational readthrough by RNA replication elements in a tombusvirus. PLoS Pathog 7:e1002423. https://doi.org/10.1371/journal.ppat.1002423.
25. Nicholson BL, Wu B, Chevtchenko I, White KA. 2010. Tombusvirus recruitment of host translational machinery via the 3′ UTR. RNA 16:1402–1419. https://doi.org/10.1261/rna.2135210.
26. Wu B, Vanti WB, White KA. 2001. An RNA domain within the 5′untranslated region of the tomato bushy stunt virus genome modulates RNA replication. J Mol Biol 305:741–756. https://doi.org/10.1006/jmbi.2000.4298.
27. Ray D, Wu B, White KA. 2003. A second functional RNA domain in the 5′ UTR of the Tomato bushy stunt virus genome: intra- and interdomain interactions mediate viral RNA replication. RNA 9:1232–1245. https://doi.org/10.1261/rna.5630203.
28. Ray D, Na H, White KA. 2004. Structural properties of a multifunctional T-shaped RNA domain that mediate efficient Tomato bushy stunt virus replication. J Virol 78:10490–10500. https://doi.org/10.1128/JVI.78.19.10490-10500.2004.
29. Lee PK, White KA. 2014. Construction and characterization of an aureusvirus defective RNA. Virology 452–453:67–74. https://doi.org/10.1016/j.virol.2013.12.033.
30. Burgyan J, Rubino L, Russo M. 1996. The 5'-terminal region of a tombusvirus genome determines the origin of multivesicular bodies. J Gen Virol 77:1967–1974. https://doi.org/10.1099/0022-1317-77-8-1967.
31. Zuker M. 2003. Mfold web server for nucleic acid folding and hybridization prediction. Nucleic Acids Res 31:3406–3415. https://doi.org/10.1093/nar/gkg595.
32. Russo J, Mundell CT, Charley PA, Wilusz C, Wilusz J. 2019. Engineered viral RNA decay intermediates to assess XRN1-mediated decay. Methods 155:116–123. https://doi.org/10.1016/j.ymeth.2018.11.019.
33. Iwakawa HO, Mizumoto H, Nagano H, Imoto Y, Takigawa K, Sarawaneeyaruk S, Kaido M, Mise K, Okuno T. 2008. A viral noncoding RNA generated by cis-element-mediated protection against 5'->3' RNA decay represses both cap-independent and cap-dependent translation. J Virol 82:10162–10174. https://doi.org/10.1128/JVI.01027-08.
34. Steckelberg A-L, Akiyama BM, Costantino DA, Sit TL, Nix JC, Kieft JS. 2018. A folded viral noncoding RNA blocks host cell exoribonucleases through a conformationally dynamic RNA structure. Proc Natl Acad Sci U S A 115:6404–6409. https://doi.org/10.1073/pnas.1802429115.
35. Allen E, Wang S, Miller WA. 1999. Barley yellow dwarf virus RNA requires a cap-independent translation sequence because it lacks a 5' cap. Virology 253:139–144. https://doi.org/10.1006/viro.1998.9507.
36. Jaag HM, Nagy PD. 2009. Silencing of Nicotiana benthamiana Xrn4p exoribonuclease promotes tombusvirus RNA accumulation and recombination. Virology 386:344–352. https://doi.org/10.1016/j.virol.2009.01.015.
37. Zhang L, Zitter TA, Palukaitis P. 1991. Helper virus-dependent replication, nucleotide sequence and genome organization of the satellite virus of maize white line mosaic virus. Virology 180:467–473. https://doi.org/10.1016/0042-6822(91)90060-o.
38. Ashton P, Wu B, D'Angelo J, Grigull J, White KA. 2015. Biologically-supported structural model for a viral satellite RNA. Nucleic Acids Res 43:9965–9977. https://doi.org/10.1093/nar/gkv917.
39. Chkuaseli T, White KA. 2018. Intragenomic long-distance RNA-RNA interactions in plus-strand RNA plant viruses. Front Microbiol 9:529. https://doi.org/10.3389/fmicb.2018.00529.
40. White KA, Morris TJ. 1994. Recombination between defective tombusvirus RNAs generates functional hybrid genomes. Proc Natl Acad Sci USA 91:3642–3646. https://doi.org/10.1073/pnas.91.9.3642.
41. Miller WA, Shen R, Staplin W, Kanodia P. 2016. Noncoding RNAs of plant viruses and viroids: sponges of host translation and RNA interference machinery. Mol Plant Microbe Interact 29:156–164. https://doi.org/10.1094/MPMI-10-15-0226-FI.
42. Cheng CP, Jaag HM, Jonczyk M, Serviene E, Nagy PD. 2007. Expression of the Arabidopsis Xrn4p 5'-3' exoribonuclease facilitates degradation of tombusvirus RNA and promotes rapid emergence of viral variants in plants. Virology 368:238–248. https://doi.org/10.1016/j.virol.2007.07.001.
43. Panavas T, Pogany J, Nagy PD. 2002. Analysis of minimal promoter sequences for plus-strand synthesis by the cucumber necrosis virus RNA-dependent RNA polymerase. Virology 296:263–274. https://doi.org/10.1006/viro.2002.1423.
44. Panavas T, Nagy PD. 2005. Mechanism of stimulation of plus-strand synthesis by an RNA replication enhancer in a tombusvirus. J Virol 79:9777–9785. https://doi.org/10.1128/JVI.79.15.9777-9785.2005.
45. Wang RY, Nagy PD. 2008. Tomato bushy stunt virus co-opts the RNA-binding function of a host metabolic enzyme for viral genomic RNA synthesis. Cell Host Microbe 3:178–187. https://doi.org/10.1016/j.chom.2008.02.005.
46. Kovalev N, Pogany J, Nagy PD. 2012. A co-opted DEAD-Box RNA helicase enhances tombusvirus plus-strand synthesis. PLoS Pathog 8:e1002537. https://doi.org/10.1371/journal.ppat.1002537.
47. Nicholson BL, White KA. 2008. Context-influenced cap-independent translation of Tombusvirus mRNAs in vitro. Virology 380:203–212. https://doi.org/10.1016/j.virol.2008.08.003.
48. Esteban R, Vega L, Fujimura T. 2008. 20S RNA narnavirus defies the antiviral activity of SKI1/XRN1 in Saccharomyces cerevisiae. J Biol Chem 283:25812–25820. https://doi.org/10.1074/jbc.M804400200.
49. Amador-Cañizares Y, Bernier A, Wilson JA, Sagan SM. 2018. miR-122 does not impact recognition of the HCV genome by innate sensors of RNA but rather protects the 5' end from the cellular pyrophosphatases, DOM3Z and DUSP11. Nucleic Acids Res 46:5139–5158. https://doi.org/10.1093/nar/gky273.
50. Thibault PA, Huys A, Amador-Cañizares Y, Gailius JE, Pinel DE, Wilson JA. 2015. Regulation of hepatitis C virus genome replication by Xrn1 and microRNA-122 binding to individual sites in the 5' untranslated region. J Virol 89:6294–6311. https://doi.org/10.1128/JVI.03631-14.
51. Mortimer SA, Doudna JA. 2013. Unconventional miR-122 binding stabilizes the HCV genome by forming a trimolecular RNA structure. Nucleic Acids Res 41:4230–4240. https://doi.org/10.1093/nar/gkt075.
52. Li Y, Masaki T, Yamane D, McGivern DR, Lemon SM. 2013. Competing and noncompeting activities of miR-122 and the 5' exonuclease Xrn1 in regulation of hepatitis C virus replication. Proc Natl Acad Sci U S A 110:1881–1886.https://doi.org/10.1073/pnas.1213515110.
53. Rubino L, Burgyan J, Russo M. 1995. Molecular cloning and complete nucleotide sequence of carnation Italian ringspot tombusvirus genomic and defective interfering RNAs. Arch Virol 140:2027–2039. https://doi.org/10.1007/BF01322690.

54. Reade R, Miller J, Robbins M, Xiang Y, Rochon D. 2003. Molecular analysis of the cucumber leaf spot virus genome. Virus Res 91:171–179. https://doi.org/10.1016/s0168-1702(02)00251-4.
55. Coutts RH, Rigden JE, Slabas AR, Lomonossoff GP, Wise PJ. 1991. The complete nucleotide sequence of tobacco necrosis virus strain D. J Gen Virol 72:1521–1529. https://doi.org/10.1099/0022-1317-72-7-1521.
56. Heaton LA, Carrington JC, Morris TJ. 1989. Turnip crinkle virus infection from RNA synthesized in vitro. Virology 170:214–218. https://doi.org/10.1016/0042-6822(89)90368-1.
57. Chkuaseli T, Newburn LR, Bakhshinyan D, White KA. 2015. Protein expression strategies in tobacco necrosis virus-D. Virology 486:54–62. https://doi.org/10.1016/j.virol.2015.08.032.
58. Johnson PZ, Kasprzak WK, Shapiro BA, Simon AE. 2019. RNA2Drawer: geometrically strict drawing of nucleic acid structures with graphical structure editing and highlighting of complementary subsequences. RNA Biol 16:1667–1671. https://doi.org/10.1080/15476286.2019.1659081.
59. Chkuaseli T, White KA. 2020. Activation of viral transcription by stepwise largescale folding of an RNA virus genome. Nucleic Acids Res 48:9285–9300. https://doi.org/10.1093/nar/gkaa675.
60. Celesnik H, Deana A, Belasco JG. 2008. PABLO analysis of RNA: 5`-phosphorylation state and 5`-end mapping. Methods Enzymol 447:83–98. https://doi.org/10.1016/S0076-6879(08)02205-2.
61. Fabian MR, White KA. 2006. Analysis of a 3′-translation enhancer in a tombusvirus: a dynamic model for RNA–RNA interactions of mRNA termini. RNA 12:1304–1314. https://doi.org/10.1261/rna.69506.

CHAPTER 4:

DISCUSSION

4.1…Study overview

Plant viruses have evolved different methods for evading and, at times, exploiting the host antiviral response system. Several studies have suggested that interactions occur between Xrn4 and members of the family *Tombusviridae*, and the results imply that Xrn4 acts primarily as an inhibitory host protein (i.e. restriction factor) during viral infections. The specific mechanisms underlying the inhibitory role of Xrn4 have not been explored prior to the work presented in this dissertation. In addition, although a canonical xrRNA structure was identified previously in the *Tombusviridae* family (i.e. SR1f in RCNMV), there were no reposts of novel resistant RNA structures that belie traditional xrRNA classification.

The focus of this dissertation was to elucidate the role of Xrn4 in the viral life-cycle of two tombusvirids, one in the genus *Tombusvirus* and the other in the genus *Betanecrovirus*. The studies conducted on these two viruses, presented in the form of published, peer-reviewed journal articles, detail the activity of Xrn4 in two distinct viral processes: 3'-noncoding RNA generation and 5'-end protection. Overall, the findings outline a novel xrRNA-like inhibitory RNA structure in the TNV-D 3'UTR that stalls Xrn4 to produce a noncoding, functionally-relevant svRNA, and a protective role for the tombusvirus 5'UTR in preventing access to Xrn4.

The two studies presented in this dissertation describe avoidance and utilization mechanisms of Xrn4 by two members of the *Tombusviridae* family. Through a highly structured 5'UTR, the tombusvirus CIRV is able to evade access and prevent decay of its viral genome by Xrn4, whereas the betanecrovirus TNV-D employs an xrRNA-like structure in its 3'UTR to stall Xrn4 and generate a proviral, noncoding RNA. These two unique examples add to the repertoire of viral mechanisms that promote infection through evasive or exploitative means when confronted by the host's antiviral defense system. The key findings of both projects are summarized below:

i) An svRNA comprising most of the TNV-D 3'UTR is generated from incomplete digestion of primarily TNV-D sg mRNA1 by Xrn4.

ii) The resistant RNA structure responsible for svRNA formation involves the base of the BTE, parts of SL2, and the replication silencer interaction, and is not transposable beyond its original viral context. The absence of this latter trait precludes its classification as a traditional xrRNA.

iii) The TNV-D svRNA is able to *trans*-inhibit protein translation from capped and uncapped RNA templates, most likely by soaking up translation initiation factors via its BTE.

iv) Cooperative interaction between secondary and tertiary level RNA structures in the tombusvirus 5'UTR act to bury and protect the 5' terminus from Xrn accessibility, and subsequent decay.

v) The tombusvirus 5'UTR does not resist actively digesting Xrn, but instead prevents 5' access to the enzyme. It is therefore not considered to be an xrRNA and is more accurately described as an Xrn-evading RNA (xeRNA).

vi) The tombusvirus 5'UTR not only protects the 5' nucleotide from Xrn4 access and decay, but also from pyrophosphatase-mediated dephoshorylation of the two 5' terminal phosphates. Since dephosphorylation of the viral RNA precedes Xrn4 digestion, this step is most likely rate-limiting for degradation of uncapped, triphosphorylated viral RNAs.

vii) Replication-deficient 5'UTR mutants generated an additional viral RNA species, most likely the product of incomplete Xrn digestion. Capping of the 5' end rescues accumulation of the defective 5'UTR mutants in protoplasts infections.

The two projects outlined in this dissertation began with the observation that a small viral RNA (svRNA) accumulates during plant protoplast infection of the betanecrovirus TNV-D. Its size, coupled with its detection in northern blots using a 3' terminal probe confirmed its origin from the viral 3'UTR. Based on previous work showing that 5'-to-3' exoribonuclease-resistant RNAs (xrRNAs) are responsible for the production of noncoding RNAs generated from the viral 3'UTR (Iwakawa et al., 2008), we tested whether a similar structure may be responsible for production of the TNV-D svRNA. We managed to confirm this, and in doing so, uncovered additional details regarding the unique stalling structure, which we determined to be an outlier among xrRNAs, not quite fulfilling all the criteria necessary for xrRNA classification (Gunawardene et al., 2019).

Following this, we wanted to determine whether 5'-to-3' exoribonucleases also interacted with the 5' end of TNV-D genomic RNA, given that these single-stranded plus-strand RNA viruses contain genomes with uncapped, and thus unprotected, 5' termini. Prior studies had shown that other members of *Tombusviridae*, i.e. tombusviruses, are negatively impacted by Xrn4 expression (Cheng et al., 2006; Cheng et al., 2007). As an initial test, we challenged the *in vitro* transcribed 5'-monophosphorylated TNV-D genome with purified Xrn1, alongside the RNA genomes of other members of the *Tombusviridae* family, including a tombusvirus, an aureusvirus, and a carmovirus. The results from this *in vitro* experiment showed that TNV-D was not as well protected from exoribonuclease activity as the tombusvirus CIRV, or the aureusvirus CLSV. More importantly, however, was that we noticed a trend in the degradation profiles of the tested RNA substrates, where those viral RNA genomes with more highly structured 5'UTRs (e.g. CIRV and CLSV) were more resistant to Xrn1 activity than those with minimal structure (e.g. TNV-D and TCV). This result, along with the fact that tombusvirus 5'UTRs had been extensively structurally characterized (Wu et al., 2001; Ray et al., 2003, 2004), led us to focus our investigation on the resistance of the CIRV 5'UTR to Xrn. The results from this second study led us to conclude that the CIRV 5'UTR uses a distinct, evasive structure-based mechanism to confound Xrn1-mediated degradation.

4.2…Two distinct modes of Xrn inhibition by tombusvirid RNAs

Xrn1/4 is a highly processive 5'-to-3' exoribonuclease that functions in the cytosol on single-stranded, 5'-monophosphorylated RNA. Early biochemical analysis of its catalytic activity showed that Xrn1 is inhibited by G-rich tracts in the RNA substrate (Stevens, 2001). The presence of G-rich regions in some RNA viruses has been shown to inhibit Xrn1, likely through the formation of G-quadruplex RNA structures (Charley et al., 2018). Other types of internal RNA structures also able to stall an actively digesting Xrn and generate decay intermediates of viral RNA genomes have also been described in detail (Kieft et al., 2015; Jones et al., 2021; Vicens and Kieft, 2021). In contrast, some viral RNA genomes contain 5'-terminal structures that do not permit Xrn engagement (Esteban et al., 2008; Gunawardene et al., 2021). Collectively, these findings indicate that there are clear distinctions in how RNAs defend themselves against the enzyme's activity; i.e. (i) stalling an actively digesting Xrn, versus (ii) preventing Xrn from gaining 5'-end access.

4.2.1. Stalling of Xrn by viral RNA

Exoribonuclease-resistant RNAs (xrRNAs) are discrete RNA sequences capable to independently blocking actively digesting 5'-to-3' exoribonucleases such as Xrn1/4. Previous studies on dianthoviruses and flaviviruses found that these viruses used xrRNA structures in their viral genomes to stall Xrn1/4 in order to generate functional noncoding RNAs, called SR1f and sfRNAs, respectively (Vicens and Kieft, 2021). The findings presented in this dissertation show that the TNV-D svRNA that accumulated in infections is the product of incomplete digestion of primarily sg mRNA1 by Xrn4 (**Figure 1**) (Gunawardene et al., 2019). Based on our findings, we determined that a potential function of the svRNA is related to protein translation, where it would act as a viral RNA sponge to soak up host translation factors (**Figure 1**). Given that the svRNA

is generated primarily from sg mRNA1, which is transcribed from the genome during late infection (Jiwan et al., 2011), its accumulation could act as a switch to downregulate genome translation and trigger encaspidation once threshold amounts of sg mRNA1 and capsid protein are attained.

The RNA structure responsible for TNV-D svRNA production is able to stall actively digesting Xrn. Stalling of Xrn in this context presumably requires the formation of some type of RNA knot, similar to the one formed by xrRNAs from flaviviruses and dianthoviruses. However, the inhibitory RNA structure in the TNV-D 3'UTR was less effective at stalling purified Xrn1 *in vitro* than the known knot-like RNA structures (Gunawardene, unpublished observations), suggesting that an alternative conformation may be involved. Also, the addition of as little as one nucleotide to the 3' end of the 3'UTR abolished Xrn stalling, indicating that the so-called silencer interaction between the 3' terminus and SL2 is an integral part of the blocking structure. Interestingly, formation of this 3'-terminal interaction in the viral RNA likely has a dual protective function related to exoribonucleases: (i) it forms part of the structure that stalls Xrn4 to generate the svRNA, and (ii) it could act to prevent access of the 3'-to-5' exosome complex to the 3' end of the viral RNA genome. Regarding the latter function, the silencer interaction would bury the 3' terminus in a tertiary interaction that could make it inaccessible to the exosome complex (Bonneau et al., 2009).

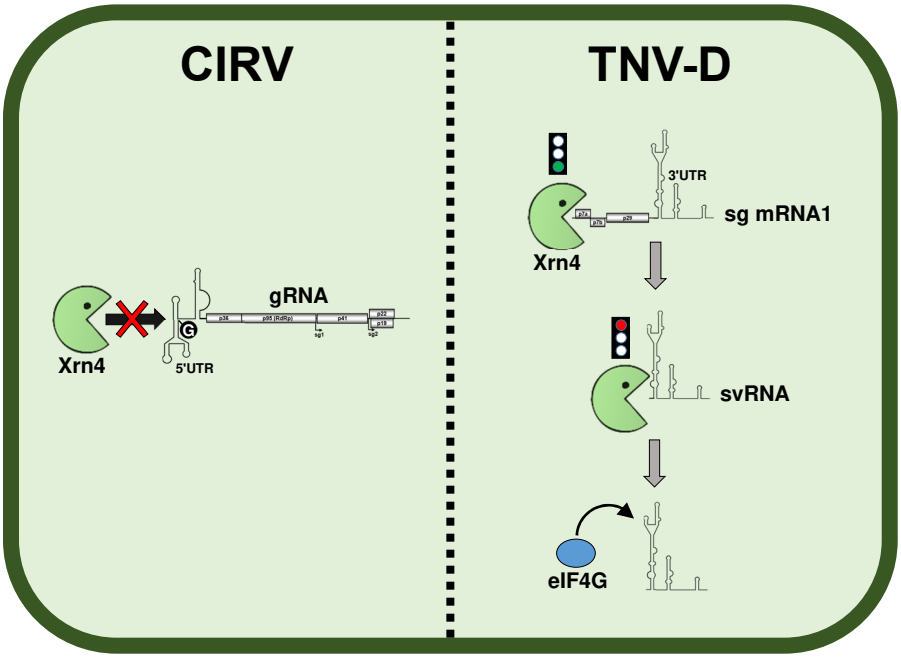

Figure 1. Model for tombusvirid evasion (CIRV) and exploitation (TNV-D) of host Xrn4. *Left panel.* Depiction of proposed interaction between plant Xrn4 and CIRV RNA genome in the cytosol. The xeRNA structure formed by the CIRV 5'UTR prevents access of the 5' terminal nucleotide to Xrn4. The white G encircled in black denotes the structurally buried 5' terminal nucleotide. *Right panel.* Proposed model for TNV-D svRNA formation and function. The svRNA is generated via incomplete digestion of TNV-D sg mRNA1 by Xrn4, which stalls just upstream of the BTE. The newly formed svRNAs likely inhibit translation, by acting as sponges for host translation factors (e.g. eIF4G), via their BTE.

4.2.2. Evasion of Xrn by viral RNA

A previous study on a yeast RNA virus demonstrated that the structural context of the 5' end of the viral RNA genome conferred resistance to Xrn1 (Esteban et al., 2008). In this dissertation, the highly structured genomic 5'UTR of the plant tombusvirus CIRV was examined for its ability to withstand exoribonuclease decay. Mutational analysis of specific 5'-proximal RNA sequences demonstrated that cooperative folding of secondary and tertiary level RNA structures are required to maintain genome integrity in the presence of Xrn1 *in vitro* (Gunawardene et al., 2021). The observed increase in genome integrity was most likely due to reduced enzyme access to the 5' terminal nucleotide of the viral genome (**Figure 1**). In light of this ability, we referred to the CIRV 5'UTR as an **X**rn-**e**vading RNA (xeRNA). For an RNA structure to be classified as an xeRNA, it must possess two main characteristics: (i) structurally, it must be located at the 5' end

and incorporate the 5' terminal nucleotide within its structure; and (ii) functionally, it must prohibit engagement by Xrn and, in doing so, protect the integrity of the downstream sequence. Burying the 5' terminal nucleotide within strong RNA structure is an essential part of the conformational fold of an xeRNA, as this prevents loading of the RNA into the Xrn1 active site (**Figure 1**). Indeed, Xrn1 requires a minimum of two to three free nucleotides to engage the substrate within its active site and initiate decay (Jinek et al., 2011), meaning that, for an RNA to avoid 5'-to-3' degradation, the 5' terminal three nucleotides must not be in ssRNA form. Accordingly, the 5'-termini of both the CIRV genome and the 20S narnavirus RNA are classified as xeRNAs based on the two aforementioned criteria.

Although the CIRV 5'UTR was also tested for its ability to function as an xrRNA via appendage of additional sequence upstream of it (i.e. poly(A) tracts), the downstream context of the 3' end was not tested thoroughly. However, treatment of the complete viral genome with Xrn1 produced results comparable to treatment of defective interfering RNA-7 (DI-7), which contains different, albeit viral, sequence downstream of the 5'UTR (Gunawardene et al., 2021). Also, the 5'UTR on its own (*i.e.* RI) demonstrated near full protection against Xrn1 activity, which suggests that the conformational fold is highly stable on its own, and would likely still be functional with different 3' sequences appended. In contrast, the inability of the blocking structure to tolerate oligonucleotide additions to its 5' end confirms that it is unable to stall an actively progressing Xrn1, and thus is not an xrRNA.

4.3…Xrn inhibition and tombusvirids

The interplay between virus and host has resulted in intricate adaptations that have evolved in viruses attempting to evade the antiviral activities of its host. In cases where evasion is not possible, some viruses have even developed contingency methods for exploiting the antiviral machinery to generate proviral elements. The antiviral factor studied in this dissertation was plant Xrn4, which is implicated as the enzyme at the root of these observations. This section will address questions related to the Xrn4's identity in these two studies, the frequency of xrRNAs in the *Tombusviridae* family, and whether or not a connection exists between RNA structures that inhibit Xrn4 and viral protein translation.

4.3.1. Is plant Xrn4 the enzyme responsible for these effects?

Plant Xrn4 is a cytoplasmic ortholog of yeast/animal nuclear Xrn2, and the functional equivalent of cytoplasmic yeast/animal Xrn1. Higher plants possess three Xrn proteins; Xrn2, Xrn3, and Xrn4, the latter two of which are Xrn2 orthologs (Kastenmeyer and Green, 2000). Xrn2 and Xrn3 are localized in the nucleus, whereas Xrn4 resides in the cytoplasm. Plant viruses in the family *Tombusviridae* are uncapped, nonpolyadenylated plus-strand RNA viruses that are strictly cytoplasmic. In addition, previous studies have identified a direct negative correlation between Xrn4 expression and tombusvirus RNA accumulation in plants (Serviene et al., 2005; Cheng et al., 2006; Cheng et al., 2007; Jaag and Nagy, 2009). Combined, these two lines of evidence support the hypothesis that Xrn4 is the enzyme responsible for the phenotypes observed in this dissertation.

However, the possibility exists that an exoribonuclease other than Xrn4 could be completely or partially responsible for the observed effects. Evidence for this line of reasoning comes from the fact that plants have two other Xrns, Xrn2 and Xrn3, and that animal Xrn2 is able

to translocate to the cytoplasm to perform certain antiviral functions (Sedano and Sarnow, 2014). Also, the active sites of the plant Xrns are highly conserved with one another, and with yeast/animal Xrn1, meaning that the possibility exists that one of the other two Xrns could potentially generate identical svRNA 5' ends with those generated by Xrn1 *in vitro*. In addition, in yeast, nuclear Xrn2 is able to substitute for loss of Xrn1 in the cytoplasm, and *vice versa* (Johnson, 1997; Kastenmeyer et al., 2001). However, given what is known about Xrn4 regarding its functional interchangeability with Xrn1 in plants (Kastenmeyer et al., 2001; Cheng et al., 2006; Cheng et al., 2007), its negative impact on tombusvirus RNA accumulation (Cheng et al., 2007), and that it is the only plant Xrn known to localize to the cytoplasm (Nagarajan et al., 2013; Kastenmeyer and Green, 2000), it seems most likely that Xrn4 is the 5'-to-3' exoribonuclease that interacts with and produces the phenotypes observed in both of the viruses studied in this dissertation.

4.3.2. How common are xrRNAs among tombusvirids?

So far, xrRNA and xrRNA-like structures have been identified and structurally characterized in the *Dianthovirus* and *Betanecrovirus* genera of the *Tombusviridae* family, which generate SR1f in RCNMV, and the TNV-D svRNA described in this dissertation, respectively. Interestingly, two additional xrRNAs may be present in the *Tombusvirus* genus. Northern blot analysis of tombusvirus infections showed that svRNAs corresponding to tombusviral 5'UTRs are detectable using a 3' terminal probe (White and Morris, 1994; Gunawardene et al., 2021). However, unlike the TNV-D svRNA, treatment of the CIRV genome and subgenomic mRNAs with purified Xrn1 did not generate any svRNA *in vitro*. This result may suggest that the CIRV svRNA is not produced by incomplete degradation of the viral 3'UTR by Xrn, but is instead produced via an unidentified subgenomic promoter. On the other hand, it is possible that production of the tombusvirus svRNA relies on additional cellular factors that either facilitate folding of the inhibitory

RNA structure, or bind to the RNA to act as a protein-based roadblock for Xrn. This could be tested by inoculating *in vitro* transcribed 5'-monophoshorylated CIRV genomic RNA into a plant cell-free extract and checking whether the svRNA is produced. The tombusvirus 3'UTRs include 3'CITEs, and thus the candidate cellular proteins that could block Xrn would include eukaryotic translation factors.

Based on the CIRV study in this dissertation, a long viral RNA (lvRNA) may also be generated by Xrn from the genome (Gunawardene et al., 2021). *In vitro* Xrn1 treatment of CIRV 5'UTR mutants generated a readily detectable lvRNA, approximately 1500 nts smaller than the full-length genome. A similar-sized product is also generated during protoplast infections of 5'UTR mutants. Whether or not these two RNAs are the same molecule remains to be tested; regardless, their characterization is of interest. The lvRNAs, which would not be capable of self-replication, could still potentially serve as templates for subgenomic transcription, given that they contain functional promoters and the long-range RNA-RNA interactions necessary for subgenomic transcription (Chkuaseli and White, 2018; Chkuaseli and White, 2020). Indeed, 5'UTR mutants with reduced genome accumulation show a corresponding spike in subgenomic mRNA production, relative to cognate genome accumulation (Gunawardene et al., 2021). Thus, the xrRNA structure responsible for lvRNA production may serve as a contingency measure for situations where the 5'UTR xeRNA structure is overcome by Xrn4, allowing for the production of a still useful viral RNA that could produce subgenomic mRNAs.

The question of why viruses, such as those in the *Tombusviridae* family, use xrRNAs to generate decay intermediates may be answered in part by the fact that they are limited in their coding capacity based on their small genomes. xrRNAs in *Tombusviridae* and other plant viruses have thus far been shown to (i) help generate translatable subgenomic mRNAs (Ilyas et al., 2021), (ii) facilitate long-distance viral movement (Flobinus et al., 2016), (iii) inhibit global protein translation as a means of potentially triggering later viral life-cycle stages (Iwakawa et al., 2008; Gunawardene et al., 2019) and (iv) potentially creating exclusive templates for subgenomic

mRNA synthesis as speculated for the CIRV lvRNA. Thus, the limited coding potential of these small plant viruses creates selective pressure for new and innovative gene expression and regulatory strategies to develop, that either help the virus to circumvent host antiviral processes, or to facilitate its own replicative cycle.

4.3.3. Potential connection between TNV-D 5'-end protection and protein translation

When testing the four tombusvirid RNA genomes with Xrn1 *in vitro*, it was found that TNV-D and TCV were significantly more susceptible to degradation than CIRV and CLSV (Gunawardene et al., 2021). During viral infections, it is unlikely that these two viruses would be much more susceptible to Xrn4 degradation than either of the other two, as all four are able to successfully replicate and accumulate viral RNAs to appreciable levels in a mutual host. Therefore, it is predicted that for TNV-D to maintain the integrity of its genome, a host factor is recruited to the 5'-end that stabilizes the region and physically impedes Xrn4 access and degradation. Interestingly, TNV-D currently has no long-range RNA-RNA interaction identified that unites its 5' and 3'UTRs (i.e. 3'CITE) to facilitate viral protein translation (Chkuaseli et al., 2015). In light of this, it is possible that a host protein that is responsible for protecting the 5' end is also involved in translation. For example, an RNA-binding protein that protects 5' end could also mediate a bridging interaction with translation factors bound to the BTE in its 3' UTRs. Thus, the 5'-UTR-binding protein would serve a dual role; aiding with recruitment of the translational machinery to the 5' end and protecting the 5' end from Xrn4 decay.

4.4…Future directions

There are several future experiments that could be performed to further expand on the findings presented in this dissertation; these possibilities are presented in the form of specific research questions.

4.4.1. Can trans-expression of the TNV-D svRNA rescue mutant viral infection in plants?

Plant infections using infectious, svRNA-deficient TNV-D transcripts (ΔsvRNA) resulted in reduced symptoms and minimal viral RNA accumulation (Gunawardene et al, 2019). To confirm that the phenotype observed during ΔsvRNA viral infection is in fact due to the absence of svRNA, the infection could be repeated with a *trans*-expressed svRNA (Shen and Miller, 2004). A vector containing ΔsvRNA could be simultaneously agroinfiltrated into *N. benthamiana* plants alongside an svRNA-expressing vector(+svRNA), or a control empty vector. If the effects observed with the ΔsvRNA mutant alone are in fact due to a lack of svRNA, then a rescue in viral RNA accumulation and symptomology would be expected in protoplasts and plants containing both the ΔsvRNA virus and the +svRNA vector. This complementation test would help to further support the conclusions drawn earlier that the TNV-D svRNA influences viral RNA accumulation and symptom generation during infections.

4.4.2. Is plant Xrn4 the enzyme that engages the CIRV 5'UTR and produces the TNV-D svRNA?

Something else worth pursuing would be to do a gene-specific knockdown of Xrn4, and observe the effects on CIRV and TNV-D replication in plants. The knockdown can be performed in *N. benthamiana* using a TRV-based gene silencing vector containing a segment of the NbXrn4 mRNA sequence (Dinesh-Kumar et al., 2003; Jaag and Nagy, 2009). Agroinfiltration of the TRV

silencing vector would occur first to allow time for Xrn4 silencing, followed by agroinfiltration of either CIRV or TNV-D several days later into the systemically Xrn4-silenced upper leaves. After allowing the infection to proceed, the infected leaves would be harvested, total RNA extracted, and probed via Northern blotting to analyse viral RNA levels. Specifically, it would be determined if replication of the defective CIRV 5'UTR mutants could be rescued, and whether TNV-D svRNA production was abolished; the results of which would allow us to more confidently assert that the enzyme responsible for the effects observed with each virus was in fact due to plant Xrn4. To add to this, knockdowns of both Xrn2 and Xrn3 could also be done in parallel, to determine if these enzymes are also involved with either the CIRV 5'UTR or the TNV-D svRNA.

4.4.3. Can 3D structural modeling of the CIRV xeRNA or TNV-D svRNA provide us with any additional information?

The findings presented in this dissertation suggest that the xeRNA structure formed by the CIRV 5'UTR represents a tightly folded RNA conformation comprising both secondary and tertiary level interactions. The lack of degradation and dephosphorylation of the 5'UTR observed when treated with Xrn1 and RppH *in vitro*, along with the near full protection demonstrated by the 5'UTR on its own against Xrn1 activity, suggests that the 5' nucleotide is buried within this tightly folded structure, granting minimal accessibility to either of these enzymes. It would be interesting to develop a 3D structural model of the CIRV xeRNA, using modern structural analysis techniques, to confirm this theory. To do this, a crystal structure of the entire wild-type CIRV 5'UTR could be solved using X-ray crystallography, or alternatively, a cryo-electron microscopy (cryo-EM) image could be generated (Ferré-D'Amaré et al., 1998; Ke and Doudna, 2004; Kappel et al., 2020). These studies rely on the structures being stable and uniform enough to form crystals or generate equivalent images by cryo-EM. The maintenance of a compact RNA structure during electrophoresis suggests that the CIRV 5'UTR may be stable enough for these studies

(Gunawardene et al., 2021). If successful, an atomic structural model would reveal how different components of the 5'UTR interact collectively to form the xeRNA structure. The xrRNA-like inhibitory structure responsible for TNV-D svRNA formation could be more challenging to model using these methods, because the stalling structure proved to be less effective than the knot-like RNA structures at stalling purified Xrn1 *in vitro*, and thus its structure may be less stable (Gunawardene, unpublished observations).

4.4.4. Is a host factor required for 5'-end protection in TNV-D and TCV?

In vitro Xrn1 treatment of tombusvirid RNA genomes yielded varying results, where the viruses with highly structured 5'UTRs (CIRV and CLSV) were more resistant to Xrn1 than those with less structure (TNV-D and TCV) (Gunawardene et al., 2021). To determine if a host factor is required for protection of the TNV-D genome, an experiment could be performed using a tobacco cell-free extract instead of purified Xrn1. Specifically, *in vitro* transcribed 5'-monophosphorylated viral RNA genomes could be incubated in cell-free extract, followed by RNA extraction and gel electrophoresis. The cell-free extract system contains all of the host factors necessary for viral replication and translation (Komoda et al., 2004; Iwakawa et al., 2007), in addition to Xrn4, and therefore any potential host factor required by the virus for 5' end protection would presumably also be present. If there is a host factor required by TNV-D and TCV, and it is present in the cell-free extract, we would expect to see similar degradation profiles between TNV-D, TCV and CIRV. The results of this experiment could potentially provide evidence that a host factor is involved in protecting the 5'UTRs of TNV-D and TCV. Further, to determine the identity of the host factor, an RNA-protein affinity purification assay can be performed (Windbichler and Schroeder, 2006). Briefly, the 5'UTRs of TNV-D and TCV would first be fused to a streptomycin-binding aptamer, called a StreptoTag, and bound to streptomycin beads in a column. Next, the cell-free extract would be added to the matrix, allowing for potential host factors to interact with

and bind to the streptotagged 5'UTR. Following several wash steps, the protein-bound streptotagged 5'UTR would then be eluted using excess streptomycin, and the proteins recovered subjected to mass spectrometry to determine their identity.

4.4.5. What is the xrRNA structure responsible for generating the CIRV lvRNA?

The formation of a long viral RNA (lvRNA) species from the CIRV genome with purified Xrn1 suggests that an xrRNA structure exists approximately 1500 nts downstream of the 5' end (Gunawardene et al., 2021). Determining the structural basis for formation of this lvRNA decay intermediate may help to identify the first xrRNA for this genus of *Tombusviridae*. The initial course of action would be to map the 5' end of the lvRNA. This could be done by gel-purifying the lvRNA directly from *in vitro* Xrn1 degradation assays and performing 5' rapid amplification of cDNA ends (5'RACE) on the purified RNA. The results of this 5' end mapping would allow for examination of the 5'-terminal sequence that would likely correspond to the xrRNA. The RNA structure in the stall region could then be examined through solution structure probing (e.g. SHAPE) and, once defined, mutated to determine its importance of the predicted structure for stalling. Transposability would also be tested via defining the minimal stalling sequence and then inserting it into a different sequence context prior to Xrn1 testing. The results of these experiments will help to determine the key structural features of the Xrn stalling structure. To determine if the lvRNA is important in infection, the xrRNA structure could be mutated to not block Xrn and the effect on infections observed.

The high amount of lvRNA that accumulated during protoplast infections suggests that it may be *trans*-replicated by functional replication proteins produced from the mutant full-length genome. To investigate this possibility, its 5'-end sequence would be examined to see if it corresponded to promoter-like sequences (i.e. GAAA….). Minus-strand analysis of infections

could also be performed to see if minus-strand lvRNA accumulate, which would support it replicating in cells. Additionally, *in vitro* transcripts of the lvRNA could be tested in co-inoculations with CIRV helper virus genomes in plant protoplasts. lvRNA accumulation would then be monitored and any observed increase in lvRNA levels over time would be consistent with its replication in the coinfection. The collective findings from these experiments will determine whether (i) the CIRV lvRNA is generated via an xrRNA, (ii) it is replicable and (iii) it is important for CIRV infections.

4.5…Final thoughts

This dissertation has provided evidence that viral RNA structures are able to inhibit 5'-to-3' exoribonucleases via two main mechanisms: by preventing access to 5'-terminal sequences in CIRV and by stalling an actively digesting exoribonuclease in TNV-D. The structures responsible for these two activities are referred to as xeRNAs (coined by us) and xrRNAs, respectively. Together, these viral RNA structures illustrate some of the mechanisms utilized by plant viruses that help to promote successful infections, either through avoidance of an antiviral factor, or exploitation of it. The work adds two further examples of the varied roles that higher-order RNA structures can play in biological systems.

4.6…References

Bonneau F, Basquin J, Ebert J, Lorentzen E, Conti E. 2009. The yeast exosome functions as a macromolecular cage to channel RNA substrates for degradation. *Cell*. **139**(3):547-559.

Charley PA, Wilusz CJ, Wilusz J. 2018. Identification of phlebovirus and arenavirus RNA sequences that stall and repress the exoribonuclease XRN1. *J Biol Chem*. **293**(1):285-295.

Cheng CP, Jaag HM, Jonczyk M, Serviene E, Nagy PD. 2007. Expression of the Arabidopsis Xrn4p 5'-3' exoribonuclease facilitates degradation of tombusvirus RNA and promotes rapid emergence of viral variants in plants. *Virology*. **368**(2):238-248.

Cheng CP, Serviene E, Nagy PD. 2006. Suppression of viral RNA recombination by a host exoribonuclease. *J Virol*. **80**(6):2631-2640.

Chkuaseli T, Newburn LR, Bakhshinyan D, White KA. 2015. Protein expression strategies in tobacco necrosis virus-D. *Virology*. **486**:54-62.

Chkuaseli T, White KA. 2018. Intragenomic long-distance RNA-RNA interactions in plus-strand RNA plant viruses. *Front Microbiol*. **9**:529.

Chkuaseli T, White KA. 2020. Activation of viral transcription by stepwise largescale folding of an RNA virus genome. *Nucleic Acids Res*. **48**(16):9285-9300.

Dinesh-Kumar SP, Anandalakshmi R, Marathe R, Schiff M, Liu Y. 2003. Virus-induced gene silencing. *Methods Mol Biol*. **236**:287-294.

Esteban R, Vega L, Fujimura T. 2008. 20S RNA narnavirus defies the antiviral activity of SKI1/XRN1 in Saccharomyces cerevisiae. *J Biol Chem*. **283**(38):25812-25820.

Ferré-D'Amaré AR, Zhou K, Doudna JA. 1998. A general module for RNA crystallization. *J Mol Biol*. **279**(3):621-631.

Flobinus A, Hleibieh K, Klein E, Ratti C, Bouzoubaa S, Gilmer D. 2016. A viral noncoding RNA complements a weakened viral RNA silencing suppressor and promotes efficient systemic host infection. *Viruses*. **8**(10):272.

Gunawardene CD, Im JSH, White KA. 2021. RNA Structure Protects the 5'-end of an Uncapped Tombusvirus RNA Genome from Xrn Digestion. *J Virol*. 95(20):e01034-21.

Gunawardene CD, Newburn LR, White KA. 2019. A 212-nt long RNA structure in the tobacco necrosis virus-D RNA genome is resistant to Xrn degradation. *Nucleic Acids Res*. **47**(17):9329-9342.

Ilyas M, Du Z, Simon AE. 2021. Opium poppy mosaic virus has an Xrn-resistant, translated subgenomic RNA and a BTE 3'CITE. *J Virol*. **95**:e02109-20.

Iwakawa HO, Kaido M, Mise K, Okuno T. 2007. Cis-acting core RNA elements required for negative-strand RNA synthesis and cap-independent translation are separated in the 3'-untranslated region of red clover necrotic mosaic virus RNA1. *Virology*. **369**(1):168-181.

Iwakawa HO, Mizumoto H, Nagano H, Imoto Y, Takigawa K, Sarawaneeyaruk S, Kaido M, Mise K, Okuno T. 2008. A viral noncoding RNA generated by cis-element-mediated protection against 5'->3' RNA decay represses both cap-independent and cap-dependent translation. *J Virol*. **82**(20):10162-10174.

Jaag HM, Nagy PD. 2009. Silencing of Nicotiana benthamiana Xrn4p exoribonuclease promotes tombusvirus RNA accumulation and recombination. *Virology*. **386**(2):344-352.

Jinek M, Coyle SM, Doudna JA. 2011. Coupled 5' nucleotide recognition and processivity in Xrn1-mediated mRNA decay. *Mol Cell*. **41**:600-608.

Jiwan SD, Wu B, White KA. 2011. Subgenomic mRNA transcription in tobacco necrosis virus. *Virology*. **418**(1):1-11.

Johnson AW. 1997. Rat1p and Xrn1p are functionally interchangeable exoribonucleases that are restricted to and required in the nucleus and cytoplasm, respectively. *Mol Cell Biol*. **17**(10):6122-6130.

Jones RA, Steckelberg AL, Vicens Q, Szucs MJ, Akiyama BM, Kieft JS. 2021. Different tertiary interactions create the same important 3D features in a distinct flavivirus xrRNA. *RNA*. **27**(1):54-65.

Kappel K, Zhang K, Su Z, Watkins AM, Kladwang W, Li S, Pintilie G, Topkar VV, Rangan R, Zheludev IN, et al. 2020. Accelerated cryo-EM-guided determination of three-dimensional RNA-only structures. *Nat Methods*. **17**(7):699-707.

Kastenmayer JP, Green PJ. 2000. Novel features of the XRN-family in Arabidopsis: evidence that AtXRN4, one of several orthologs of nuclear Xrn2p/Rat1p, functions in the cytoplasm. *Proc Natl Acad Sci U S A*. **97**(25):13985-13990.

Kastenmayer JP, Johnson MA, Green PJ. 2001. Analysis of XRN orthologs by complementation of yeast mutants and localization of XRN-GFP fusion proteins. *Methods Enzymol*. **342**:269-282.

Ke A, Doudna JA. 2004. Crystallization of RNA and RNA-protein complexes. *Methods*. **34**(3):408-414.

Kieft JS, Rabe JL, Chapman EG. 2015. New hypotheses derived from the structure of a flaviviral Xrn1-resistant RNA: conservation, folding, and host adaptation. *RNA Biol*. **12**(11):1169-1177.

Komoda K, Naito S, Ishikawa M. 2004. Replication of plant RNA virus genomes in a cell-free extract of evacuolated plant protoplasts. *Proc Natl Acad Sci U S A*. **101**(7):1863-1867.

Nagarajan VK, Jones CI, Newbury SF, Green PJ. 2013. XRN 5'→3' exoribonucleases: structure, mechanisms and functions. *Biochim Biophys Acta*. **1829**(6-7):590-603.

Ray D, Na H, White KA. 2004. Structural properties of a multifunctional T-shaped RNA domain that mediate efficient tomato bushy stunt virus RNA replication. *J Virol*. **78**(19):10490-10500.

Ray D, Wu B, White KA. 2003. A second functional RNA domain in the 5' UTR of the tomato bushy stunt virus genome: intra- and interdomain interactions mediate viral RNA replication. *RNA*. **9**(10):1232-1245.

Sedano CD, Sarnow P. 2014. Hepatitis C virus subverts liver-specific miR-122 to protect the viral genome from exoribonuclease Xrn2. *Cell Host Microbe*. **16**(2):257-264.

Serviene E, Shapka N, Cheng CP, Panavas T, Phuangrat B, Baker J, Nagy PD. 2005. Genome-wide screen identifies host genes affecting viral RNA recombination. *Proc Natl Acad Sci U S A*. **102**(30):10545-10550.

Shen R, Miller WA. 2004. Subgenomic RNA as a riboregulator: negative regulation of RNA replication by barley yellow dwarf virus subgenomic RNA 2. *Virology*. **327**(2):196-205.

Stevens A. 2001. 5'-exoribonuclease 1: Xrn1. *Methods Enzymol*. **342**:251-259.

Vicens Q, Kieft JS. 2021. Shared properties and singularities of exoribonuclease-resistant RNAs in viruses. *Comput Struct Biotechnol J*. **19**:4373-4380.

White KA, Morris TJ. 1994. Recombination between defective tombusvirus RNAs generates functional hybrid genomes. *Proc Natl Acad Sci U S A*. **91**(9):3642-3646.

Windbichler N, Schroeder R. 2006. Isolation of specific RNA-binding proteins using the streptomycin-binding RNA aptamer. *Nat Protoc*. **1**(2):637-640.

Wu B, Vanti WB, White KA. 2001. An RNA domain within the 5' untranslated region of the tomato bushy stunt virus genome modulates viral RNA replication. *J Mol Biol*. **305**(4):741-756.

APPENDIX A:

ADDITIONAL RESEARCH CONTRIBUTIONS

Gunawardene CD, Donaldson LW, White KA. 2017. Tombusvirus polymerase: structure and function. *Virus Res*. **234**:74-86.

Gunawardene CD, Jaluba K, White KA. 2015. Conserved motifs in a tombusvirus polymerase modulate genome replication, subgenomic transcription, and amplification of defective interfering RNAs. *J Virol*. **89**(6):3236-3246.

APPENDIX B:

LIST OF COPYRIGHT PERMISSIONS

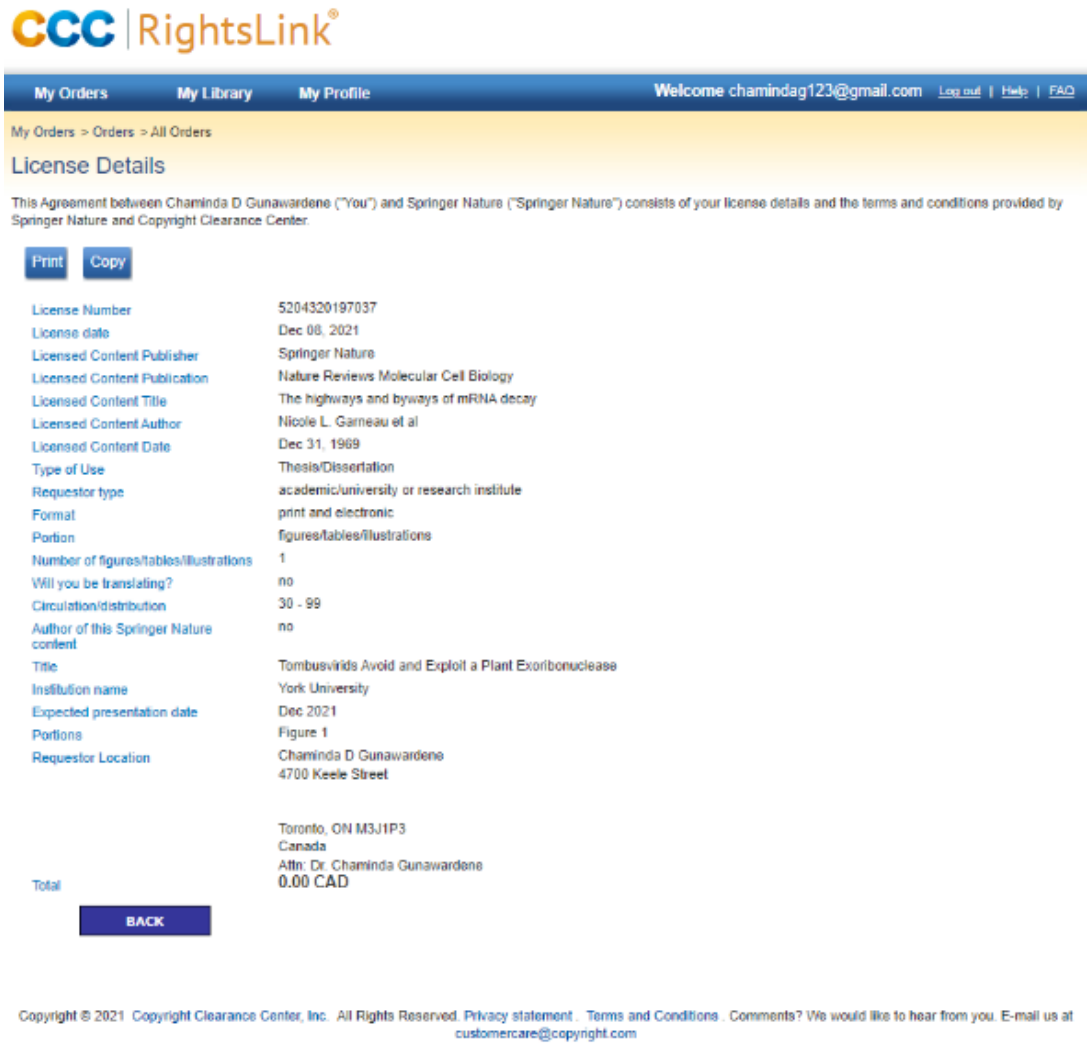

CCC | RightsLink®

My Orders | My Library | My Profile | Welcome chamindag123@gmail.com | Log out | Help | FAQ

My Orders > Orders > All Orders

License Details

This Agreement between Chaminda D Gunawardene ("You") and Springer Nature ("Springer Nature") consists of your license details and the terms and conditions provided by Springer Nature and Copyright Clearance Center.

Print | Copy

License Number	5204320197037
License date	Dec 08, 2021
Licensed Content Publisher	Springer Nature
Licensed Content Publication	Nature Reviews Molecular Cell Biology
Licensed Content Title	The highways and byways of mRNA decay
Licensed Content Author	Nicole L. Garneau et al
Licensed Content Date	Dec 31, 1969
Type of Use	Thesis/Dissertation
Requestor type	academic/university or research institute
Format	print and electronic
Portion	figures/tables/illustrations
Number of figures/tables/illustrations	1
Will you be translating?	no
Circulation/distribution	30 - 99
Author of this Springer Nature content	no
Title	Tombusviruses Avoid and Exploit a Plant Exoribonuclease
Institution name	York University
Expected presentation date	Dec 2021
Portions	Figure 1
Requestor Location	Chaminda D Gunawardene 4700 Keele Street Toronto, ON M3J1P3 Canada Attn: Dr. Chaminda Gunawardene
Total	0.00 CAD

BACK

Figure 1. Copyright permission for CHAPTER 1, Figure 1.

Chaminda G. <cdgunawa@yorku.ca> Tue, Dec 7, 7:11 PM

to PNASpermissions

Hi,

I am requesting permission to use Figure 1 from the following article for reuse in my dissertation at York University:

https://doi.org/10.1073/pnas.97.25.13985

I tried going through the Copyright Clearance Center, but this article is not registered for use in dissertations.

Here is my information:

Name/Title: Chaminda Gunawardene, PhD
Institution: York University
Mailing Address: 4700 Keele St, Toronto, ON M3J 1P3
Phone Number: 416-736-5152 X70352
Email Address: cdgunawa@yorku.ca
Volume/Issue/Date: 97/25/2000
Article Title: Novel features of the XRN-family in Arabidopsis: Evidence that AtXrn4, one of several orthologs of nuclear Xrn2p/Rat1p, functions in the cytoplasm
Authors' Names: JP Kastenmayer and PJ Green
Page Numbers: 13985-13990
Figure to be reused: Figure 1

Title of dissertation: Tombusvirids avoid and exploit a plant exoribonuclease
Authors: Chaminda Gunawardene
Publisher of work: York University

Please let me know if there are any issues.

Thanks for your time,
Chaminda Gunawardene

PNAS Permissions via yuoffice.onmicrosoft.com Dec 9, 2021, 4:31 PM

to Chaminda

Dear Dr. Gunawardene,

Thank you for your message. Permission is granted for your use of the material as described in your request. Please include a complete citation for the original PNAS article when reusing the material, and include "Copyright (2000) National Academy of Sciences, U.S.A." as a copyright note. Because this material published between 1993 and 2008, a copyright note is needed. There is no charge for this material, either. Let us know if you have any questions.

Best regards,
Greg McCoy for
Diane Sullenberger
PNAS Executive Editor

Figure 2. Copyright permission for CHAPTER 1, Figure 2.

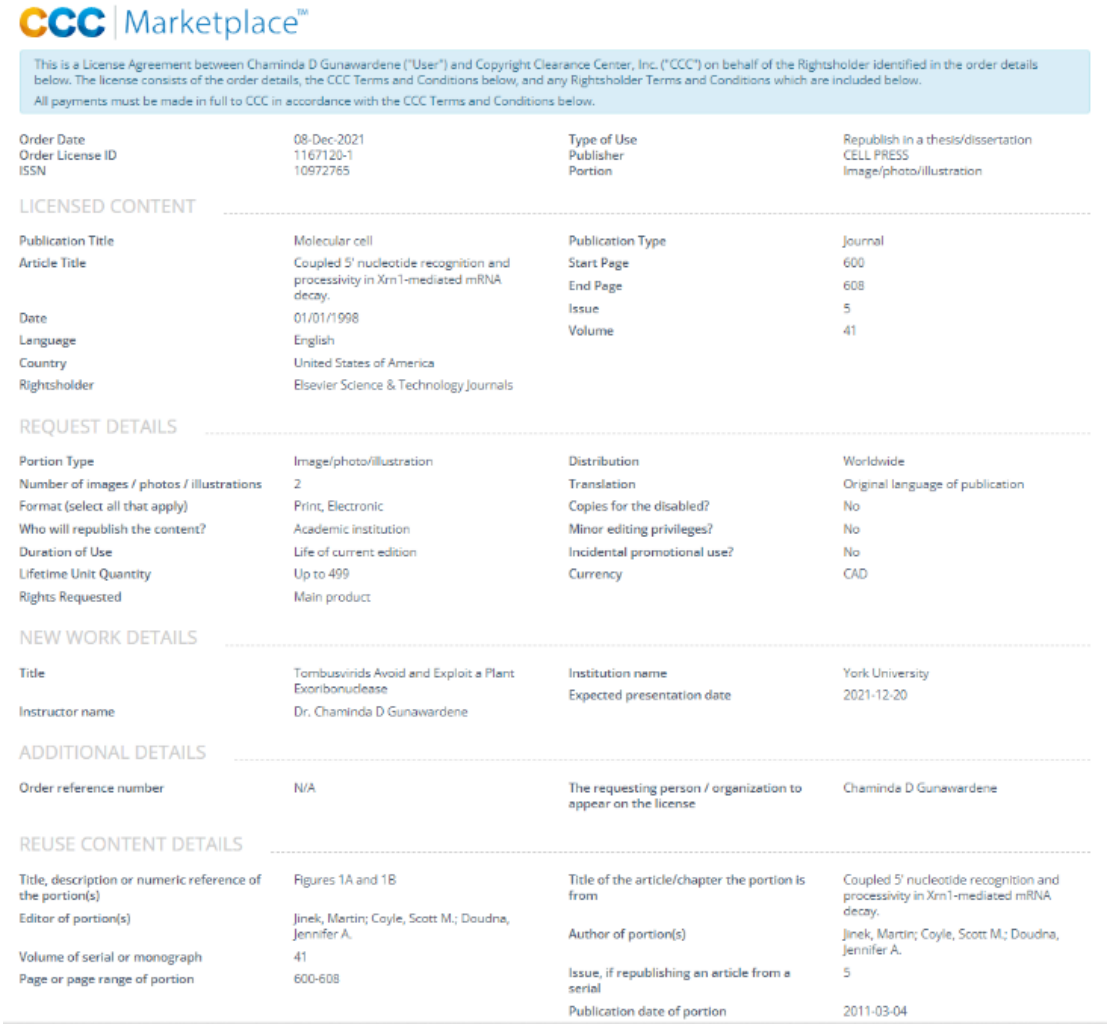

CCC Marketplace™

This is a License Agreement between Chaminda D Gunawardene ("User") and Copyright Clearance Center, Inc. ("CCC") on behalf of the Rightsholder identified in the order details below. The license consists of the order details, the CCC Terms and Conditions below, and any Rightsholder Terms and Conditions which are included below.

All payments must be made in full to CCC in accordance with the CCC Terms and Conditions below.

Order Date	08-Dec-2021	Type of Use	Republish in a thesis/dissertation
Order License ID	1167120-1	Publisher	CELL PRESS
ISSN	10972765	Portion	Image/photo/illustration

LICENSED CONTENT

Publication Title	Molecular cell	Publication Type	Journal
Article Title	Coupled 5' nucleotide recognition and processivity in Xrn1-mediated mRNA decay.	Start Page	600
		End Page	608
Date	01/01/1998	Issue	5
Language	English	Volume	41
Country	United States of America		
Rightsholder	Elsevier Science & Technology Journals		

REQUEST DETAILS

Portion Type	Image/photo/illustration	Distribution	Worldwide
Number of images / photos / illustrations	2	Translation	Original language of publication
Format (select all that apply)	Print, Electronic	Copies for the disabled?	No
Who will republish the content?	Academic institution	Minor editing privileges?	No
Duration of Use	Life of current edition	Incidental promotional use?	No
Lifetime Unit Quantity	Up to 499	Currency	CAD
Rights Requested	Main product		

NEW WORK DETAILS

Title	Tombusviruses Avoid and Exploit a Plant Exoribonuclease	Institution name	York University
		Expected presentation date	2021-12-20
Instructor name	Dr. Chaminda D Gunawardene		

ADDITIONAL DETAILS

Order reference number	N/A	The requesting person / organization to appear on the license	Chaminda D Gunawardene

REUSE CONTENT DETAILS

Title, description or numeric reference of the portion(s)	Figures 1A and 1B	Title of the article/chapter the portion is from	Coupled 5' nucleotide recognition and processivity in Xrn1-mediated mRNA decay.
Editor of portion(s)	Jinek, Martin; Coyle, Scott M.; Doudna, Jennifer A.	Author of portion(s)	Jinek, Martin; Coyle, Scott M.; Doudna, Jennifer A.
Volume of serial or monograph	41		
Page or page range of portion	600-608	Issue, if republishing an article from a serial	5
		Publication date of portion	2011-03-04

Figure 3. Copyright permission for CHAPTER 1, Figure 3.

CCC Marketplace™

This is a License Agreement between Dr. Chaminda D Gunawardene ("User") and Copyright Clearance Center, Inc. ("CCC") on behalf of the Rightsholder identified in the order details below. The license consists of the order details, the CCC Terms and Conditions below, and any Rightsholder Terms and Conditions which are included below.

All payments must be made in full to CCC in accordance with the CCC Terms and Conditions below.

Order Date	08-Dec-2021	Type of Use	Republish in a thesis/dissertation
Order License ID	1167111-1	Publisher	AMERICAN SOCIETY FOR MICROBIOLOGY.
ISSN	0022-538X	Portion	Chapter/article

LICENSED CONTENT

Publication Title	Journal of virology	Rightsholder	American Society for Microbiology - Journals
Article Title	RNA Structure Protects the 5'-end of an Uncapped Tombusvirus RNA Genome from Xrn Digestion	Publication Type	Journal
		Issue	20
Author/Editor	AMERICAN SOCIETY FOR MICROBIOLOGY.	Volume	95
Date	01/01/1967	URL	https://journals.asm.org/journal/jvi
Language	English		
Country	United States of America		

REQUEST DETAILS

Portion Type	Chapter/article	Rights Requested	Main product
Page range(s)	1-17	Distribution	Worldwide
Total number of pages	17	Translation	Original language of publication
Format (select all that apply)	Print, Electronic	Copies for the disabled?	No
Who will republish the content?	Academic institution	Minor editing privileges?	No
Duration of Use	Current edition and up to 10 years	Incidental promotional use?	No
Lifetime Unit Quantity	Up to 499	Currency	CAD

NEW WORK DETAILS

Title	Tombusvirids Avoid and Exploit a Plant Exoribonuclease	Institution name	York University
		Expected presentation date	2021-12-20
Instructor name	Dr. Chaminda D Gunawardene		

ADDITIONAL DETAILS

Order reference number	N/A	The requesting person / organization to appear on the license	Dr. Chaminda D Gunawardene

REUSE CONTENT DETAILS

Title, description or numeric reference of the portion(s)	Whole Article	Title of the article/chapter the portion is from	RNA Structure Protects the 5'-end of an Uncapped Tombusvirus RNA Genome from Xrn Digestion
Editor of portion(s)	Gunawardene, Chaminda D.; Im, Jennifer S. H.; White, K. Andrew	Author of portion(s)	Gunawardene, Chaminda D.; Im, Jennifer S. H.; White, K. Andrew
Volume of serial or monograph	95		
Page or page range of portion	1-17	Issue, if republishing an article from a serial	20
		Publication date of portion	2021-09-27

Figure 4. Copyright permission for CHAPTER 1, Figure 5 and 6; CHAPTER 3.

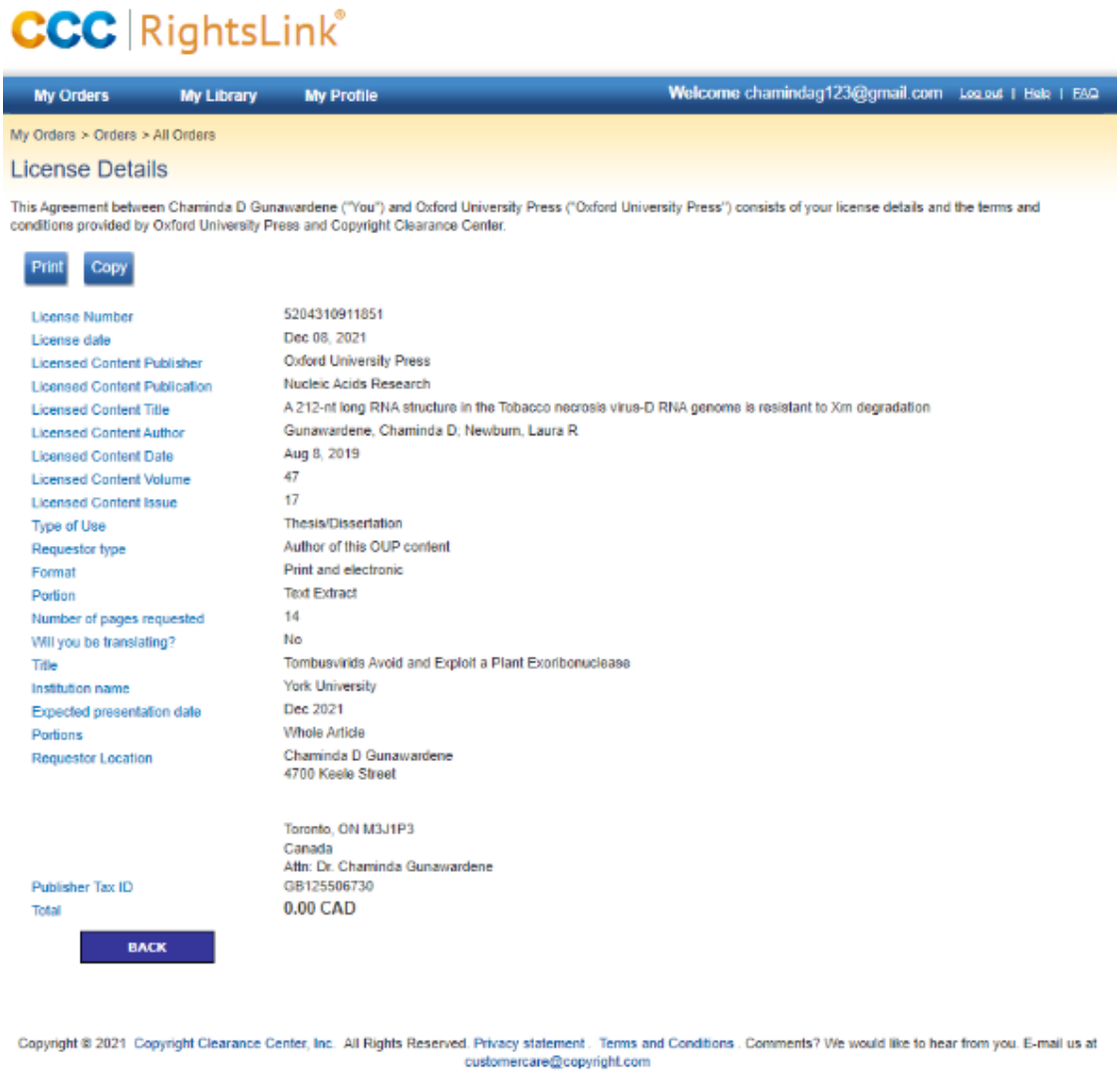

CCC RightsLink®

My Orders | My Library | My Profile | Welcome chamindag123@gmail.com | Log out | Help | FAQ

My Orders > Orders > All Orders

License Details

This Agreement between Chaminda D Gunawardene ("You") and Oxford University Press ("Oxford University Press") consists of your license details and the terms and conditions provided by Oxford University Press and Copyright Clearance Center.

Print | Copy

License Number	5204310911851
License date	Dec 08, 2021
Licensed Content Publisher	Oxford University Press
Licensed Content Publication	Nucleic Acids Research
Licensed Content Title	A 212-nt long RNA structure in the Tobacco necrosis virus-D RNA genome is resistant to Xrn degradation
Licensed Content Author	Gunawardene, Chaminda D; Newburn, Laura R
Licensed Content Date	Aug 8, 2019
Licensed Content Volume	47
Licensed Content Issue	17
Type of Use	Thesis/Dissertation
Requestor type	Author of this OUP content
Format	Print and electronic
Portion	Text Extract
Number of pages requested	14
Will you be translating?	No
Title	Tombusviridis Avoid and Exploit a Plant Exoribonuclease
Institution name	York University
Expected presentation date	Dec 2021
Portions	Whole Article
Requestor Location	Chaminda D Gunawardene 4700 Keele Street Toronto, ON M3J1P3 Canada Attn: Dr. Chaminda Gunawardene
Publisher Tax ID	GB125506730
Total	0.00 CAD

BACK

Copyright © 2021 Copyright Clearance Center, Inc. All Rights Reserved. Privacy statement . Terms and Conditions . Comments? We would like to hear from you. E-mail us at customercare@copyright.com

Figure 5. Copyright permission for CHAPTER 1, Figure 7; CHAPTER 2.

CCC Marketplace™

This is a License Agreement between Chaminda D Gunawardene ("User") and Copyright Clearance Center, Inc. ("CCC") on behalf of the Rightsholder identified in the order details below. The license consists of the order details, the CCC Terms and Conditions below, and any Rightsholder Terms and Conditions which are included below.

All payments must be made in full to CCC in accordance with the CCC Terms and Conditions below.

Order Date	09-Dec-2021	Type of Use	Republish in a thesis/dissertation
Order License ID	1167385-1	Publisher	Research Network of Computational and Structural Biotechnology
ISSN	2001-0370	Portion	Image/photo/illustration

LICENSED CONTENT

Publication Title	Computational and structural biotechnology journal	Rightsholder	Elsevier Science & Technology Journals
Article Title	Shared properties and singularities of exoribonuclease-resistant RNAs in viruses	Publication Type	Journal
Author/Editor	Research Network of Computational and Structural Biotechnology.	Start Page	4373
Date	01/01/2012	End Page	4380
Language	English	Volume	19
Country	Netherlands	URL	http://www.sciencedirect.com/science/jo...

REQUEST DETAILS

Portion Type	Image/photo/illustration	Distribution	Worldwide
Number of images / photos / illustrations	1	Translation	Original language of publication
Format (select all that apply)	Print, Electronic	Copies for the disabled?	No
Who will republish the content?	Academic institution	Minor editing privileges?	No
Duration of Use	Life of current edition	Incidental promotional use?	No
Lifetime Unit Quantity	Up to 499	Currency	CAD
Rights Requested	Main product		

NEW WORK DETAILS

Title	Tombusvirids Avoid and Exploit a Plant Exoribonuclease	Institution name	York University
Instructor name	Dr. Chaminda D Gunawardene	Expected presentation date	2021-12-20

ADDITIONAL DETAILS

Order reference number	N/A	The requesting person / organization to appear on the license	Chaminda D Gunawardene

REUSE CONTENT DETAILS

Title, description or numeric reference of the portion(s)	Figures 2A and 2B	Title of the article/chapter the portion is from	Shared properties and singularities of exoribonuclease-resistant RNAs in viruses
Editor of portion(s)	Vicens, Quentin; Kieft, Jeffrey S.	Author of portion(s)	Vicens, Quentin; Kieft, Jeffrey S.
Volume of serial or monograph	19	Issue, if republishing an article from a serial	N/A
Page or page range of portion	4373-4380	Publication date of portion	2021-07-01

Figure 6. Copyright permission for CHAPTER 1, Figure 9.